Quantifying Agreement Between Sampling Methods to Estimate Deoxynivalenol (DON) Contamination of Maize Grain in Commercial Fields and Characterizing its Heterogeneity at Multiple Spatial Scales across Ohio

Thesis

Presented in Partial Fulfillment of the Requirements for the Degree Master of Science in the Graduate School of The Ohio State University

By

Jorge Valle Torres

Graduate Program in Plant Pathology

The Ohio State University

2024

Thesis Committee

Dr. Pierce A. Paul, Advisor

Dr. Horacio Lopez-Nicora

Dr. Osler Ortez

ABSTRACT

Gibberella ear rot (GER) is a maize ear disease caused primarily by the necrotrophic toxigenic fungus *Fusarium graminearum* in the United States (US). Deoxynivalenol (DON) contamination of grain represents the greatest economic impact of GER because it reduces the market value of the crop and poses a threat to human and animal health. Sampling for DON at the field level is important for making harvest and postharvest management decisions, evaluating the efficacy of in-field management approaches, and validating risk assessment models. Accurate estimates of DON contamination are also useful for avoiding unfair price discounts and the utilization of grain with unsafe levels of the toxin. No information is available on how crop fields should be sampled for DON, how many samples should be collected to accurately estimated mean DON contamination, or whether sampling protocols should be adjusted based on baseline GER and DON levels, cultural practices, or local weather conditions. In addition, DON contamination of grain can be highly variable at multiple spatial scales, but estimates of such variability, which are important for developing sampling protocols, are lacking. Because of this, the agreement between two sampling methods, combine- and hand-sampling, in detecting fields with DON above an established threshold of 2 parts per million (ppm) and in estimating field-level mean DON contamination was quantified along with the characterization of the heterogeneity of DON contamination of grain at multiple spatial

scales. During three growing seasons, 2021, 2022, and 2023, eleven to twenty-nine fields were sampled using either or both sampling methods. Combine sampling consisted in pulling grain from the grain stream of the combine during harvest every 2 hectares or every 25,400 kg of grain, and hand-sampling was performed by collecting ten maize ears from each of 9 twelve-meter-long transects (pairs of rows) established in an M-pattern across a field.

Fields that were sampled with both methods were used to assess the agreement between combine- and hand-sampling in detecting fields with DON above 2 ppm, a threshold that is generally used by the grain industry, and in estimating field-level mean contamination in ppm, using DON as a continuous variable. Cohen's Kappa coefficient (*K*) was estimated for the former and Lin's concordance correlation coefficient (*CCC*) for the latter. Agreement in detecting DON above 2 ppm was moderate in 2021, 2022, and for the data pooled across years (*K* = 0.61, 0.79, and 0.64, respectively), but weak in 2023 (*K* = 0.42), with *K* not significantly different from zero. *K* was low in 2023 likely due to the relatively small sample size. However, assuming that there is low or no bias in sampling, observed agreement was moderate to strong (OA = 0.72 to 0.90). For field-level mean DON contamination, agreement was weak in 2021 and 2022 (*CCC* = 0.48 and 0.55) and moderate in 2023 and for the pooled data (*CCC* = 0.75 and 0.67, respectively). Low *CCC* values were due to imprecision between sampling methods, as there was high variability in mean DON contamination between fields. These results suggest that either method would be suitable for sampling to estimate DON if the goal is to detect fields with contamination below/above 2 ppm.

To characterize the heterogeneity of DON at multiple spatial scales, the complete DON dataset was used, including fields that were sampled with either or both methods. Two spatial scales were established, a three-level scale consisting of region (group of counties that share some similarities in growing conditions and/or topography), fields nested within regions, and samples (samples for combine-sampling and transects for hand-sampling) nested within fields within regions, and a two-level scale (only for 2023) using transects and ears nested within transects. Two separate dependent variables were used, one for DON as a binary response (i.e., DON incidence; 1 or 0, representing the presence or absence of DON above 2 ppm), and a second for DON as a continuous response using ppm results. Heterogeneity of DON contamination at multiple spatial scales was characterized for the binary response by fitting a generalized linear mixed model to the incidence data using the complementary log-log (CLL) link function, and to the field-level mean DON contamination (ppm) data by fitting unconditional hierarchical linear models. Estimated variances from the fit of the models were used to calculate variance partition coefficients and intracluster correlation coefficients (ICC). Separate models were fitted to the data for each year × sampling method combination. With DON as a continuous response, the variability between fields within regions was the greatest source of heterogeneity with combine-sampling in all cases, whereas sample/transect accounted for the highest proportion of the total variability with hand-sampling in all years, except 2022. Low ICC values indicated that this high transect-level variability was most likely due to ear-to-ear variability in DON contamination within transects. For DON as a binary response, field was the spatial scale with the highest variability on the CLL link scale. High

intracluster correlation coefficient indicated a high degree of similarity of the DON contamination status (above or below 2 ppm) within transects on the CLL link scale. These results suggest that combine-sampling tended to produce less variable field-level mean DON estimates than hand-sampling, and that the high heterogeneity within transects in hand-sampling was mostly due to ear-to-ear variability.

DEDICATION

To my parents, Jorge Valle and Yessica Torres, siblings Roberto and Yessica, and my grandparents Jorge, Teresa, and Ercilia

ACKNOWLEDGMENTS

I would like to extend my deepest gratitude to my advisor and mentor, Dr. Pierce Paul, for granting me the invaluable opportunity to be part of his lab and for his continuous support, patience, and guidance throughout this academic journey. His leadership and mentorship have profoundly inspired me and shaped the researcher I aspire to become. Words cannot express the depth of my appreciation.

I would also like to thank my student advisory committee members, Dr. Horacio Lopez-Nicora and Dr. Osler Ortez, for their advice, guidance, and for fostering a welcoming environment that nurtured my curiosity in various aspects of my research.

I am grateful to my current lab mates (Dr. Isaack Kikway, Doyeon Park, Joseph Chonza, Arianna Plaza) and former lab members (Nicole Winkler, Gabriela Silva, Rosita Martinez, Filipe Binotti, Luiz Soroldoni, Dr. Marian Luis, Dr. Maira Duffeck, and Dr. Wanderson Moraes) for their friendship, support, and the many memories shared during field and lab activities. I consider myself fortunate to have learned from each of you, especially Dr. Moraes, whom I also regard as a mentor.

Special thanks to Dr. Cristhian Cruz and Dr. Carolina Avellaneda, who provided me with my first research experiences at Purdue University and Zamorano University, respectively. Their mentorship and recommendations laid the foundation for my journey at The Ohio State University.

I would also like to express my sincere appreciation to the Department of Plant Pathology at The Ohio State University for their support and the knowledge gained from the faculty in every class. I am equally thankful to the friends I have made within and outside the department, whose presence made this journey more enjoyable and enriching.

Finally, I would like to thank my family in Ecuador—my parents, Jorge and Yessica, my siblings, Roberto and Yessica, and Xiomara—for their constant encouragement, unwavering support, and unconditional love, which sustained me throughout this journey.

VITA

2019……. B.Sc. Agricultural Sciences and Production, Zamorano University, Honduras.

2023……. Master in Sustainable Agribusiness, ESPAE, Ecuador.

2022 to present…… Graduate Research Assistant, Department Plant Pathology, The Ohio State University.

PUBLICATIONS.

Valle-Torres, J., Ross, T. J., Plewa, D., Avellaneda, M. C., Check, J., Chilvers, M. I., Cruz, A. P., Dalla Lana, F., Groves, C., Gongora-Canul, C., Henriquez-Dole, L., Jamann, T., Kleczewski, N., Lipps, S., Malvick, D., McCoy, A. G., Mueller, D. S., Paul, P. A., Puerto, C., Schloemer, C., Raid, R. N., Robertson, A., Roggenkamp, E. M., Smith, D. L., Telenko, D. E. P., and Cruz, C. D. 2020. Tar Spot: An Understudied Disease Threatening Corn Production in the Americas. Plant Dis. 104:2541–2550.

FIELDS OF STUDY

Major Field: Plant Pathology

TABLE OF CONTENTS

LIST OF TABLES

LIST OF FIGURES

CHAPTER 1: Introduction

IMPORTANCE OF MAIZE IN THE UNITED STATES

Maize (*Zea mays*), a cereal crop product of the domestication of the wild grass Teosinte in southern Mexico (Matsuoka et al. 2002), has been of importance for the United States (US) since it was introduced about 4000 years ago (Fonseca et al. 2015). Maize is an important ingredient for food and industrial products, feed for livestock, and for fuel ethanol production (USDA-NASS 2023). After the acceptance of hybrid maize in 1930 (Russel 1993), productivity and yield of the crop have increased steadily over the years. Currently, maize is the most widely grown crops in the US, being cultivated on 36.58, 37.59, 35.69, 38.28, and 37.06 million hectares in 2020, 2021, 2022, 2023, and 2024, respectively (USDA-NASS 2024a). The average annual production of maize over the last four growing seasons (2020-2023) was 360 million metric tons, with an average yield of 11.24 metric tons per acre (USDA-NASS 2024b, c). At an average grain price of USD 5.5 per 25.45 kilograms, the net value of the maize crop from 2020 to 2023 was USD 79.75 billion.

An estimated 40% of the maize produced in the US is used for livestock feed, whereas the other 60% is used for food, seed, and ethanol fuel and related co-products (USDA-NASS 2023). Maize accounts for 95% of the main energy ingredient in feed (USDA-NASS 2023). It is also an important source of calories in human diets (Awika 2011). High fructose corn syrup, starch, oil, beverage alcohol, fuel ethanol, industrial alcohol, glucose, dextrose, corn flakes, flour, and corn meal can all be produced from maize

(USDA-NASS 2023). In addition, by products from ethanol production such as distillers dried grains with soluble (DDGS) have been used as a primary ingredient in livestock feed (Iram et al. 2020). Given the importance of maize in the US, farmers need to maintain and increase its productivity, but their efforts to do so are constrained by limited arable land, water scarcity, more expensive inputs, and climate change-driven pests and diseases that often reduce grain yield and quality.

On average, plant diseases accounted for approximately 6% reduction in maize yield in the US from 2016 to 2019, representing USD 20,000 million in estimated losses during that period (Mueller et al. 2020). Of the diseases that affect maize, those caused by fungi belonging to the genus *Fusarium* are some of the most common and economically important. For instance, during 2016-2019, 28% of the total estimated yield losses in corn was reported to be due to diseases such as Fusarium stalk rot, Gibberella stalk rot, Fusarium ear rot, Gibberella ear rot (GER), and corn root rot, all of which are caused by *Fusarium* species, resulting in an estimated 1,598 million bushels in losses (Mueller et al. 2020). The main concern with maize diseases caused by *Fusarium* species is the risk of grain contamination with mycotoxins that reduce the market value and utilization of the crop. In the US, *F. graminearum* is the primary causal agent of GER, an ear disease of significant concern in terms of food safety, and because it has the potential to reduce yield (Dalla Lana et al. 2022; Vigier et al. 2010) and lead to grain contamination with mycotoxins such as deoxynivalenol (DON) and nivalenol, among others (Sutton 1982).

GIBBERELLA EAR ROT AND MYCOTOXINS

THE CAUSAL AGENT

Gibberella ear rot is caused by *Fusarium graminearum* Schwabe [Teleomorph: *Gibberella zeae* (Schwein.) Petch], a toxigenic, necrotrophic fungus with a wide host range that includes several small grain cereals such as wheat (*Triticum*), barley (*Hordeum*), oats (*Avena*), rice (*Oryza*) (Islam et al. 2021; Lee et al. 2010; Salas et al. 1999; Xue et al. 2019), as well as other field crops such as soybean (Broders et al. 2007; Xue et al. 2007). On wheat, barley, and rice, *F. graminearum* causes Fusarium head blight (FHB), leading to grain yield and quality reductions. *F. graminearum* was initially thought to be the only causal agent of GER and FHB. It was believed to be a single panmictic species throughout the world (O'Donnell et al. 2004). However, the development of genealogical concordance phylogenetic species recognition (GCPSR) has led to the conclusion that the dominant Fusarium species causing FHB varied among geographic regions, depending on climatic and agronomic factors (O'Donnell et al. 2000, 2004; Petronaitis et al. 2021). Knowledge of the dominant Fusarium species causing GER is limited to a small number of studies (Boutigny et al. 2011, 2014; Desjardins and Proctor 2011; Kuhnem et al. 2016; Lee et al. 2010; Qiu and Shi 2014; Samprieto et al. 2011), but they provided sufficient information to demonstrate that the causal agent might vary according to geographic locations due to pathogen migration, and/or environmental adaptation.

Each region is now believed to have its own population of Fusarium species that differ in pathogenicity, toxigenicity, and fungicide sensitivity (Akinsanmi et al. 2006; Kuhnem et al. 2016; Nielsen et al. 2012). Those causing FHB and GER are now considered part of the *Fusarium graminearum* species complex (FGSC) that consists of *F. brasilicum, F. austroamericanum, F. meridionale, F. cortaderiae, F. mesoamericanum, F. asiaticum,*

F. vorosii, F. acacia-mearnsii, F. cortaderiae, F. aethiopicum, F. ussurianum, F. boothi, and *F. gerlachii* (O'Donnell et al. 2000, 2004, 2008; Starkey et a. 2007; Yli et al. 2009). However, only *F. graminearum, F. graminearum sensu stricto* (Qiu and Shi 2014), *F. meridionale* (Machado et al. 2021; Samprieto et al. 2011), *Fusarium boothii* (Samprieto et al. 2011), *Fusarium cortaderiae* (Kuhnem et al. 2016) and *F. asiaticum* (Kawakami et al. 2015) have been recorded as causal agents of GER, with *F. graminearum* being the most prevalent GER-causing species in the US.

F. graminearum is an hemibiotrophic pathogen that belongs to the order of the *Hypocreales* and is genotypically diverse around the world and within North America (O'Donnell et al. 2000; Walker et al. 2001; Zeller et al. 2004). Based on results from multilocus sequencing experiments of different isolates collected from around the world, O'Donnell et al. (2000) revealed that *F. graminearum* can be grouped in seven biogeographical lineages. *F. graminearum* isolates from the US belong to lineages four and seven (O'Donnell et al. 2000), with populations showing recombination events and high genotypic diversity (Zeller et al. 2004) that are indicative of a strong evolutionary potential.

Populations of FGSC have also been classified into chemotypes on the bases of the mycotoxins they produce. The three main chemotypes are: 3-acetyldeoxynivalenol (3-ADON), 15-acetyldeoxynivalenol (15-ADON), and Nivalenol (NIV) (Alexander et al. 2011), and some authors suggest that they might be correlated with geographical origin (Suga et al. 2008). For instance, although *F. graminearum* is the main causal agent FHB in North America, the two chemotypes of this pathogen (3-ADON and 15-ADON) can be found in different regions (Ward et al. 2008). Chemotype population shifts are possible, as

Ward et al. (2008) showed a 14-fold increase in the frequency of the 3-ADON chemotype in western Canada over the usual 15-ADON chemotype in wheat samples. Since 3-ADON chemotype produces more mycotoxin and has higher fecundity rates than 15-ADON isolates (Ward. et al. 2008), it represents a significant concern for food security and plant breeders. Chemotype distribution and prevalence seems to vary by geographic location. The NIV chemotype predominates in South America from *F. meridionale* in Brazil and Argentina (Kunhem et al. 2016; Samprieto et al. 2011), whereas the 15-ADON chemotype was more frequently recovered in China from *F. graminearum sensu stricto* (Qui and Shi 2014), in France from *F. graminearum* (Boutigny et al. 2014), and South Africa from *F. boothii* (Boutigny et al. 2011).

PATHOGEN ECOLOGY AND DISEASE EPIDEMIOLOGY

Survival and inoculum sources. The ability of *F. graminearum* to produce an array of cell-wall and polysaccharide degrading enzymes allows it to use crop residue as a nutrient source and to survive between crops (Belien et al. 2006; Leplat et al. 2013). The pathogen is known to survive in the residue of small grain host crops such as wheat, barley, and corn, as well as soybean (Baird et al. 1997; Pereyra and Dill-Macky 2008). Mycelium in crop residue produces macroconidia in sporodochia and ascospores in perithecia that together constitute the primary inoculum for GER development (Sutton 1982). However, survival and sporulation of the pathogen and the type of inoculum produced are dependent on the type of residue and whether it is located on or below the soil surface (Khonga and Sutton 1988). For instance, Khonga and Sutton (1988) observed that *F. graminearum* survived and produced macroconidia and/or perithecia on one or more types of corn (ears

and stalks) and wheat (stems, spikelets, and grain) residue left on or above the soil during the first two years of a three-year study. In contrast, neither macroconidia nor perithecia were produced on any of the tested types of residue buried 10 cm below the soil surface (Khonga and Sutton 1988). Pereyra and Dill-Macky (2008) showed that *F. graminearum* was also able to colonize and survive in the residue of non-host such as fescue, sunflower, and different gramineous weeds (*D. sanguinalis, Cyno-don dactylon, Lolium multiflorum* and *Setaria* spp.), but colonization and survival were considerably lower when compared to cereal host crops. In addition to crop residue, soil and seeds are also considered *F. graminearum* inoculum sources (Sutton 1982).

Besides residue type and location, several other factors may affect sporulation and survival of *F. graminearum* in crop residue. For instance, the stage of decomposition and the nutritional status of residue were found to influence macroconidia and ascospores production (Khonga and Sutton 1988). Macroconidia of *F. graminearum* were produced mainly on freshly colonized tissue (early stages of residue decomposition), whereas ascospore production peaked at later stages of residue decomposition, usually when macroconidia production declined (Khonga and Sutton 1988). Wetting residue for long periods suppressed sporulation of the pathogen, probably due to increases in the presence and abundance of other microbes that likely competed with *F. graminearum* for resources (Khonga and Sutton 1988).

Dispersal. Dispersal of plant pathogens occurs in three distinct phases, discharge or release (passive or active), transport (short- or long-distant), and deposition, all of which are influenced weather conditions (Keller et al. 2014; Tar 1972). Ascospores of *F. graminearum* are produced in sac-like structure called asci that are borne in perithecia,

whereas macroconidia are borne on sporodochia. Under the right set of environmental conditions, asci extend within the perithecium to the ostiole to actively discharge the ascospores into the air (Trail et al. 2002). Trail et al. (2002) found that ascospore discharge was slightly higher under light compared to complete darkness. The complete process of ascospore release lasted up to 6 hours at 20°C under simulated rain and illumination. The launch speed of ascospore release was measured as 34.5 m/s, at a pressure of 1.54 MPa and an acceleration of 870,000 g (Trail et al. 2005). Trail et al. (2005) reposted that when ascospores were released into the air, they were accompanied by droplets of epiplasmic fluid, which may help to generate the necessary pressure for spore discharge.

Based on experiments similar to those conducted by Trail et al. (2005), Schmale III et al. (2005) reported that ascospore discharge distance varied slightly according to the age of the perithecia. Six-day-old perithecia discharge ascospores 4.6 mm on average, whereas twelve-day-old perithecia discharge ascospores to 3.9 mm, with settling velocity ranging from 0.93 to1.6 mm/s, and a settling time for deposition of 3.1-3.6 seconds (Schmale III et al. 2005). The authors concluded that the 3.9-4.6 discharge distances were enough to surpass the laminar boundary layer of the air, with this occurring much easier during the day than during the night. This suggests a higher probability of ascospores becoming airborne during the day than during the night (Schmale III et al. 2005). Ascospore release in wheat fields was found to occur 1-6 days after a rainfall event, and in some cases, on the same day as the event (De Luna et al. 2002). However, the concentration of ascospore released decreased as the time after the rain event increased.

Once released or discharged, *F. graminearum* ascospores and conidia can be transported by wind and rain splash (McMullen et al. 2012; Paul et al. 2004), with the

former contributing to long-distance movement of the pathogen. Paul et al. (2004) showed that spores (macroconidia and ascospores) of the pathogen can be splash dispersed through the wheat canopy, reaching heights of up to 100 cm above the soil surface. They noted that spores collected at 100 cm may have been splashed not only from the ground, but also from leaves within the canopy. Maldonado-Ramirez et al. (2005) reported that *F. graminearum* was transported by wind to long distances and postulated that long-distance transport of inoculum might play a role in regional epidemics in FHB. They observed that significantly more viable *F. graminearum* spores were present in the atmosphere under cloudy conditions compared to clear conditions, with spores traveling several kilometers to tens of kilometers. Relatedly, Francl et al. (1999) recovered the pathogen from places that were far from sources of inoculum (including roofs of buildings, urban yards and campus grounds).

Infection and colonization F. graminearum infects maize primarily during the silking growth stage (R1; Hesseltine and Bothast 1976; Sutton and Baliko 1981; Sutton 1982). Miller et al. (2007) reported that under field conditions, germination of the spores occurred 24 hours after inoculation (hai) and penetration occurs 48 hai. However, in vitro experiments showed faster spore germination (4-6 hai) (Miller et al. 2007). Studies of the infection and colonization of maize silks with macroconidia of *F. graminearum* revealed that attachment and penetration of the pathogen occurs mainly through the silk epidermal cells and hairs and are enhanced by the presence of pollen grain (Miller et al. 2007). However, penetration of the pathogen can also be facilitated by insect/bird damage (Sutton et al. 1980, 1982).

After penetration, the time taken for the pathogen to colonize and reach the developing grain varied with to the ear rot susceptibility of the cultivar, taking 12-15 days in resistant cultivars in contrast to 7-9 days in susceptible cultivars (Miller et al. 2007). Colonization was reported to be directed by the morphology of epidermal cells, as it progressed longitudinally down the silk at the junction of two epidermal cells towards the rachis and around immature kernels (Miller et al. 2007). Inside the rachis, hyphae were observed in the parenchyma and the vascular elements.

The role of the mycotoxin deoxynivalenol in the development of GER. Mycotoxins are low-molecular-weight organic compounds produced as secondary metabolites by some species of fungi. *F. graminearum* produces a wide range of mycotoxins such as deoxynivalenol (DON) and its derivatives 3-acetyl-deoxynivalenol (3-ADON), 15-acetyl-deoxynivalenol (15-ADON) (Xu and Nicholson 2009) that belong to the type B trichothecenes group and are synthesized from trichodiene (Zamir et al. 1989). DON is the most common mycotoxin produced by *F. graminearum* (Desjardins 2006). Nivalenol, another type B trichothecene, its derivatives (Desjardins 2006; Xu and Nicholson 2009), and other mycotoxins such as zearalenone (Jimenez et al. 1996) are also produced by *F. graminearum* and related species (Bottalico and Perrone 2002; Caldwell et al. 1970).

DON is considered a virulence factor in the development of GER (Harris et al. 1999). Its production is not essential for initial infection, as research showed that trichothecene-non-producing strains were able to infect and colonize maize tissue. However, the virulence of trichothecene-minus strains of pathogen was compromised (in terms of disease severity) compared to wild type strains (Harris et al. 1999). Trichothecene-producing strains also led significant yield losses compared to trichothecene-non-

producing strains. The main effect this group of mycotoxins at cellular level is interference in protein synthesis as it binds to the enzyme peptidyl transferase (Feinberg and McLaughlin 2017). Electrolyte loss (K+) from tissues occurs within 24 hours of DON production, indicating a disruption of the plasmalemma (Cossette and Miller 1995). DON concentration increased as GER severity increased, starting two weeks after inoculation, reaching a peak after six weeks, and then decreasing, stabilizing, or increasing, depending on genotype (Atanasova-Penichon et al. 2012; Miller et al. 1983; Reid and Sinha 1998). The exponential growth of *F. graminearum* started following the peak in DON concentration (Atanasova-Penichon et al. 2012).

Symptom development and sporulation. Reid and Sinha (1998) showed that the incubation period of *F. graminearum* was approximately 2 weeks. After the first symptoms developed, disease severity increased exponentially until the 4th week and reached a peak at 6-8 weeks (Miller et al. 1983; Reid and Sinha 1998). This is explained in part by the process of drying and hardening of the grain, which increase the barrier to infect and spread to other kernels. Typical signs and symptoms of GER develop a pinkish fungal mat on and between the kernels, starting at the tip of the ear. However, symptoms may develop at any point on the ear, depending on its orientation at dry-down (Crop Observation and Recommendation Network 2020; Enerson and Hunter 1980; Sutton 1982) and where cob and kernel wounds occur. Under highly favorable conditions for GER development, signs of the disease may be seen on the husk leaves (Munkvold 2003; Sutton 1982).

Perithecial development is influenced by temperature and moisture, as shown by Dufault et al. (2006). They showed that the favorable range of temperature and moisture for this fruiting body to develop on corn stalks was from 16 to 24°C and -0.45 to -1.30

MPa, respectively. In contrast, temperatures between 12 and 28°C and moisture levels between -2.36 and -4.02 MPa slowed perithecial development and prevented its maturation and production of ascospores (Dufault et al. 2006). Tschanz et al. (1975) determined that low intensity ultraviolet light (below 320 nm) stimulated the production of perithecia. On the other hand, Beyer et al. (2004) showed that macroconidia germination is enhanced by high relative humidity (80%), temperature of 20 °C, and complete darkness. Incubation under light conditions and a decrease in temperature prolonged the time to 50% germination of macroconidia, but did not prevent the process (Beyer et al. 2004).

ECONOMIC IMPACT OF GER AND DON

GER has steadily increased in prevalence and severity in the US, particularly in northern maize-growing states. GER reduces grain yield and yield components (Dalla Lana et al. 2022; Vigier et al. 2001). High levels of GER usually result in smaller, lighter ears and kernels, reducing grain weight by up to 50% in susceptible hybrids (Dalla Lana et al. 2022). However, the greatest impact of GER disease is DON contamination of grain, which may lead to economic losses (Dalla Lana et al. 2022) as a result of price reductions and grain rejection. DON contaminated grain, food and feed are unsafe for human and animal consumption. DON, commonly referred to as “Vomitoxin”, may cause feed refusal, vomiting, anorexia, impaired immune function, reproductive disorders, and emesis in mammals if fed with contaminated grains (Foroud and Eudes 2009; Pestka et al. 1987; Vesonder et al., 1976; Wu et al. 2014). Swine are particularly sensitive to DON. Consequently, DON contamination often reduces the market value and utilization of affected crops and their co-products (Schaafsma et al. 2009).

DON contamination may render DDGS, a nutrient-rich co-product of ethanol production, unfit for us as a low-cost ingredient for livestock and poultry feed (Iram et al. 2020). If contaminated grain is used in the dry-milling ethanol production process, DON can potentially increase by a factor of 3 in the final DDGS, making it unsafe for animal consumption, in some cases, even when initial levels of contamination are relatively low (Schaafsma et al. 2009). Due to the aforementioned adverse effects of GER and associated DON contamination of grain on the corn and ethanol industries, animal health, and food safety, maximum allowable limits for DON have been established for grain commercialization and utilization. For instance, in the US, the Food and Drug Administration recommends several advisory limits for DON in wheat grain for different end uses (FDA 2010). For maize commercialization, the DON thresholds at which grain is rejected or priced down are usually established by grain buyer at the point of sale.

MANAGEMENT OF GER AND DON

Several management strategies can be used to minimize the negative effects of GER and DON, including cultural practices, the use of resistant hybrids, and fungicide applications (Anderson et al. 2017; Andriolli et al 2016; Chungu et al. 1996; Khonga and Sutton 1988). Hybrid resistance is most effective, cheapest, and commonly recommended strategy for managing GER and DON (Dalla Lana et al. 2020). Two types of resistance to GER have been identified in maize, namely, silk and kernel resistance (Chungu et al. 1996; Reid et al. 1992; Reid and Hamilton 1997). These types of resistance target silk infection and kernel-to-kernel spread of *F. graminearum*, respectively. Silk resistance helps to reduce GER severity by reducing the growth of the pathogen down the silk due to a thicker

wax coating covering the silks (Reid et al. 1992; Reid and Hamilton 1997), whereas kernel resistance functions by reducing fungal spread from kernel to kernel from the initial point of infection (Chungu et al. 1996; Reid and Hamilton 1997).

Several authors have demonstrated that both types of resistance are controlled by several genes and are highly influenced by environmental conditions (Ali et al. 2005; Bolduan et al. 2009; Butron et al. 2015; Chungu et al. 1996; Reid et al. 1992, 1994). Ali et al. (2005) demonstrated that both resistance mechanisms are controlled by multiple and largely distinct loci throughout the genome, identifying at least 1 QTL for resistance on all but 2 chromosomes. Proteomic analysis after *F. graminearum* infection showed that, compared to susceptible varieties, resistant varieties had a greater abundance of Bowman-Birk-type wound-induced proteinase inhibitor WIP1, a phenolic O-methyltransferase, lipoxygenase (LOX)1, a lipase, calreticulin, and a 4SNc-Tudor domain protein that would promote resistance to kernel infection (Mohammadi et al. 2011). These same authors found significant increases of defense proteins in resistant varieties, including PR-10, chitinases, proteinase inhibitors, xylanase inhibitors, thaumatin-like and germin-like proteins.

Fungicides have been shown to reduce GER severity in some small-plot experiments where backpack sprayers were used to make targeted treatment applications and inoculations of the silks, with percent controls ranging 10 to 20% (Anderson et al. 2017) and 9 to 52% (Andriolli et al. 2016), depending on location, fungicide active ingredient, hybrid resistance, and application timing. However, fungicide efficacy against DON tends to be much more variable and inconsistent. For instance, Anderson et al. (2017) did not see a decrease in DON contamination with the use of DMI and QoI fungicides in Indiana, but Eli et al. (2021) observed a 50% reduction in DON when testing the active

ingredient pydiflumetofen in Ontario, Canada. Efficacy tended to be greatest when applications are made at early-to-mid silking (R1). Under commercial field conditions, fungicide efficacy against GER and DON is often more variable than in small-plot experiments, partly because of ear-to-ear variability in silking and the challenge of getting the fungicide on the ears/silks.

Crop rotation and tillage or any soil cultivation practice that results in the removal, destruction, or burial of infected crop residue are good strategies to manage GER, since the pathogen overwinters in these inoculum sources (McMullen et al. 2012; Nyvall 1970; Pereyra and Dill-Macky 2008). Khonga and Sutton (1988) showed that perithecia and macroconidia are not produced when corn residue is buried, limiting the production of primary inoculum the following seasons. Soil conservation practices such as no-till or reduced tillage that result in more inoculum being available on the surface were shown increase disease severity when susceptible host crop residue were not buried (Dill-Macky and Jones 2000; Pfordt et al. 2020). Fertilizer regimes (type and application rate) may also influence disease severity in some pathosystems, including GER of maize. In susceptible hybrids, amending the soils with appropriate rates of NH4NO3 in continuous corn production resulted in relatively lower GER severity and DON accumulation compared to non-treated plots (0 kg N/ha). However, when very high N rates are used (i.e., 200 kg N/ha), disease severity tended to increase (Reid et al. 2001).

Due to the possibility of *F. graminearum* infecting corn ears through insect damage and wounds (Sutton et al. 1980), some studies have focus on determining the effect insect pest management strategies on the management of GER and DON in the field (Parker et al. 2017; Schaafsma et al. 2002). Parker et al. (2017) showed a positive correlation between

the presence of western bean cutworm [*Striacosta albicosta* (Smith)] feeding damage and GER severity in field, suggesting the importance of controlling insects to limit disease severity by reducing wound-based infections. Schaafsma et al. (2002) observed that the control of the European corn borer, *Ostrinia nubilalis*, with Bt-corn hybrids contributed to the reduction of mycotoxin accumulation (mainly DON over Fumonisin B_1) when high incidence of the pest was present.

Other traits contribute to differences in hybrid reactions to GER and DON. These include kernel dry-down rate (KDD), husk tightness, and ear position during dry-down (Enerson and Hunter 1980; Kebebe et al. 2015; Munkvold 2003). For instance, Enerson and Hunter (1980) showed that ears that tended to dry in an upright position with tight husk generally had higher disease severity compared to pendant ears with loose husk. This is presumably because tight husk delay drying and residual water from rain accumulate at the base of ears that dry in an upright position. A higher KDD allows faster drying of the kernels, preventing further mycotoxin contamination and fungal colonization (Kebebe et al. 2015). Based on the fact that GER development requires moisture, KDD was seen as a promising trait to quantify when breeding for GER resistance. KDD can be used to reduce breeding time and costs, as it could limit pathogen development by reducing available moisture inside the ear. However, even though faster KDD resulted in lower GER severity, Kebebe et al. (2015) observed that traditional direct selection of cultivars for resistance was more effective than using KDD (Kebebe et al. 2015). Physical traits such as the position of the ear during dry-down and husk tightness are important to consider when screening for resistance to GER (Munkvold 2003) since both may affect KDD and grain contamination with DON.

SAMPLING FOR DON

Efforts to develop and evaluate GER and DON management strategies, particularly in commercial fields, requires accurate estimates to disease incidence and severity and grain contamination. In addition, to complement in-field management strategies such as hybrid resistance and fungicide application, farmers can also rely on grain harvesting and post-harvest handling (cleaning and screening) strategies to further reduce DON contamination. Field scouting for GER sampling and testing for DON are extremely important for evaluating in-field GER/DON management strategies and for making harvest and post-harvest grain cleaning, testing, and marketing decisions. However, relying on visual symptoms alone may lead to erroneous conclusions about DON contamination and the efficacy management strategies against DON, and consequently, incorrect management and grain handling decisions. Asymptomatic grain may still have DON concentration higher than regulatory advisory limits (Dalla Lana et al. 2021b). In addition, inadequate sampling may result in inaccurate estimates of mean disease intensity and DON at the field level (Moraes et al. 2022), and consequently, unfair price discounts, or conversely, contaminated gran being commercialized with adverse downstream effects on the various industries (e.g., ethanol, livestock, food ingredients).

GER and DON contamination of grain are known to be highly variable within fields, with high variability among ears and among kernels within ears. Consequently, inadequate scouting and sampling may lead to over or underestimation of DON contamination. Forecasting systems (Dalla Lana et al. 2021a) can be used to compliment or as an alternative to field scouting to assess the risk of DON contamination, but testing and validation of these tools for accuracy also require sampling. Alternatively, since insect feeding may lead to infection and GER development, scouting for insect damage may

provide a good indirect indicator of possible DON contamination (Parker et al. 2017). However, for more direct estimation of DON contamination, fields should be scouted after the R3 growth stage (milk) when the grain is already formed and developing, and pathogen colonization, GER symptom development, and DON production reach their peaks. Farmers are encouraged to sample at least ten ears from randomly selected locations across the field (Purdue Extension 2010) or sample grain directly from the grain stream during harvest. However, established field sampling protocols for mycotoxin estimation before or during harvest are not available for farmers.

Post harvest, five to ten samples can be drawn from multiple locations in the grain bin or truckload (Willyerd et al. 2016). As recommended by the Federal Grain Inspection Service-USDA (2016), hand or mechanical probes are the only effective method for sampling from stationary grain, with the minimum recommended sample size of 1,000 grams of grain drawn along an "X"-shape pattern (FGIS-USDA 2023; Willyerd et al. 2016). Sampling from conveyor belts can be performed using Ellis cup samplers, diverter- or woodside-type mechanical samplers, whereas sampling from falling stream should be performed using pelican samplers (FGIS-USDA 2016). However, regardless of the pre-sampling method used, the Ohio law (section 926.31) indicates that a licensed commodity handler shall allow an agricultural commodity tester to draw a sample to test for the quality of the grain for sale or storage under a bailment agreement (Ohio Law and Administrative Rules 2010). Farmers have the option of asking that a second sample to be drawn if they believe the first was not representative, or alternatively, they have the option of rejecting the agricultural commodity tester's result and requesting that the sample be sent to a federally licensed grain inspector for retesting.

THE RESEARCH QUESTIONS

GER and associated grain contamination with DON continue to be a problem in maize in the state of Ohio. None of the existing management strategies are full effective against GER and DON. In particular, no hybrid is immune to GER or DON, and resistance to GER does not always lead to reductions in DON contamination below critical thresholds. Similarly, no fungicide is 100% effective against GER and DON. Promising results from small-plot experiments do not directly translate into acceptable levels of fungicide efficacy in commercial fields. On-farm research is ongoing to screen commercial hybrids for resistance to GER and DON; evaluate the efficacy of fungicides and application methods using commercial spray equipment; determine the efficacy and efficiency of commercial grain cleaners, and validate DON risk assessment models. However, since DON contamination of grain is highly variable at multiple spatial scales, sampling at the field level is critical for evaluating the efficacy and economic benefit of these management and mitigation strategies, and for making important harvest and post-harvest decisions. But no information is available on how field should be sampled for DON, how many samples should be collected to accurately estimate mean DON contamination, or whether sampling protocols should be adjusted based on baseline GER and DON levels, cultural practices, or local weather conditions.

Sampling before or at harvest is critical for making informed grain handling and marketing decisions and for evaluating cultivar resistance and fungicide efficacy. Pre-harvest sampling (hand sampling) can be done by randomly collecting ears from multiple locations across the field, whereas at-harvest sampling (combine sampling) can be performed by pulling samples from the grain stream during harvest. Both methods have

advantages and disadvantages. For instance, with hand sampling, one may be better able to systematically sample from different locations of the field based on GER intensity and in-field microclimatic conditions, with the resulting estimates of GER and DON being useful for making informed grain harvesting decisions. However, this process can be laborious and time-consuming. On the other hand, sampling from the grain stream during harvest may be quicker and easier than hand-sampling and results in samples being drawn from a larger, more representative area of the field. However, an obvious disadvantage of this approach is that the resulting DON estimates are of no value for making grain harvesting decision.

Estimates of variability are extremely important for developing sampling protocols. Further research is needed to determine the variability associated with each of these sampling methods and at what level of the spatial hierarchy the variability is highest. This information is critical for determining sample sizes. In addition, given the aforementioned advantages and disadvantaged of the two methods, research is also needed to determine the level of agreement between them in terms of estimated mean DON and estimation of contamination above critical thresholds. Perfect or an acceptable level of agreement would suggest that either method could be used to estimate DON in commercial fields, whereas poor agreement would suggest that one method may be better that the other. The choice of method would then be made based of variability, cost, convenience, and the aforementioned advantages/disadvantages.

RESEASRCH OBJECTIVES

The specific objectives of the study were to (1) determine the level of agreement in estimating mean DON contamination at the field level (measured in ppm) between hand-

and combine-harvested grain sampling methods; (2) determine the level of agreement in detecting the presence/absence of DON contamination above a 2 ppm threshold (binary response); and (3) determine the variability in estimated mean DON contamination of grain at different spatial sampling (variability within fields, between fields in the same region, and between regions) scales when using hand- and combine-sampling methods.

REFERENCES

Akinsanmi, O. A., Backhouse, D., Simpfendorfer, S., and Chakraborty, S. 2006. Genetic diversity of australian *Fusarium graminearum* and *F. pseudograminearum*. Plant Pathol. 55:494–504.

Alexander, N. J., McCormick, S. P., Waalwijk, C., van der Lee, T., and Proctor, R. H. 2011. The genetic basis for 3-ADON and 15-ADON trichothecene chemotypes in *Fusarium*. Fungal Genet. Biol. 48:485–495.

Ali, M. L., Taylor, J. H., Jie, L., Sun, G., William, M., Kasha, K. J., Reid, L. M., and Pauls, K. P. 2005. Molecular mapping of QTLs for resistance to Gibberella ear rot, in corn, caused by *Fusarium graminearum*. Genome 48:521–533.

Anderson, N. R., Romero Luna, M. P., Ravellette, J. D., and Wise, K. A. 2017. Impact of foliar fungicides on Gibberella ear rot and deoxynivalenol levels in Indiana corn. Plant Health Progress 18:186–191.

Andriolli, C. F., Casa, R. T., Kuhnem, P. R., Bogo, A., Zancan, R. L., and Reis, E. M. 2016. Timing of fungicide application for the control of Gibberella ear rot of maize. Trop. plant pathol. 41:264–269.

Atanasova-Penichon, V., Pons, S., Pinson-Gadais, L., Picot, A., Marchegay, G., Bonnin-Verdal, M.-N., Ducos, C., Barreau, C., Roucolle, J., Sehabiague, P., Carolo, P., and Richard-Forget, F. 2012. Chlorogenic acid and maize ear rot resistance: a dynamic study investigating *Fusarium graminearum* development, deoxynivalenol production, and phenolic acid accumulation. Mol. Plant-Microbe in. 25:1605–1616.

Awika, J. M. 2011. Major cereal grains production and use around the world. In advances in cereal science: implications to food processing and health promotion. ACS Symposium Series. American Chemical Society pp. 1–13.

Baird, R. E., Mullinix, B. G., Peery, A. B., and Lang, M. L. 1997. Diversity and longevity of the soybean debris mycobiota in a no-tillage system. Plant Dis. 81:530–534.

Beliën, T., Van Campenhout, S., Robben, J., and Volckaert, G. 2006. Microbial endoxylanases: effective weapons to breach the plant cell-wall barrier or, rather, triggers of plant defense systems?. Mol. Plant-Microbe in. 19:1072–1081.

Beyer, M., Röding, S., Ludewig, A., and Verreet, J. A. 2004. Germination and survival of *Fusarium graminearum* macroconidia as affected by environmental factors. J. Phytopathol. 152:92–97.

Bolduan, C., Miedaner, T., Schipprack, W., Dhillon, B. S., and Melchinger, A. E. 2009. Genetic variation for resistance to ear rots and mycotoxins contamination in early european maize inbred lines. Crop Sci. 49:2019–2028.

Bottalico, A., and Perrone, G. 2002. Toxigenic Fusarium species and mycotoxins associated with head blight in small-grain cereals in Europe. In Mycotoxins in Plant Disease: Under the aegis of COST Action 835 'Agriculturally Important Toxigenic Fungi 1998-2003', EU project (QLK 1-CT-1998-01380), and ISPP 'Fusarium Committee,' eds. A. Logrieco, J. A. Bailey, L. Corazza, and B. M. Cooke. Springer.

Boutigny, A. L., Ward, T. J., Ballois, N., Iancu, G., and Ioos, R. 2014. Diversity of the *Fusarium graminearum* species complex on French cereals. Eur. J. Plant Pathol. 138:133–148.

Boutigny, A. L., Ward, T. J., Van Coller, G. J., Flett, B., Lamprecht, S. C., O'Donnell, K., and Viljoen, A. 2011. Analysis of the *Fusarium graminearum* species complex from wheat, barley and maize in South Africa provides evidence of species-specific differences in host preference. Fungal Genet. Biol. 48:914–920.

Broders, K. D., Lipps, P. E., Paul, P. A., and Dorrance, A. E. 2007. Evaluation *of Fusarium graminearum* associated with corn and soybean seed and seedling disease in Ohio. Plant Dis. 91:1155–1160.

Butrón, A., Reid, L. M., Santiago, R., Cao, A., and Malvar, R. A. 2015. Inheritance of maize resistance to Gibberella and Fusarium ear rots and kernel contamination with deoxynivalenol and fumonisins. Plant Pathol. 64:1053–1060.

Caldwell, R. W., Tuite, J., Stob, M., and Baldwin, R. 1970. Zearalenone production by *Fusarium* species. Appl. Microbiol. 20:31–34.

Chungu, C., Mather, D. E., Reid, L. M., and Hamilton, R. I. 1996. Inheritance of kernel resistance to *Fusarium graminearum* in maize. J. of Hered. 87:382–385.

Cossette, F., and Miller, J. D. 1995. Phytotoxic effect of deoxynivalenol and Gibberella ear rot resistance of com. Nat. Toxins 3:383–388.

Dalla Lana, F., Madden, L. V., and Paul, P. A. 2021a. Logistic models derived via lasso methods for quantifying the risk of natural contamination of maize grain with deoxynivalenol. Phytopathology 111:2250–2267.

Dalla Lana, F., Madden, L. V., and Paul, P. A. 2021b. Natural occurrence of maize Gibberella ear rot and contamination of grain with mycotoxins in association with weather variables. Plant Dis. 105:114–126.

David Miller, J., Culley, J., Fraser, K., Hubbard, S., Meloche, F., Ouellet, T., Lloyd Seaman, W., Seifert, K. A., Turkington, K., and Voldeng, H. 1998. Effect of tillage practice on Fusarium head blight of wheat. Can. J. Plant Pathol. 20:95–103.

Desjardins, A. E. 2006. *Fusarium* mycotoxins: chemistry, genetics and biology. J. Agric. Sci. 145:539–539.

Desjardins, A. E., and Proctor, R. H. 2011. Genetic diversity and trichothecene chemotypes of the *Fusarium graminearum* clade isolated from maize in Nepal and identification of a putative new lineage. Fungal Biol. 115:38–48.

Dill-Macky, R., and Jones, R. K. 2000. The effect of previous crop residues and tillage on Fusarium head blight of wheat. Plant Dis. 84:71–76.

Dufault, N. S., De Wolf, E. D., Lipps, P. E., and Madden, L. V. 2006. Role of temperature and moisture in the production and maturation of *Gibberella zeae* perithecia. Plant Dis. 90:637–644.

Eli, K., Schaafsma, A. w., Limay-Rios, V., and Hooker, D. c. 2021. Effect of pydiflumetofen on Gibberella ear rot and *Fusarium* mycotoxin accumulation in maize grain. World Mycotoxin J. 14:495–512.

Enerson, P. M., and Hunter, R. B. 1980. Response of maize hybrids to artificially inoculated ear mold incited by Gibberella zeae. Can. J. Plant Sci. 60:1463–1465.

Federal Grain Inspection Service-United States Department of Agriculture. 2016. Inspecting grain: practical procedures for grain handlers. Available: https://www.ams.usda.gov/sites/default/files/media/PracticalProceduresBook2017.pdf

Federal Grain Inspection Service-United States Department of Agriculture. 2023. Mycotoxin handbook. Available at: https://www.ams.usda.gov/sites/default/files/media/MycotoxinHB.pdf

Feinberg, B., and McLaughlin, C. S. 1989. Biochemical mechanism of action of trichothecene mycotoxins. 1st ed. In Trichothecene Mycotoxicosis Pathophysiologic Effects (1989), CRC Press, Boca Raton, Fl.

Da Fonseca, R. R., Smith, B. D., Wales, N., Cappellini, E., Skoglund, P., Fumagalli, M., Samaniego, J. A., Carøe, C., Ávila-Arcos, M. C., Hufnagel, D. E., Korneliussen, T. S., Vieira, F. G., Jakobsson, M., Arriaza, B., Willerslev, E., Nielsen, R., Hufford, M. B., Albrechtsen, A., Ross-Ibarra, J., and Gilbert, M. T. P. 2015. The origin and evolution of maize in the Southwestern United States. Nat. Plants 1:1–5.

Foroud, N. A., and Eudes, F. 2009. Trichothecenes in cereal grains. Int. J. Mol. Sci. 10:147–173.

Francl, L., Shaner, G., Bergstrom, G., Gilbert, J., Pedersen, W., Dill-Macky, R., Sweets, L., Corwin, B., Jin, Y., Gallenberg, D., and Wiersma, J. 1999. Daily inoculum levels of Gibberella zeae on wheat spikes. Plant Dis. 83:662–666.

Harris, L. J., Desjardins, A. E., Plattner, R. D., Nicholson, P., Butler, G., Young, J. C., Weston, G., Proctor, R. H., and Hohn, T. M. 1999. Possible role of trichothecene mycotoxins in virulence of *Fusarium graminearum* on maize. Plant Dis. 83:954–960.

Hesseltine, C. W., and Bothast, R. J. 1977. Mold development in ears of corn from tasseling to harvest. Mycologia 69:328–340.

Iram, A., Cekmecelioglu, D., and Demirci, A. 2020. Distillers' dried grains with solubles (DDGS) and its potential as fermentation feedstock. Appl. Microbiol. Biotechnol. 104:6115–6128.

Islam, M. N., Tabassum, M., Banik, M., Daayf, F., Fernando, W. G. D., Harris, L. J., Sura, S., and Wang, X. 2021. Naturally occurring *Fusarium* species and mycotoxins in oat grains from Manitoba, Canada. Toxins 13:670.

Jiménez, M., Máñez, M., and Hernández, E. 1996. Influence of water activity and temperature on the production of zearalenone in corn by three *Fusarium* species. Int. J. Food Microbiol. 29:417–421.

Kawakami, A., Kato, N., Sasaya, T., Tomioka, K., Inoue, H., Miyasaka, A., and Hirayae, K. 2015. Gibberella ear rot of corn caused by *Fusarium asiaticum* in Japan. J. Gen. Plant Pathol. 81:324–327.

Kebebe, A. Z., Reid, L. M., Zhu, X., Wu, J., Woldemariam, T., Voloaca, C., and Xiang, K. 2015. Relationship between kernel drydown rate and resistance to Gibberella ear rot in maize. Euphytica 201:79–88.

Keller, M. D., Bergstrom, G. C., and Shields, E. J. 2014. The aerobiology of *Fusarium graminearum*. Aerobiologia 30:123–136.

Khonga, E. B., and Sutton, J. C. 1988. Inoculum production and survival of *Gibberella zeae* in maize and wheat residues. Can. J. Plant Pathol. 10:232–239.

Kuhnem, P. R., Ward, T. J., Silva, C. N., Spolti, P., Ciliato, M. L., Tessmann, D. J., and Del Ponte, E. M. 2016. Composition and toxigenic potential of the *Fusarium graminearum* species complex from maize ears, stalks and stubble in Brazil. Plant Pathol. 65:1185–1191.

Lana, F. D., Madden, L. V., Carvalho, C. P., and Paul, P. A. 2022. Impact of Gibberella ear rot on grain quality and yield components in maize as influenced by hybrid reaction. Plant Dis. 106:3061–3075.

Lana, F. D., Paul, P. A., Minyo, R., Thomison, P., and Madden, L. V. 2020. Stability of hybrid maize reaction to Gibberella ear rot and deoxynivalenol contamination of grain. Phytopathology 110:1908–1922.

Lee, S.-H., Lee, J.-K., Nam, Y.-J., Lee, S.-H., Ryu, J.-G., and Lee, T. 2010. Population structure of *Fusarium graminearum* from maize and rice in 2009 in Korea. Plant Pathol. J. 26:321–327.

Leplat, J., Friberg, H., Abid, M., and Steinberg, C. 2013. Survival of *Fusarium graminearum*, the causal agent of Fusarium head blight. Agron. Sustain. Dev. 33:97–111.

Liu, K. 2011. Chemical composition of distillers grains, a review. J. Agric. Food Chem. 59:1508–1526.

Machado, F. J., Kuhnem, P. R., Casa, R. T., McMaster, N., Schmale, D. G., Vaillancourt, L. J., and Del Ponte, E. M. 2021. The dominance of *Fusarium meridionale* over *F. graminearum* causing Gibberella ear rot in Brazil may be due to increased aggressiveness and competitiveness. Phytopathology 111:1774–1781.

Maldonado-Ramirez, S. L., Schmale, D. G., Shields, E. J., and Bergstrom, G. C. 2005. The relative abundance of viable spores of *Gibberella zeae* in the planetary boundary layer suggests the role of long-distance transport in regional epidemics of Fusarium head blight. Agric. For. Meteorol. 132:20–27.

Matsuoka, Y., Vigouroux, Y., Goodman, M. M., Sanchez G., J., Buckler, E., and Doebley, J. 2002. A single domestication for maize shown by multilocus microsatellite genotyping. Proc. Natl. Acad. Sci. 99:6080–6084.

McMullen, M., Bergstrom, G., De Wolf, E., Dill-Macky, R., Hershman, D., Shaner, G., and Van Sanford, D. 2012. A unified effort to fight an enemy of wheat and barley: Fusarium head blight. Plant Dis. 96:1712–1728.

Miller, J. D., Young, J. C., and Trenholm, H. L. 1983. *Fusarium* toxins in field corn. I. Time course of fungal growth and production of deoxynivalenol and other mycotoxins. Can. J. Bot. 61:3080–3087.

Miller, S. S., Reid, L. M., and Harris, L. J. 2007. Colonization of maize silks by *Fusarium graminearum*, the causative organism of Gibberella ear rot. Can. J. Bot. 85:369–376.

Mohammadi, M., Anoop, V., Gleddie, S., and Harris, L. J. 2011. Proteomic profiling of two maize inbreds during early Gibberella ear rot infection. Proteomics 11:3675–3684.

Moraes, W. B., Madden, L. V., and Paul, P. A. 2022. Characterizing heterogeneity and determining sample sizes for accurately estimating wheat Fusarium head blight index in research plots. Phytopathology 112:315–334.

Mueller, D. S., Wise, K. A., Sisson, A. J., Allen, T. W., Bergstrom, G. C., Bissonnette, K. M., Bradley, C. A., Byamukama, E., Chilvers, M. I., Collins, A. A., Esker, P. D., Faske, T. R., Friskop, A. J., Hagan, A. K., Heiniger, R. W., Hollier, C. A., Isakeit, T., Jackson-Ziems, T. A., Jardine, D. J., Kelly, H. M., Kleczewski, N. M., Koehler, A. M., Koenning, S. R., Malvick, D. K., Mehl, H. L., Meyer, R. F., Paul, P. A., Peltier, A. J., Price, P. P., Robertson, A. E., Roth, G. W., Sikora, E. J., Smith, D. L., Tande, C. A., Telenko, D. E. P., Tenuta, A. U., Thiessen, L. D., and Wiebold, W. J. 2020. Corn yield loss estimates due to diseases in the United States and Ontario, Canada, from 2016 to 2019. Plant Health Progress 21:238–247.

Munkvold, G. P. 2003. Epidemiology of *Fusarium* diseases and their mycotoxins in maize ears. Eur. J. Plant Pathol. 109:705–713.

Nielsen, L. K., Jensen, J. D., Rodríguez, A., Jørgensen, L. N., and Justesen, A. F. 2012. *TRI12* based quantitative real-time PCR assays reveal the distribution of trichothecene genotypes of *F. graminearum* and *F. culmorum* isolates in Danish small grain cereals. Int. J.Food Microbiol. 157:384–392.

Nyvall, R. F. 1970. Chlamydospores of *Fusarium roseum 'graminearum'* as survival structures. Phytopathology 60:1175-1177.

O'Donnell, K., Kistler, H. C., Tacke, B. K., and Casper, H. H. 2000. Gene genealogies reveal global phylogeographic structure and reproductive isolation among lineages of *Fusarium graminearum*, the fungus causing Wheat scab. Proc. Natl. Acad. Sci. 97:7905–7910.

O'Donnell, K., Ward, T. J., Aberra, D., Kistler, H. C., Aoki, T., Orwig, N., Kimura, M., Bjørnstad, Å., and Klemsdal, S. S. 2008. Multilocus genotyping and molecular phylogenetics resolve a novel head blight pathogen within the *Fusarium graminearum* species complex from Ethiopia. Fungal Genet. Biol. 45:1514–1522.

O'Donnell, K., Ward, T. J., Geiser, D. M., Corby Kistler, H., and Aoki, T. 2004. Genealogical concordance between the mating type locus and seven other nuclear genes supports formal recognition of nine phylogenetically distinct species within the *Fusarium graminearum* clade. Fungal Genet. Biol. 41:600–623.

Ohio Law and Administrative Rules. 2010. Section 926.31 - Ohio revised code | Ohio laws. Available: https://codes.ohio.gov/ohio-revised-code/section-926.31

O. Zamir, L., J. Gauthier, M., A. Devor, K., Nadeau, Y., and Sauriol, F. 1989. Trichodiene is a precursor to trichothecenes. J. Chem. Soc., Chem. Commun. 0:598–600.

Parker, N. S., Anderson, N. R., Richmond, D. S., Long, E. Y., Wise, K. A., and Krupke, C. H. 2017. Larval western bean cutworm feeding damage encourages the development of Gibberella ear rot on field corn. Pest Manag. Sci. 73:546–553.

Paul, P. A. 2020. Gibberella ear rots showing up in corn: how to tell it apart from other ear rots. Agronomic Crops Network. Ohio State Univ. Extension. Available: https://agcrops.osu.edu/newsletter/corn-newsletter/2020-34/gibberella-ear-rots-showing-corn-how-tell-it-apart-other-ear-rots .

Paul, P. A., El-Allaf, S. M., Lipps, P. E., and Madden, L. V. 2004. Rain splash dispersal of *Gibberella zeae* within wheat canopies in Ohio. Phytopathology 94:1342–1349.

Pereyra, S. A., and Dill-Macky, R. 2008. Colonization of the residues of diverse plant species by Gibberella zeae and their contribution to Fusarium head blight inoculum. Plant Dis. 92:800–807.

Pestka, J. J., Lin, W.S., and Miller, E. R. 1987. Emetic activity of the trichothecene 15-acetyldeoxynivalenol in swine. Food Chem. Toxicol. 25:855–858.

Petronaitis, T., Simpfendorfer, S., and Hüberli, D. 2021. Importance of *Fusarium* spp. in wheat to food security: a global perspective. in: Plant Diseases and Food Security in the 21st Century, eds. Peter Scott, Richard Strange, Lise Korsten, and Maria Lodovica Gullino. Cham: Springer International Publishing.

Pfordt, A., Ramos Romero, L., Schiwek, S., Karlovsky, P., and von Tiedemann, A. 2020. Impact of environmental conditions and agronomic practices on the prevalence of *Fusarium* species associated with ear- and stalk rot in maize. Pathogens 9:236.

Przemieniecki, S., Tomasz, K., and Korzekwa, K. 2015. Chemotypes and geographic distribution of the *Fusarium graminearum* species complex. Environmental Biotechnology 10:45–54.

Qiu, J., and Shi, J. 2014. Genetic relationships, carbendazim sensitivity and mycotoxin production of the *Fusarium graminearum* populations from maize, wheat and rice in eastern China. Toxins 6:2291–2309.

Reid, L. M., and Hamilton, R. I. 1997. Breeding maize for ear rot resistance in Canada. Cereal Res. Commun. 25:639–642.

Reid, L. M., Mather, D. E., Bolton, A. T., and Hamilton, R. I. 1994. Evidence for a gene for silk resistance to *Fusarium graminearum* schw. ear rot of maize. J. Hered. 85:118–121.

Reid, L. M., Mather, D. E., Hamilton, R. I., and Bolton, A. T. 1992. Diallel analysis of resistance in maize to *Fusarium graminearum* infection via the silk. Can. J. Plant Sci. 72:915–923.

Reid, L. M., and Sinha, R. C. 1998. Maize maturity and the development of Gibberella ear rot symptoms and deoxynivalenol after inoculation. Eur. J. Plant Pathol. 104:147–154.

Reid, L. M., Zhu, X., and Ma, B. L. 2001. Crop rotation and nitrogen effects on maize susceptibility to Gibberella (*Fusarium graminearum*) ear rot. Plant Soil 237:1–14.

Russell, W. A. 1993. Achievements of maize breeders in North America. in: International Crop Science I. John Wiley & Sons, Ltd. Madison, WI.

Salas, B., Steffenson, B. J., Casper, H. H., Tacke, B., Prom, L. K., Fetch, T. G., and Schwarz, P. B. 1999. *Fusarium* species pathogenic to barley and their associated mycotoxins. Plant Dis. 83:667–674.

Sampietro, D. A., Díaz, C. G., Gonzalez, V., Vattuone, M. A., Ploper, L. D., Catalan, C. A. N., and Ward, T. J. 2011. Species diversity and toxigenic potential of *Fusarium graminearum* complex isolates from maize fields in northwest Argentina. Int. J. Food Microbiol. 145:359–364.

Schaafsma, A. W., Hooker, D. C., Baute, T. S., and Illincic-Tamburic, L. 2002. Effect of bt-corn hybrids on deoxynivalenol content in grain at harvest. Plant Dis. 86:1123–1126.

Schaafsma, A. W., Limay-Rios, V., Paul, D. E., and Miller, J. D. 2009. Mycotoxins in fuel ethanol co-products derived from maize: a mass balance for deoxynivalenol. J. Sci. Food Agric. 89:1574–1580.

Schaafsma, A. W., Tamburic-Ilincic, L., and Hooker, D. C. 2005. Effect of previous crop, tillage, field size, adjacent crop, and sampling direction on airborne propagules of *Gibberella zeae/Fusarium graminearum*, Fusarium head blight severity, and deoxynivalenol accumulation in winter wheat. Can. J. Plant Pathol. 27:217–224.

Schmale III, D. G., Arntsen, Q. A., and Bergstrom, G. C. 2005. The forcible discharge distance of ascospores of *Gibberella zeae*. Can. J. Plant Pathol. 27:376–382.

Starkey, D. E., Ward, T. J., Aoki, T., Gale, L. R., Kistler, H. C., Geiser, D. M., Suga, H., Tóth, B., Varga, J., and O'Donnell, K. 2007. Global molecular surveillance reveals novel Fusarium head blight species and trichothecene toxin diversity. Fungal Genet. Biol. 44:1191–1204.

Suga, H., Karugia, G. W., Ward, T., Gale, L. R., Tomimura, K., Nakajima, T., Miyasaka, A., Koizumi, S., Kageyama, K., and Hyakumachi, M. 2008. Molecular characterization of the *Fusarium graminearum* species complex in Japan. Phytopathology 98:159–166.

Sutton, J. C. 1982. Epidemiology of wheat head blight and maize ear rot caused by *Fusarium graminearum*. Can. J. Plant Pathol. 4:195–209.

Sutton, J. C., and Baliko, W. 1981. Methods for quantifying partial resistance to *Gibberella zeae* in maize ears. Can. J. Plant Pathol. 3:26–32.

Sutton, J. C., Baliko, W., and Liu, H. J. 1980. Fungal colonization and zearalenone accumulation in maize ears injured by birds. Can. J. Plant Sci. 60:453–461.

Tarr, S. A. J. 1972. The dispersal of plant pathogens. In Principles of Plant Pathology, ed. S. A. J. Tarr. London: Macmillan Education UK. Palgrave, London.

Trail, F., and Common, R. 2000. Perithecial development by *Gibberella zeae*: a light microscopy study. Mycologia 92:130–138.

Trail, F., Gaffoor, I., and Vogel, S. 2005. Ejection mechanics and trajectory of the ascospores of *Gibberella zeae* (anamorph *Fuarium graminearum*). Fungal Genet. Biol. 42:528–533.

Trail, F., Xu, H., Loranger, R., and Gadoury, D. 2002. Physiological and environmental aspects of ascospore discharge in *Gibberella zeae* (anamorph *Fusarium graminearum*). Mycologia 94:181–189.

Tschanz, A. T., Horst, R. K., and Nelson, P. E. 1976. The effect of environment on sexual reproduction of *Gibberella Zeae*. Mycologia 68:327–340.

U.S. Food and Drug Administration. 2010. Guidance for industry and FDA: advisory levels for deoxynivalenol (don) in finished wheat products for human consumption and grains and grain by-products used for animal feed. Available: https://www.fda.gov/regulatory-information/search-fda-guidance-documents/guidanceindustry-and-fda-advisory-levels-deoxynivalenol-don-finished-wheat-products-human.

USDA-NASS. 2023. Corn & other feedgrains. Available at: https://www.ers.usda.gov/topics/crops/corn-and-other-feedgrains/.

USDA-NASS. 2024a. Corn acreage planted. Available at: https://www.nass.usda.gov/Charts_and_Maps/graphics/cornac.pdf

USDA-NASS. 2024b. Corn production. Available at: https://www.nass.usda.gov/Charts_and_Maps/graphics/cornprod.pdf

USDA-NASS. 2024c. Corn yield. Available at: https://www.nass.usda.gov/Charts_and_Maps/graphics/cornyld.pdf

Vesonder, R. F., Ciegler, A., Jensen, A. H., Rohwedder, W. K., and Weisleder, D. 1976. Co-identity of the refusal and emetic principle from *Fusarium*-infected corn. Appl. Environ. Microbiol. 31:280–285.

Vigier, B., Reid, L. M., Dwyer, L. M., Stewart, D. W., Sinha, R. C., Arnason, J. T., and Butler, G. 2001. Maize resistance to Gibberella ear rot: symptoms, deoxynivalenol, and yield. Can. J. Plant Pathol. 23:99–105.

Walker, S. L., Leath, S., Hagler, W. M., and Murphy, J. P. 2001. Variation among isolates of *Fusarium graminearum* associated with Fusarium head blight in North Carolina. Plant Dis. 85:404–410.

Ward, T. J., Clear, R. M., Rooney, A. P., O'Donnell, K., Gaba, D., Patrick, S., Starkey, D. E., Gilbert, J., Geiser, D. M., and Nowicki, T. W. 2008. An adaptive evolutionary shift in Fusarium head blight pathogen populations is driving the rapid spread of more toxigenic *Fusarium graminearum* in North America. Fungal Genet. Biol. 45:473–484.

Willyerd, K. T., Thomison, P., and Paul, P. A. 2016. Gibberella ear rot and mycotoxins in corn: sampling, testing, and storage. Ohio State Univ. Extension. Available: https://ohioline.osu.edu/factsheet/plpath-cer-04

Wu, Q.-H., Wang, X., Yang, W., Nüssler, A. K., Xiong, L.-Y., Kuča, K., Dohnal, V., Zhang, X.-J., and Yuan, Z.-H. 2014. Oxidative stress-mediated cytotoxicity and metabolism of T-2 toxin and deoxynivalenol in animals and humans: an update. Arch Toxicol. 88:1309–1326.

Xu, X., and Nicholson, P. 2009. Community ecology of fungal pathogens causing wheat head blight. Annu. Rev. Phytopathol. 47:83–103.

Xu, X.-M., Parry, D. W., Nicholson, P., Thomsett, M. A., Simpson, D., Edwards, S. G., Cooke, B. M., Doohan, F. M., Monaghan, S., Moretti, A., Tocco, G., Mule, G., Hornok, L., Béki, E., Tatnell, J., and Ritieni, A. 2008. Within-field variability of Fusarium head blight pathogens and their associated mycotoxins. Eur. J. Plant Pathol. 120:21–34.

Xue, A. G., Chen, Y., Seifert, K., Guo, W., Blackwell, B. A., Harris, L. J., and Overy, D. P. 2019. Prevalence of *Fusarium* species causing head blight of spring wheat, barley and oat in Ontario during 2001–2017. Can. J. Plant Pathol. 41:392–402.

Xue, A. G., Cober, E., Voldeng, H. D., Voldeng, H. D., Babcock, C., and Clear, R. M. 2007. Evaluation of the pathogenicity of *Fusarium graminearum* and *Fusarium pseudograminearum* on soybean seedlings under controlled conditions. Can. J. Plant Pathol. 29:35–40.

Yli-Mattila, T., Gagkaeva, T., Ward, T. J., Aoki, T., Kistler, H. C., and O'Donnell, K. 2009. A novel Asian clade within the *Fusarium graminearum* species complex includes a newly discovered cereal head blight pathogen from the Russian Far East. Mycologia 101:841–852.

Zeller, K. A., Bowden, R. L., and Leslie, J. F. 2004. Population differentiation and recombination in wheat scab populations of *Gibberella zeae* from the United States. Mol. Ecol. 13:563–571.

CHAPTER 2: Determining Agreement between Sampling methods in Quantifying Deoxynivalenol Contamination of Maize Grain in Commercial Fields in Ohio

ABSTRACT

Gibberella ear rot (GER) and deoxynivalenol (DON) contamination of grain are major concerns for maize production in Ohio. Sampling is important for estimating field-level DON contamination and for evaluating GER/DON management strategies. Twenty-six, 20, and 11 commercial maize fields in Ohio were hand- and combine-sampled during the 2021, 2022, and 2023 growing seasons, respectively. Hand-sampling consisted of randomly collecting 10 ears from each of nine transects across a field, whereas combine-sampling involved pulling samples from the grain stream of the combine during harvest every two hectares or every 25,400 kg of grain. DON estimates were averaged across samples to obtain field-level means. Agreement between the methods in detecting the presence of DON above a 2-ppm threshold and in estimating field-level mean contamination was determined with Cohen's kappa coefficient (*K*) and concordance correlation coefficient (*CCC*), respectively. Agreement was moderate in 2021, 2022, and for the data pooled across years (*K* = 0.61, 0.79, and 0.64), but weak, with *K* not significantly different from zero in 2023 (*K* = 0.42). Assuming that there is low or no bias in sampling, observed agreement was moderate to strong (OA = 0.72 to 0.90). For field-level mean contamination, agreement was weak in 2021 and 2022 (*CCC* = 0.48 and 0.55) and moderate in 2023 and for pooled data (*CCC* = 0.75 and 0.67). These results suggest

that, assuming there is no sampling bias, either method would be suitable for sampling to estimate DON if the goal is to detect fields with contamination below/above 2 ppm.

INTRODUCTION

Gibberella ear rot (GER) is a maize ear disease caused primarily by the toxigenic, necrotrophic ascomycete fungus *Fusarium graminearum* in North America. GER has steadily increased in prevalence and severity in the state of Ohio (Dalla Lana et al. 2020) and other parts of the United States (Mueller et al. 2016; Sutton 1982) over the past decade. The pathogen infects maize ears primarily during the R1 growth stage (Hesseltine and Bothast 1976; Sutton 1982; Sutton and Baliko 1981), leading to the development of a pinkish fungal mat starting at the tip of the ear. However, infections may occur at any point on the ear where cob and kernel wounds occur or at the base of ears drying down in an upright position (Enerson and Hunter 1980; Sutton 1982). Under favorable weather conditions, signs of the disease may develop on husk leaves of the ear (Magarini et al. 2023; Munkvold 2003; Sutton 1982).

GER may lead to yield loss by reducing grain weight and ear dimensions (Dalla Lana et al. 2022; Vigier et al. 2001), but grain contamination with mycotoxins such as zearalenone and deoxynivalenol (DON) is often of greater importance from an economic and food and feed safety standpoint, since they pose a threat to human and animal health (Da Rocha et al. 2014; Pestka 2010). DON, frequently referred to as “Vomitoxin”, may cause feed refusal, vomiting, anorexia, impaired immune function, reproductive disorders, and emesis in mammals if fed highly contaminated grains (Foroud and Eudes 2009; Pestka 2010; Vesonder et al. 1976; Wu et al. 2014). Consequently, several countries have set maximum allowable limits for DON in contaminated grain destined for human and animal

consumption. For instance, in the United States, the Food and Drug Administration (2010) established DON thresholds for different end uses of grain, including 1 ppm in finished wheat products, 5 ppm in grains and grain by-product for swine consumption, and 10 ppm in grain and by-products for cattle.

Farmers attempting to commercialize grain with DON contamination exceeding the aforementioned thresholds may face price reductions or even complete grain rejected at grain elevators. DON contamination also reduces the utilization of the crop (Schaafsma et al. 2009). For instance, DON contamination my prevent the use of distillers' dried grains with solubles (DDGS), a co-product of ethanol production that is often used as a nutrient-rich, low-cost ingredient for livestock and poultry feed (Iram et al. 2020). When GER-affected grain is used in the dry-milling process, DON contamination of the final DDGS may increase by a factor of 3 over the amount of the toxin found in the grain, making the co-product unfit for animal consumption. In some cases, this occurs even when initial levels of contamination are relatively low (Schaafsma et al. 2009). Consequently, DON contamination may reduce the market value of the crop through price discounts, grain rejection, and rejection of coproducts such as DDGS, all of which lead to lost revenue (Dalla Lana et al. 2022; Vigier et al. 2001).

Several management strategies can be used to reduce the adverse effects of GER, with hybrid resistance being the most effective and commonly recommended (Dalla Lana et al. 2020), followed by fungicide application and cultural practices (Anderson et al. 2017; Reid et al. 2001). Results from a limited number of studies showed that fungicides reduced GER severity and DON contamination in small-plot experiments, but efficacy in terms of percent control tended to be highly variable (Anderson et al. 2017; Andriolli et al. 2016;

Eli et al. 2021), depending on location, fungicide active ingredient, hybrid resistance, and application timing. In addition, results for small-plot trials do not necessarily translate into effective GER and DON control in commercial fields. Research is ongoing to evaluate the efficacy of fungicide treatments and applications methods for GER/DON control using commercial spray equipment and to screen commercial hybrids for resistance under a range of field conditions.

Harvest and post-harvest grain handling strategies such as harvesting early, and the use of grain cleaner and screens may also help to mitigate DON contamination. Field scouting for GER and grain sampling and testing for DON are important for harvest and post-harvest management decision-making, for evaluating the efficacy of fungicide treatments, and for largescale screening of hybrid for resistance in on-farm trials. However, relying on visual symptoms alone may lead to erroneous conclusions about DON contamination and incorrect management and marketing decisions. Asymptomatic grain may still have DON concentration higher than regulatory limits (Dalla Lana et al. 2021b). In addition, inadequate sampling may result in inaccurate estimates of field levels mean GER severity and DON contamination (Moraes et al. 2022), and consequently, erroneous conclusions about fungicide efficacy and hybrid resistance, unfair price discounts at the point of sale, or contaminated gran being commercialized. Forecasting models (Dalla Lana et al. 2021a) have been developed to compliment or as alternatives to field scouting to assess the risk of DON contamination, but testing and validation of these tools for accuracy also require adequate sampling.

Protocols and guidelines are available for sampling from grain trucks or wagons after harvest (FGIS-USDA 2023; Willyerd et al. 2016), but less is known about sampling

before or during harvest. Several methods can be used to sample corn fields to estimate grain contamination with DON, including hand-harvesting and shelling ears and pulling samples from the grain stream during harvest. Each of these methods have advantages and disadvantages. For instance, with hand-sampling prior to harvest, one may be better able to systematically collect ears from different locations of the field and adjust sampling frequency based on GER intensity or microclimatic conditions, and the resulting information would be useful for making grain harvest decisions. However, this process can be laborious and time-consuming. On the other hand, sampling from the grain stream during harvest may be quicker and easier than hand-sampling and result in samples being drawn from larger, more representative areas of the field, but the resulting information will be of no value for informing grain harvest decisions.

Given the advantages and disadvantages of hand- and combine-sampling listed above, research is needed to estimate the level of agreement between the two sampling methods at detecting the presence/absence of DON above critical thresholds and estimating mean DON contamination. Acceptable levels of agreements between the methods would suggest that either can be used to sample for DON contamination, whereas weak agreement may indicate that one method should be chosen other the other. The specific objectives of the study were to (1) determine the level of agreement in estimating mean DON contamination at the field level (measured in ppm) between hand and combine grain sampling methods and (2) determine the level of agreement between the methods in estimating mean DON above/below a 2-ppm threshold (binary response). To accomplish these objectives, fields across the state of Ohio were sampled using the two methods in each of three growing seasons (2021, 2022, and 2023). Concordance correlation coefficient

and Cohen's Kappa coefficient were used to determine the levels of agreement between the methods when estimating DON contamination as a continuous and binary response, respectively.

MATERIALS AND METHODS

Site selection and grain sampling. Twenty-six, twenty, and eleven corn fields across the state of Ohio were both hand- and combine-sampled during the 2021, 2022, and 2023 growing seasons, respectively. Fields were sampled in Crawford, Darke, Delaware, Holmes, Knox, Morrow, Pickaway, Putnam, Richland, Wayne, Williams, Madison, Licking, and Seneca counties, representing regions with different production practices, topographical features, and weather patterns (Table 2.1). Field locations in counties, grouped based by production regions, are shown on Fig. 2.1. Each field was planted and managed in ways determined by each producer, in many cases, following fertility and weed and pest management guidelines recommended in the Ohio Agronomic Guide (2017). The specific production practices and other metadata such as crop rotation, tillage, and fungicide treatment, planting date, and hybrid varied among fields (Table 2.1).

For sampling Method 1, *Hand-sampling*, nine transects (pairs of row sections) of approximately 12 meters long were established along an M-shape pattern across each commercial field for sampling (Fig. 2.2). A random sample of 10 ears were collected per transect, 5 from each row, giving a total of 90 ears per field. Whereas for sampling Method 2, *Combine-sampling*, three to twenty-four samples of approximately 110 to 450 grams of grain were pulled from the grain stream of the combine during harvest every 2 hectares or every 25,400 kg of grain. All ear and grain samples were collected in paper bags appropriately labelled with field and sample identification codes and GPS coordinates.

Combine samples were not collected from the same locations in the field where transects for hand-sampling were established. Additional field information (Table 2.1) and metadata were collected from growers.

Sample processing and deoxynivalenol analysis. Samples were shipped or transported to the laboratory and maintained on greenhouse benches with the paper bags open to allow grain/ear to dry to approximately 14-15% grain moisture. The husks were then removed from hand-harvested ears and GER severity was estimated with the aid of a standard area diagram as described (Dalla Lana et al. 2022). The incidence of insect damage (yes/no) was also recorded. Each ear was individually threshed using a Hand Field Corn Sheller (Model #50-CS; Decker Manufacturing Company, Keokuk, IA, U.S.A.), and the resulting grain from the 10 ears from a given transect were pooled in the initial paper bag to form a composite transect samples. This was done in 2021 and 2022. In 2023, the grain from each ear were kept in a separate paper bag as an individual ear sample.

Each grain sample was processed separately for mycotoxin analysis. Samples were first homogenized in a 5-gallon bucket before a subsample of approximately 60 g of grain was drawn and ground using a laboratory disc mill (Model LM3310; Perten Instruments Inc., Springfield, IL, U.S.A.) set to give the finest possible degree of grind. A subsample of approximately 60 grams of ground grain was collected in a Ziploc bag and shipped to the mycotoxin testing laboratory at the University of Minnesota for the mycotoxin deoxynivalenol (DON) analysis by gas chromatography-mass spectrometry (GC-MS). The limit of detection for DON was 0.05 ppm and samples below this limit were assumed to contain 0.025 ppm of the toxin.

Data analysis. Because we are interested in how accurate the two methods are in providing the same, or similar, estimates of DON contamination of grain, analyses of agreement were performed to account for the precision and accuracy of the estimates rather than simply quantifying the relationship between the methods through correlation analysis. Given the importance of identifying fields with DON contamination above established regulatory thresholds in a timely manner, the first set of analyses were performed to determine the agreement between the sampling methods in estimating the presence of DON above specific thresholds (binary responses; yes/no), in addition to estimating mean field level of contamination (ppm).

Agreement in estimating field-levels mean DON above a 2-ppm threshold. For each field and sampling method, data from individual samples (transects in the case of hand-sampling) were used to estimate field level mean DON contamination (ppm). Means estimated based on each sampling method were then converted to a binary response by coding those with DON less than 2 ppm as 0 and those with estimated means greater than or equal to 2 ppm as 1. Using the resulting dataset with pairs of 1s and 0s for each field, two-way contingency tables were developed using the FREQ procedure of SAS (SAS Institute, Cary, NC) showing the number of observations (fields in this case) in which the sampling methods agreed in the estimates of mean DON $\geq$ 2 ppm (number of fields coded 1 for both sampling methods) or < 2 ppm (number of fields coded 0 for both methods) or disagreed (number of coded 1 for one method and 0 for the other) in estimating mean DON above the 2 ppm threshold. The 2-ppm threshold was chosen because it is commonly used be grain buyers to make decisions about grain quality and prices.

Separate analyses were performed by year as well as on the data pooled across years. Observed agreement (P_o; equation 1), agreement by chance (P_e; equation 2), and Cohen's Kappa coefficient ($\hat{k}$; equation 3) (Cohen 1960) were estimated for using the *agree(kappadetails)* option in the *tables* statement of the FREQ procedure in SAS as:

$$P_o = \sum_i p_{ii} \tag{1}$$

$$P_e = \sum_i p_{i.} p_{.i} \tag{2}$$

$$\hat{k} = \frac{(P_o - P_e)}{(1 - P_e)} \tag{3}$$

where p_{ii} is the total probability of agreement in table cell (i, i), $p_{i.}$ is the estimate of the proportion in row i, and $p_{.i}$ is the estimate of the proportion in column i. Estimated *K* values range from -1 to 1, with values > 0.90 indicating almost perfect agreement, from 0.80 to 0.90 strong agreement, 0.60 to 0.79 moderate agreement, 0.40 to 0.59 weak agreement, and 0.39 to 0 indicating minimal to no agreement (McHugh 2012). A value of 0 indicates agreement by random chance and 1 indicates perfect agreement. The asymptomatic standard error (ASE) of, and 95% confidence intervals around, *K* were also estimated (Madden et al. 2007).

Agreement in estimating field-level mean DON contamination. Hand- and combine-samples within each field were considered subsamples and were averaged to obtain an estimated mean DON level per field (ppm). Agreement between sampling methods in estimating field-level mean DON (ppm) was determined using Lin's concordance correlation coefficient (equation 4a; Lin 1989) calculated as:

$$CCC = \frac{2\sigma_{ch}}{(\mu_c - \mu_h)^2 + \sigma_c^2 + \sigma_h^2} \tag{4a}$$

where σ_{ch} is the covariance between estimates for combine- and hand-sampling, μ_c and μ_h are the means and σ_c^2 and σ_h^2 the variances for combine- and hand-sampling,

respectively. In order to obtain estimates of precision and accuracy, equation 4a was rewritten as follows:

$$CCC = r.C_b \tag{4b}$$

where r is the Pearson's product-moment correlation coefficient for the relationship between estimated means for combine- and hand-sampling (parameter of precision; equation 5) and C_b is a bias estimate (parameter of accuracy; equation 6) calculated as:

$$r = \frac{\sum(x_i - \bar{x})(y_i - \bar{y})}{\sqrt{\sum(x_i - \bar{x})^2 \sum(y_i - \bar{y})^2}} \tag{5}$$

$$C_b = \frac{2}{v + \frac{1}{v} + (u)^2} \tag{6}$$

where v is the ratio of the variances of estimates from the two sampling methods (equation 6.1) and helps to determine the presence of scale shifts (the slope of the best fitting line of the data being different from the slope of the concordance line) and u is the difference in estimated mean DON between the sampling methods divided by the square root of the product of their standard deviations (equation 6.2); u indicates the presence of location shifts (when the intercept of the best fitting line of the data is different from the intercept of the concordance line).

$$v = \frac{\sigma_c}{\sigma_h} \tag{6.1}$$

$$u = \frac{\mu_c - \mu_h}{\sqrt{\sigma_c . \sigma_h}} \tag{6.2}$$

RESULTS

*Exploratory data analysis***.** A total of 26 commercial fields were both hand- and combine-sampled for DON in 2021, four each in Morrow and Wayne counties, three each in Crawford, Delaware, Holmes, Knox, and Putnam counties, two in Madison county and

one in Darke county (Fig. 2.1A). Fifteen of the sampled fields were tilled, 10 had corn surface residue (coverage ranging from 18 to 77%) and four were under continuous corn production. Planting dates ranged from April 18th to May 27th, with silking (R1 growth) dates from July 12th to August 4th. Eleven of the fields received a fungicide application either in-furrow at planting or between VT (tasseling) and R3 (milk) growth stages (Table 2.1). In 2022, fields were sampled in Crawford (2), Darke (1), Delaware (1), Holmes (2), Knox (3), Morrow (3), Pickaway (1), Putnam (1), Richland (1), Wayne (3), and Williams (2) counties (Fig. 2.1B). Ten of the 20 fields were tilled, nine had corn residue (coverage between 8 to 60%) and five were under continuous corn production. Planting dates in 2022 ranged from May 2nd to May 26th and R1 dates from July 27th to August 5th. Seven fields received a fungicide application either in-furrow at planting or between after VT (tasseling) and R1 (silking) growth stages (Table 2.1). Less information was available for the 11 fields sampled in 2023 (Table 2.1). Five were in Crawford County, three in Knox County, and one each in Licking, Morrow and Seneca counties (Fig. 2.1C). Seven were tilled, all were under crop rotation, and one was treated with a fungicide application.

Average across fields and samples, mean DON contamination (ppm) was higher in 2023 than in 2022 and 2021 (Fig. 2.3, Table 2.2). Field-level means ranged from 0.06 to 6.93 and 0.03 to 11 in 2021, from 0.08 to 10.4 and 0.04 to 17.64 in 2022, and from 1.66 to 24.04 and 0.5 to 21.24 in 2023 for combine- and hand-sampling, respectively (Table 2.3). Averaged across all sampled fields, mean DON was comparable between combine- and hand-sampling methods in 2021 (2.31 vs 2.80), higher for hand- than combine-sampling in 2022 (5.14 vs 3.80) and higher for combine- than hand-sampling in 2023 (7.40 vs 5.93) (Fig. 2.3, Table 2.3). Similar trends were observed for standard deviations, with values of

2.28, 5.6, 6.55 for hand-sampling and 2.31, 3.79, and 6.90 for combine-sampling in 2021, 2022, and 2023, respectively (Table 2.2). Pooled across years, hand-sampling had a slightly higher mean and standard deviation (4.22, SD 4.76) than combine-sampling (3.81, SD = 4.09). The 20th, 40th, 60th, and 80th percentiles were 0.80, 1.82, 3.52, and 6.60 for hand-sampling and 1.07, 1.92, 3.15, and 6.10 for combine-sampling (Table 2.2).

*Agreement in estimating mean DON contamination above 2 ppm***.** Mean DON contamination above 2 ppm was found in 50, 55, and 81% of the fields sampled with combine-sampling, and 61, 55, and 54% of those hand sampled, in 2021, 2022, and 2023 respectively. In 2021, 2022, and 2023, respectively, combine-sampling estimated that mean DON contamination was above the 2-ppm threshold in 10, 11, and 60% of the fields that were estimated by hand-sampling to have had mean DON below this threshold. Conversely, hand-sampling estimated mean DON above the threshold in 31, 11, and 0% of the fields that were estimated to have had mean DON below 2 ppm by combine-sampling. For the pooled data, both sampling methods estimated DON contamination to be above 2 ppm in 49% of the fields (Fig 2.4).

Observed agreement between sampling methodologies was 0.80, 0.90, and 0.72, with AC values of 0.50, 0.51, and 0.52 for 2021, 2022, and 2023 (Table 2.4). Following the interpretation of Kappa results from McHugh (2012), agreement in estimating DON above 2 ppm (*K*) was moderate for 2021 and 2022 (*K* = 0.61 and 0.79), weak in 2023 (*K* = 0.42), and moderate for the data pooled across years (K = 0.64). *K* values were significantly different from zero in 2021 and 2022 ($P < 0.05$) but not in 2023 ($P > 0.086$) (Table 2.4, Fig. 2.5). Upper and lower 95% confidence intervals around *K* were 0.32 to 0.91 (SE =

0.15) in 2021, 0.53 to 1 (SE = 0.13) in 2022, and -0.034 to 0.87 (SE = 0.23) in 2023 (Table 2.4, Fig. 2.5).

*Agreement in estimating mean field-level DON contamination***.** All summary statistics (means, variances, and standard deviations) varied among sampling method x year combinations (Table 2.5), leading to similar variations in *v*, *u*, *r* (Pearson's product moment correlation coefficient, which provides a measure of precision), and C_b (the bias coefficient, eq. 5), and by definition, estimates of *CCC* (concordance correlation coefficients, eq 4a and 4b). *CCC* was 0.48 in 2021, 0.55 in 2022 and 0.75 in 2023 (Table 2.5), indicating that the agreement in estimated field-level mean DON (ppm) contamination between combine- and hand-sampling was weak in 2021 and 2022 and moderate in 2023. The overall agreement based on the pooled data was also moderate (*CCC* = 0.67). Hand-sampling tended to lead to higher estimate of mean DON compared to combine-sampling generated estimates, particularly at relatively higher levels of contamination (Fig. 2.6D).

Less-then-perfect agreement (*CCC* < 1) could be attributed to imprecision, inaccuracy, or both. The slope and location of the best-fit relative to the line of concordance are indicators of accuracy and precision. The slopes of the best-fit lines were 0.66, 1.25, 0.73, and 0.80 with intercepts of 1.26, 0.40, 0.55, and 1.18 for 2021, 2022, 2023, and the pooled data, respectively (Fig. 2.6A-D). As indicated by the magnitude of the *r* values, precision was lowest in 2021 (*r* = 0.51) and highest in 2023 (*r* = 0.77). Estimated *r* was the same, 0.68, for 2022 and for the pooled data (Table 2.5). Only in 2022 was the best fitting line completely above the concordance line (Fig. 2.6B). For the other years and the pooled data, the lines intersected at 3.74 (2021), 2.00 (2023), and 5.83 (pooled data) (Fig. 2.6A, C, D).

Differences in means and variances between the combine- and hand-sampling methods resulted in C_b values that were less than 1 (i.e. the best fitting line of the data not identical to the concordance line). The ratios of the standard deviations, v, indicators of scale shift (i.e. slope of the best-fit line different from 1) and the standardized differences in the means, u, indicators of location shift (i.e. different in intercept between the best-fit line and the concordance line), the statistics used to estimate C_b (eq 6), ranged from 0.54 to 1.05 and from -0.32 to 0.21, respectively. Location and scale shifts can be seen in figure 6A-D. Non-zero u values and values of v different from 1 resulted in estimated C_b values that were less than 1, indicating bias in the estimated *CCC*. However, C_b values were still very high (0.93, 0.80, 0.97, and 0.98 for 2021, 2022, 2023, and the pooled data, respectively) indicating fairly high accuracy or relatively little bias in the estimated *CCC* (Table 2.5).

DISCUSSION

Increases in the natural occurrence of GER and associated DON contamination of grain in Ohio (Dalla Lana et al. 2021b), with potentially negative consequences for the maize, ethanol, and livestock industries (Kathibi et al. 2014), have become a cause for concern among stakeholders and researchers. One of the first steps to developing and evaluating disease management strategies is to establish sampling methods and protocols. This is particularly true for pathosystems such as *F. graminearum*-maize where visual assessments alone might not provide enough information for appropriate and timely decision-making. For instance, high variability in GER symptom expression across fields and disparity between visual symptoms and toxin contamination may lead to erroneous

conclusions about the level of DON contamination and the need for management intervention. In order to evaluate the efficacy of fungicides in on-farm trials, screen commercial hybrids for resistance, and validate forecasting systems, appropriate sampling methods are needed. Sampling is also important for postharvest grain handling, management, and marketing decision-making to avoid unfair price discounts, grain rejection, or the commercialization of highly contaminated grain. This has naturally led to question about which sampling methodology to rely on to accurately estimate DON contamination of grain in production fields. Here we quantified agreements between hand- and combine-sampling methods in estimating field-level mean DON contamination and contamination above a 2-ppm threshold.

Both sampling methods can be used before or during harvest. Among the advantages of sampling by hand (Figure 2.2), farmers have more time to obtain estimates of DON and make informed decisions before or during harvest to mitigate grain contamination (e.g. harvest early, change combine configurations to remove lightweight kernels that are usually heavily contaminated with DON, or grain cleaning and screening). However, the main drawbacks of this method are that it is time consuming, labor intensive, and in very large fields, may not result in samples that are representative. Combine-sampling would address these drawbacks by providing more homogenized and representative samples from large fields in less time by sampling grain at regular intervals from the grain stream. With combine-sampling, several rows are harvested at a time with natural mixing and homogenization of the grain without needing the assistance of additional people. However, the main limitation of combine-sampling is timing. Because it is performed at harvest, farmers would not be able to make informed harvest-related

decisions based on DON test results. However, DON estimates from combine sampling are still of value for making post-harvest grain cleaning and screening decision to remove fines and cob pieces that are usually more DON contaminated than the grain (Reid et al. 1996; Visconti et al. 1990). Although scientists and farmers can use either method to sample for DON in production fields, understanding their agreement, accurate, and precise would be valuable for choosing between the two methods.

Field-level mean DON contamination of grain varied among seasons and locations for both sampling methods, with the highest mean levels and field-to-field variability of the toxin in 2023. Differences in baselines DON contamination between years could be attributed, at least in part, to differences in production practices. For instance, in 2023 only one of the 11 sampled fields was treated with a fungicide, compared to 12 of 26 in 2021 and 7 of 20 in 2022. There is some evidence, both anecdotal and research-based, that some of the fungicides applied to the fields in this study do contribute to DON reduction, albeit with highly variable levels of efficacy, particularly when applied at the R1 growth state as was the case in several of the treated fields (Anderson et al. 2017; Andriolli et al. 2016; Eli et al. 2021). Other possible contributors to variations in mean DON contamination among growing seasons and fields within seasons were differences in crop rotation, tillage practices, surface residue cover, in-field weather condition, and hybrid reactions. Although we were unable to gather information on the susceptibility and resistance of the hybrids used on each farm, resistance likely played a role in the variability because hybrids are known to vary in their reaction to DON contamination (Dalla Lana et al. 2022). Despite the similarity in mean temperature and relative humidity among seasons and locations, weather likely also contributed to differences in mean DON among fields by virtue of its

interactions with other factors such as surface residue cover, tillage, crop rotation, and hybrid resistance. Regardless of the reasons for the DON variability among field, the wide range of baseline DON levels was important for us to evaluate and compare sampling methods.

Given the importance of regulatory advisory DON limits for the commercialization of grain (FDA 2010), and since the use of these limits tend to vary among grain buyers as a function of the supply and demand of DON-free grain and grain market prices, we used an established and standard threshold of 2 ppm to assess agreement between the two sampling methods evaluated in this study based on Cohen's kappa coefficient (*K*; Cohen 1960). Only during the 2023 growing season was *K* not significantly different from zero ($P > 0.08$), with a weak agreement between the sampling methods ($K = 0.42$). This could have been due to the considerably smaller sample size in 2023 ($n = 11$) compared to 2021 and 2022, and consequently, lower precision in the estimate of *K*, as evidenced by the relatively large standard error (SE = 0.23) and wide confidence interval that included zero (lower limit of the CI = -0.03 and upper limit = 0.87). Some argue that a sample size of at least 30 observations is necessary to reduce the CI and increase precision (McHugh 2012; Ross 2017). In 2021 and 2022, the sample sizes were larger than in 2023, likely contributing, at least in part, to the higher and more precisely estimated *K* values ($K = 62$ [SE = 0.15] and 0.80 [SE = 0.14]) in those two years. Based on results from 2021, 2022, and the pooled data, and interpretations of the *K* values suggested by McHugh (2012), agreement was moderate between combine- and hand-sampling for identifying fields with mean DON contamination above 2 ppm. McHugh (2012) suggested that researchers might also consider using observed agreement (OA, also known as percent agreement) as a better

measure of agreement when there is no potential sampling bias. If we consider that bias was indeed low in our sampling, agreement between the two sampling methods would be considered moderate to strong based on OA values ranging from 0.72 to 0.90.

To gain an understanding on the precision and accuracy of hand- and combine-sampling, we measured their agreement in estimating field-level mean DON contamination based on Lin's concordance correlation coefficient (*CCC*; Lin 1989). In theory, *CCC* is used to compare a 'gold standard' with a new method or technique. However, since there is no true gold standard protocol for sampling commercial maize fields for mycotoxins, we used combine-sampling as our gold standard based on the assumption that it is quicker and easier, and likely generates more representative and homogenized samples than hand-sampling. *CCC* was higher in 2023 (0.75) than in 2021 (0.48) and 2022 (0.55), indicating that the agreement between the two sampling methods was weak to moderate. In order to obtain perfect agreement (*CCC* = 1), both the precision estimate (r) and accuracy coefficient (C_b) would have to be equal to one. Since C_b values were close to 1 (ranging from 0.80 to 0.98), less-then-perfect agreement between the sampling methods were more likely due to the low precision ($r < 1$), particularly in 2021 ($r = 0.51$ in 2021, 0.68 in 2022, and 0.77 in 2023). This can be explained mathematically by the high standard deviations for the sampling methods, particularly hand-sampling in 2021 and 2022, which increased the denominator in equation 5, leading to relatively low r. In addition, the covariance between the methods likely affected r. Although the covariances were all positive, values were considerably lower in 2021 (COV = 2.04) and 2022 (COV = 11.84) than in 2023 (COV = 34.64).

Less-than-perfect agreement between sampling methods due to low precision could be attributed to spatial heterogeneity in *F. graminearum* spore density, ear development and infection, GER intensity, and consequently, DON contamination of grain. Although both hand- and combine-sampling were done in the same fields, the specific locations of the line transects hand-sampled likely did not coincide with the two-hectare areas from which the combine samples were pulled, leading to differences in estimated plot-level mean DON between the two methods. Little specific information is available on the spatial patterns of DON in commercial maize fields, but work done on the spatial deposition of *F. graminearum* spore in corn and wheat fields (Del Ponte et al. 2003; Oerke et al. 2010; Schmale III et al. 2005a, b) would be useful for gaining insights into possible spatial heterogeneity of GER/DON in maize fields. Schmale III et al. (2005a) indicated that the deposition patterns of *F. graminearum* spores on maize silks and tassel where randomly in 92% of the fields sampled and aggregated in only 8%. Comparable results were reported from a similar study by the same team of researchers in wheat fields (Schmale III et al. 2005b). Del Ponte et al. (2003) also reported random patterns of FHB in 64 fields and a strong aggregation pattern in only 3 of the tested fields. However, none of the fields in the research conducted by Schmale III et al. (2005a, b) had crop residue, and the few fields in the studies by Del Ponte et al. (2003) that had corn residue, all showed aggregated patterns of spore deposition and infection. Oerke et al. (2010) also found one out of four fields with aggregated patterns of *F. graminearum* infection.

Random and aggregated patterns of *F. graminearum* spore deposition and infection likely led of random and aggregated patterns of infection, disease development and grain contamination with DON in our study. Of the fields sampled, 42% (2021), 30% (2022),

and 27% (2023) were no-till, with crop residue on the soil surface, serving an overwinter source of the pathogen (Broders et al. 2007; Sutton 1982). Reasons for the apparent association between in-field crop residue and the spatial heterogeneity of GER/DON is unknow, but could be due to variations in the amount of residue cover, associated weather conditions (moisture in particular), and consequently, spore production. With different microenvironmental conditions among field as well as the adoption of reduced- or no-till practices that favor the survival of *F. graminearum*, the hypothesis of high within-field variability in *F. graminearum* infection, GER development, and DON contamination following an aggregated distribution patterns in fields with crop residue needs to be tested in future research.

In conclusion, the fact that the agreement between the two sampling methods was moderate to strong in detecting fields with DON contamination above the 2-ppm threshold, based on observed agreement, suggests that farmers might be able to use either method if they are not interested in the actual level of contamination, but only in whether contamination exceeds the limit of 2 ppm. Agreements in estimating the actual level of DON contamination (*CCC*) between the two sampling methods were weak to moderate. As discussed above, this was likely due to high within-field variability in DON contamination, given that accuracy (C_b) was high, but precision (r) was low. Chapter 3 of this thesis focuses on characterizing the heterogeneity of DON contamination at different spatial scales to determine where DON is most variable as a guide for increasing the precision in field-level estimates of contamination by increasing sample size. Increasing precision will likely lead to stronger agreements between the hand-and combine-sampling methods.

REFERENCES

Anderson, N. R., Romero Luna, M. P., Ravellette, J. D., and Wise, K. A. 2017. Impact of foliar fungicides on Gibberella ear rot and deoxynivalenol levels in Indiana Corn. Plant Health Progress 18:186–191.

Andriolli, C. F., Casa, R. T., Kuhnem, P. R., Bogo, A., Zancan, R. L., and Reis, E. M. 2016. Timing of fungicide application for the control of Gibberella ear rot of maize. Trop. Plant Pathol. 41:264–269.

Broders, K. D., Lipps, P. E., Paul, P. A., and Dorrance, A. E. 2007. Evaluation of *Fusarium graminearum* associated with corn and soybean seed and seedling disease in Ohio. Plant Dis. 91:1155–1160.

Burlakoti, R. R., Neate, S. M., Adhikari, T. B., Gyawali, S., Salas, B., Steffenson, B. J., and Schwarz, P. B. 2011. Trichothecene profiling and population genetic analysis of *Gibberella zeae* from barley in North Dakota and Minnesota. Phytopathology 101:687–695.

Cohen, J. 1960. A coefficient of agreement for nominal scales. Educ. Psychol. Meas. 20:37–46.

Dalla Lana, F., Madden, L. V., and Paul, P. A. 2021a. Logistic models derived via lasso methods for quantifying the risk of natural contamination of maize grain with deoxynivalenol. Phytopathology 111:2250–2267.

Dalla Lana, F., Madden, L. V., and Paul, P. A. 2021b. Natural occurrence of maize Gibberella ear rot and contamination of grain with mycotoxins in association with weather variables. Plant Dis. 105:114–126.

Del Ponte, E. M., Shah, D. A., and Bergstrom, G. C. 2003. Spatial patterns of Fusarium head blight in New York wheat fields suggest role of airborne inoculum. Plant Health Progress 4:6.

Edite Bezerra da Rocha, M., Freire, F. da C. O., Erlan Feitosa Maia, F., Izabel Florindo Guedes, M., and Rondina, D. 2014. Mycotoxins and their effects on human and animal health. Food Control 36:159–165.

Eli, K., Schaafsma, A. W., Limay-Rios, V., and Hooker, D. C. 2021. Effect of pydiflumetofen on Gibberella ear rot and *Fusarium* mycotoxin accumulation in maize grain. World Mycotoxin J. 14:495–512.

Enerson, P. M., and Hunter, R. B. 1980. Response of maize hybrids to artificially inoculated ear mold incited by *Gibberella zeae*. Can. J. Plant Sci. 60:1463–1465.

Federal Grain Inspection Service-United States Department of Agriculture. 2016. Inspecting grain: practical procedures for grain handlers. Available: https://www.ams.usda.gov/sites/default/files/media/PracticalProceduresBook2017.pdf

U.S. Food and Drug Administration. 2010. Guidance for industry and FDA: advisory levels for deoxynivalenol (don) in finished wheat products for human consumption and grains and grain by-products used for animal feed. Available: https://www.fda.gov/regulatory-information/search-fda-guidance-documents/guidanceindustry-and-fda-advisory-levels-deoxynivalenol-don-finished-wheat-products-human.

Foroud, N. A., and Eudes, F. 2009. Trichothecenes in cereal grains. Int. J. Mol. Sci. 10:147–173.

Hesseltine, C. W., and Bothast, R. J. 1977. Mold development in ears of corn from tasseling to harvest. Mycologia 69:328–340.

Iram, A., Cekmecelioglu, D., and Demirci, A. 2020. Distillers' dried grains with solubles (DDGS) and its potential as fermentation feedstock. Appl. Microbiol. Biotechnol. 104:6115–6128.

Khatibi, P. A., McMaster, N. J., Musser, R., and Iii, D. G. S. 2014. Survey of mycotoxins in corn distillers' dried grains with solubles from seventy-eight ethanol plants in twelve states in the U.S. In 2011. Toxins 6:1155–1168.

Lana, F. D., Madden, L. V., Carvalho, C. P., and Paul, P. A. 2022. Impact of Gibberella ear rot on grain quality and yield components in maize as influenced by hybrid reaction. Plant Dis. 106:3061–3075.

Lana, F. D., Paul, P. A., Minyo, R., Thomison, P., and Madden, L. V. 2020. Stability of hybrid maize reaction to Gibberella ear rot and deoxynivalenol contamination of grain. Phytopathology 110:1908–1922.

Lin, L. I.-K. 1989. A concordance correlation coefficient to evaluate reproducibility. Biometrics 45:255–268.

Madden, L. V., Hughes, G., and Van Den Bosch, F. 2007. The Study of Plant Disease Epidemics. American Phytopathological Society, St. Paul, MN.

Magarini, A., Passera, A., Ghidoli, M., Casati, P., and Pilu, R. 2023. Genetics and environmental factors associated with resistance to *Fusarium graminearum*, the causal agent of Gibberella ear rot in maize. Agronomy 13:1836.

McHugh, M. L. 2012. Interrater reliability: the kappa statistic. Biochem. Med. 22:276–282.

Moraes, W. B., Madden, L. V., and Paul, P. A. 2022. Characterizing heterogeneity and determining sample sizes for accurately estimating wheat Fusarium head blight index in research plots. Phytopathology 112:315–334.

Morrison, J. E., Huang, C. H., Lightle, D. T., and Daughtry, C. S. 1993. Residue measurement techniques. J. Soil Water Conserv. 48:478-483.

Mueller, D. S., Wise, K. A., Sisson, A. J., Allen, T. W., Bergstrom, G. C., Bissonnette, K. M., Bradley, C. A., Byamukama, E., Chilvers, M. I., Collins, A. A., Esker, P. D., Faske, T. R., Friskop, A. J., Hagan, A. K., Heiniger, R. W., Hollier, C. A., Isakeit, T., Jackson-Ziems, T. A., Jardine, D. J., Kelly, H. M., Kleczewski, N. M., Koehler, A. M., Koenning, S. R., Malvick, D. K., Mehl, H. L., Meyer, R. F., Paul, P. A., Peltier, A. J., Price, P. P., Robertson, A. E., Roth, G. W., Sikora, E. J., Smith, D. L., Tande, C. A., Telenko, D. E. P., Tenuta, A. U., Thiessen, L. D., and Wiebold, W. J. 2020. Corn yield loss estimates due to diseases in the United States and Ontario, Canada, from 2016 to 2019. Plant Health Progress 21:238–247.

Munkvold, G. P. 2003. Epidemiology of *Fusarium* diseases and their mycotoxins in maize ears. Eur. J. Plant Pathol. 109:705–713.

Oerke, E.-C., Meier, A., Dehne, H.-W., Sulyok, M., Krska, R., and Steiner, U. 2010. Spatial variability of Fusarium head blight pathogens and associated mycotoxins in wheat crops. Plant Pathol. 59:671–682.

Pestka, J. J. 2010. Deoxynivalenol: mechanisms of action, human exposure, and toxicological relevance. Arch. Toxicol. 84:663–679.

Puri, K. D., and Zhong, S. 2010. The 3ADON population of *Fusarium graminearum* found in North Dakota is more aggressive and produces a higher level of DON than the prevalent 15ADON population in spring wheat. Phytopathology 100:1007–1014.

Reid, L. M., Zhu, X., and Ma, B. L. 2001. Crop rotation and nitrogen effects on maize susceptibility to Gibberella (*Fusarium graminearum*) ear rot. Plant Soil 237:1–14.

Reid, L. M., Mather, D. E., and Hamilton, R. I. 1996. Distribution of deoxynivalenol in *Fusarium graminearum*-infected maize ears. Phytopathology 86: 110-114.

Ross, S. M. 2017. Introductory Statistics. Fourth edition ed. Academic Press, Burlington, MA.

Schaafsma, A. W., Limay-Rios, V., Paul, D. E., and Miller, J. D. 2009. Mycotoxins in fuel ethanol co-products derived from maize: a mass balance for deoxynivalenol. J. Sci. Food Agric. 89:1574–1580.

Schmale, D. G., Bergstrom, G. C., and Shah, D. A. 2005a. Spatial patterns of viable spore deposition of the corn ear rot pathogen, *Gibberella zeae*, in first-year corn fields. Can.J. Plant Pathol. 27:225–233.

Schmale, D. G., Shah, D. A., and Bergstrom, G. C. 2005b. Spatial patterns of viable spore deposition of *Gibberella zeae* in wheat fields. Phytopathology 95:472–479.

Sutton, J. C. 1982. Epidemiology of wheat head blight and maize ear rot caused by *Fusarium graminearum*. Can. J. Plant Pathol. 4:195–209.

Sutton, J. C., and Baliko, W. 1981. Methods for quantifying partial resistance to *Gibberella zeae* in maize ears. Can. J. Plant Pathol. 3:26–32.

Vesonder, R. F., Ciegler, A., Jensen, A. H., Rohwedder, W. K., and Weisleder, D. 1976. Co-identity of the refusal and emetic principle from *Fusarium*-infected corn. Appl. Environ. Microbiol. 31:280–285.

Vigier, B., Reid, L. M., Dwyer, L. M., Stewart, D. W., Sinha, R. C., Arnason, J. T., and Butler, G. 2001. Maize resistance to Gibberella ear rot: symptoms, deoxynivalenol, and yield1. Can. J. Plant Pathol. 23:99–105.

Visconti, A., Chelkowski, J., Solfrizzo, M., and Bottalico, A. 1990. Mycotoxins in corn ears naturally infected with *Fusarium graminearum* and *F. crookwellense*. Can. J. Plant Pathol. 12:187–189.

Ward, T. J., Clear, R. M., Rooney, A. P., O'Donnell, K., Gaba, D., Patrick, S., Starkey, D. E., Gilbert, J., Geiser, D. M., and Nowicki, T. W. 2008. An adaptive evolutionary shift in Fusarium head blight pathogen populations is driving the rapid spread of more toxigenic *Fusarium graminearum* in North America. Fungal Genet. Biol. 45:473–484.

Willyerd, K. T., Thomison, P., and Paul, P. A. 2016. Gibberella ear rot and mycotoxins in corn: sampling, testing, and storage. Ohio State Univ. Extension. Available: https://ohioline.osu.edu/factsheet/plpath-cer-04

Wu, F., Groopman, J. D., and Pestka, J. J. 2014. Public health impacts of foodborne mycotoxins. Annu. Rev. Food Sci. Technol. 5:351–372.

Table 2.1. Agricultural practices, field characteristics, crop development stages, and number of samples collected per field in 2021, 2022, and 2023.

Field[a]	Residue[b]	PreviousCrop	Tillage	Planting date	Maturity[c]	R1[d]	Fungicide application		Combine	Hand[f]
							Product	GS[e]		
					2021					
Crawford_1	78	Corn	Yes	5/19/21	107	7/28/21	Headline Amp	R2-R3	8	9
Crawford_4	31	Corn	Yes	5/5/21	107	7/28/21	Miravis Neo	R1	5	9
Crawford_5	0	Wheat	Yes	5/26/21	109	7/28/21	No	No	4	8
Darke_2	29	Corn	Yes	4/28/21	110	7/12/21	No	No	20	9
Delaware_1	50	Soybean	No	5/15/21	111	7/21/21	Veltyma	R2	17	9
Delaware_2	0	Wheat	Yes	4/27/21	112	7/21/21	Xyway	Planting	9	9
Delaware_3	0	Wheat	Yes	4/26/21	112	7/21/21	Headline	R2	20	9
Holmes_2	0	Soybean	Yes	5/21/21	107	7/19/21	No	No	6	9
Holmes_3	0	Wheat	No	5/18/21	111	7/19/21	No	No	11	9
Holmes_4	0	Wheat	No	4/26/21	111	7/19/21	No	No	20	9
Knox_1	18	Soybean	Yes	4/26/21	108	7/21/21	No	No	20	9
Knox_2	0	Soybean	Yes	5/27/21	111	8/4/21	Zolera	VT	20	9
Knox_3	77	Soybean	No	4/25/21	115	7/21/21	No	No	20	9
Madison_1	56	Soybean	No	5/24/21	108	7/23/21	Headline Amp	R1	19	9
Madison_2	35	Soybean	No	4/18/21	112	7/23/21	Quilt Xcel	R2	20	9
Morrow_1	0	Soybean	Yes	5/24/21	105	8/4/21	No	No	11	9
Morrow_2	0	Soybean	No	4/27/21	104	7/21/21	No	No	4	9
Morrow_3	0	Soybean	No	5/18/21	103	7/21/21	Miravis Neo	R1	22	9
Morrow_4	70	Wheat	No	4/28/21	109	7/21/21	Zolera	R1	20	9
Putnam_1	0	Wheat	No	5/19/21	111	7/30/21	Aproach Prima	R1	7	9
Putnam_2	0	Soybean	Yes	5/19/21	108	7/30/21	No	No	14	9
Putnam_3	0	Tomato	Yes	5/17/21	107	7/30/21	Miravis Neo	…[g]	9	9
Wayne_1	0	Soybean	Yes	4/28/21	105	7/19/21	No	No	9	9
Wayne_2	45	Corn	Yes	5/14/21	105	7/19/21	No	No	18	9
Wayne_3	0	Wheat	No	5/20/21	104	7/19/21	No	No	4	9
Wayne_4	0	Clover	Yes	5/19/21	108	7/19/21	No	No	6	9

Table 2.1. Continued

Field[a]	Residue[b]	PreviousCrop	Tillage	Planting date	Maturity[c]	R1[d]	Fungicide application		Combine	Hand[f]
							Product	GS[e]		
					2022					
Crawford_4	11	Corn	Yes	5/14/22	107	7/25/22	Miravis Neo	R1	4	9
Crawford_5	31	…	…	…	…	7/25/22	No	No	24	9
Darke_3	0	Wheat	Yes	5/24/22	…	7/27/22	No	No	4	12
Delaware_1	33	Soybean	No	5/12/22	114	7/29/22	Aproach Prima	R1	13	9
Holmes_2	8	Corn	Yes	5/23/22	110	8/5/22	No	No	5	9
Holmes_3	0	Soybean	No	5/14/22	101	7/22/22	Xyway	Planting	15	9
Knox_1	38	Corn	Yes	5/2/22	103	7/29/22	No	No	20	9
Knox_2	0	Soybean	No	5/19/22	…	7/29/22	No	No	20	9
Knox_3	0	Soybean	Yes	5/17/22	113	7/29/22	Trivapro	R1	20	9
Morrow_1	0	Soybean	Yes	5/13/22	110	7/29/22	No	No	9	9
Morrow_2	14	Soybean	Yes	5/19/22	101	7/29/22	No	No	3	9
Morrow_3	0	Wheat	No	5/13/22	111	7/29/22	Brixen	VT	20	9
Richland_2	...	...	...	...	...	...	...	...	2	9
Pickaway_2	0	…	…	…	…	7/20/22	No	No	14	9
Putnam_3	0	…	…	…	…	7/21/22	...	...	3	9
Wayne_1	0	Soybean	Yes	5/26/22	105	8/4/22	No	No	6	9
Wayne_2	36	Corn	Yes	5/11/22	109	7/22/22	No	No	20	9
Wayne_3	0	Wheat	No	5/12/22	112	7/22/22	Xyway	Planting	3	9
Williams_1	60	Soybean	No	5/11/22	104	7/21/22	No	No	6	9
Williams_3	0	Corn	Yes	5/17/22	109	8/3/22	Aproach Prima	R1	20	9
					2023					
Crawford_1	…	...	...	...	...	...	No	No	3	90
Crawford_2	...	Wheat	Yes	5/12/23	...	...	No	No	8	90
Crawford_3	...	Cover crop	Yes	5/17/23	...	...	Miravis neo	...	10	90
Crawford_4	...	Wheat	Yes	5/12/23	...	...	No	No	9	90
Crawford_5	...	Wheat	Yes	5/12/23	...	...	No	No	10	90
Knox_1	...	Soybeans	Yes	5/20/23	...	...	No	No	10	90

Continued

Table 2.1. Continued

Field[a]	Residue[b]	PreviousCrop	Tillage	Planting date	Maturity[c]	R1[d]	Fungicide application		Combine	Hand[f]
							Product	GS[e]		
					2023					
Knox_2	...	Soybeans	No	5/20/23	...	...	No	No	10	90
Knox_3	...	Soybeans	No	5/16/23	...	...	No	No	10	90
Lickng_1	...	Soybeans	Yes	5/18/23	...	...	No	No	10	90
Morrow_1	...	Soybean	No	5/25/23	...	...	No	No	5	90
Seneca_1	...	Wheat	Yes	5/12/23	...	...	No	No	5	90

[a]Fields combine- and hand-sampled for deoxynivalenol (DON), coded with name of the name of the County in which the field was located and a number indicating the specific field sampled in that county, [b]percent corn surface residue cover measured using the line-transect method (Morrison et al. 1993), [c]hybrid relative maturity in number days to physiological maturity, [d]silking date (R1 growth stage), [e]growth stage (GS) when fungicide was applied, [f]2021 and 2022, number of transects from each of which 10 ears were hand-harvested, and in 2023, the total number of ears samples (10 ears from the 9 transects) and individually sent for DON analysis instead of being pooling as in 2021 and 2022, and [g]Ellipses indicate information not provided.

Table 2.2. Summary statistics for deoxynivalenol contamination of maize grain (ppm) across fields hand- and combine-sampled in Ohio by growing field season and pooled across seasons.

	Combine				Hand			
Statistic[a]	2021	2022	2023	All[b]	2021	2022	2023	All
N	343	231	84	658	233	183	989	1,405
Mean	2.31	3.8	7.40	3.81	2.80	5.14	5.93	4.22
SD	1.75	3.08	6.91	4.08	2.28	5.66	6.55	4.76
Variance	3.07	9.49	47.75	16.69	5.22	31.99	43.00	22.68
Median	1.99	3.29	6.45	2.63	2.55	3.44	2.48	2.68
P20	0.69	0.74	2.14	1.07	1.26	0.42	1.30	0.81
P40	1.39	1.73	2.5	1.92	2.19	1.61	1.82	1.82
P60	2.72	5.25	7.42	3.15	2.99	4.64	4.28	3.52
P80	3.50	6.50	11.66	6.10	3.75	9.76	10.40	6.60

[a]N = Total number of samples (samples x field) tested for deoxynivalenol, SD = standard deviation, P20 = 20th percentile, P40 = 40th percentile, P60 = 60th percentile, P80 = 80th percentile, and [b]All = data from 2021, 2022, and 2023 pooled.

Table 2.3. Estimated mean DON (ppm) contamination of maize grain by field for samples collected using the combine- and hand-sampling methods in Ohio in 2021, 2022, and 2023.

		DON (ppm)[b]		DON (binary)[c]	
Year	Field[a]	Combine	Hand	Combine	Hand
2021	Crawford_1	0.69	1.27	0	0
	Crawford_4	1.24	1.68	0	0
	Crawford_5	1.28	1.26	0	0
	Darke_2	0.27	1.38	0	0
	Delaware_1	0.66	0.54	0	0
	Delaware_2	5.47	3.81	1	1
	Delaware_3	6.93	3.66	1	1
	Holmes_2	3.50	6.60	1	1
	Holmes_3	5.21	3.75	1	1
	Holmes_4	1.39	3.68	0	1
	Knox_1	1.08	2.27	0	1
	Knox_2	2.01	0.91	1	0
	Knox_3	3.15	4.24	1	1
	Madison_1	2.94	2.42	1	1
	Madison_2	3.73	3.34	1	1
	Morrow_1	1.96	2.19	0	1
	Morrow_2	2.63	2.99	1	1
	Morrow_3	0.92	0.79	0	0
	Morrow_4	2.72	11.00	1	1
	Putnam_1	0.62	0.03	0	0
	Putnam_2	0.06	1.31	0	0
	Putnam_3	0.11	0.04	0	0
	Wayne_1	3.14	4.73	1	1
	Wayne_2	1.90	2.68	0	1
	Wayne_3	3.83	2.82	1	1
	Wayne_4	2.75	3.29	1	1
2022	Crawford_4	7.28	3.35	1	1
	Crawford_5	3.77	5.54	1	1
	Darke_3	1.58	0.81	0	0
	Delaware_1	2.80	0.32	1	0
	Holmes_2	0.21	0.41	0	0
	Holmes_3	5.19	7.31	1	1
	Knox_1	1.26	0.42	0	0
	Knox_2	6.10	7.19	1	1
	Knox_3	10.4	17.64	1	1
	Morrow_1	5.31	5.7	1	1
	Morrow_2	5.77	3.52	1	1
	Morrow_3	1.07	14.97	0	1
	Richland_2	6.9	12.2	1	1
	Pickaway_2	0.30	0.04	0	0

Continued

Table 2.3. Continued

		DON (ppm)[b]		DON (binary)[c]	
Year	Field[a]	Combine	Hand	Combine	Hand
2022	Putnam_3	0.08	0.57	0	0
	Wayne_1	8.03	15.48	1	1
	Wayne_2	1.88	1.87	0	0
	Wayne_3	6.00	3.74	1	1
	Williams_1	1.58	0.41	0	0
	Williams_3	0.42	1.36	0	0
2023	Crawford_1	2.50	1.30	1	0
	Crawford_2	11.66	10.40	1	1
	Crawford_3	2.20	2.48	1	1
	Crawford_4	13.70	21.24	1	1
	Crawford_5	24.04	12.36	1	1
	Know_1	1.66	0.81	0	0
	Knox_2	2.14	0.51	1	0
	Knox_3	6.45	1.55	1	0
	Licking_1	7.77	4.28	1	1
	Morrow_1	1.92	1.82	0	0
	Seneca_1	7.42	8.50	1	1

[a] Fields combine- and hand-sampled for DON, coded with name of the County in which the field was located and a number indicating the specific field sampled in that county, [b]results from combine- and hand-harvested grain averaged across samples to obtain an estimate of field-level mean DON that was used for agreement analysis, and [c]code assigned to fields with 1 indicating field-level mean DON grain contamination ≥ 2 ppm and 0 contamination below 2 ppm.

Table 2.4. Cohen's Kappa (K) coefficients with corresponding statistics used to measure agreement between combine- and hand-sampling methods in detecting commercial maize fields in Ohio with mean DON contamination of grain above or below a 2-ppm threshold during the 2021, 2022, and 2023 growing seasons and pooled across seasons.

Statistics[a]	2021	2022	2023	Pooled data
OA	0.81	0.90	0.73	0.82
AC	0.50	0.51	0.53	0.51
K	0.62	0.80	0.42	0.64
SE	0.15	0.14	0.23	0.10
CL_L	0.32	0.53	-0.03	0.44
CL_U	0.91	1.00	0.88	0.84
Z	3.22	3.57	1.71	4.83
P > |Z|	0.001	< 0.001	0.087*	<0.001

[a] OA = observed agreement; AC = agreement by chance; *K* = Cohen's Kappa coefficient (1 = perfect agreement; 0 = agreement by random chance); SE = standard error; CL_L = lower limit of 95% confidence interval; CL_U = upper limit of 95% confidence interval; Z = test statistic of the null hypothesis (*K* = 0); P > |Z| = level of significance, and * indicates not significant at *P* < 0.05

Table 2.5. Concordance correlation coefficients (CCC) and corresponding statistics used to measure agreement between combine- and hand-sampling methods in estimating field-level mean DON contamination (ppm) in commercial maize fields in Ohio during the 2021, 2022, and 2023 growing seasons and pooled across seasons.

	2021		2022		2023		Pooled data	
Statistic[a]	Combine	Hand	Combine	Hand	Combine	Hand	Combine	Hand
Mean	2.31	2.79	3.79	5.15	7.40	5.93	3.81	4.22
Variance	3.08	5.23	9.5	31.9	47.69	42.98	16.69	22.68
SD	1.76	2.29	3.08	5.64	6.9	6.55	4.09	4.76
Covariance	2.04		11.84		34.64		13.32	
r	0.51		0.68		0.77		0.68	
v	0.77		0.54		1.05		0.86	
u	-0.23		-0.32		0.21		-0.02	
C_b	0.94		0.80		0.98		0.98	
CCC	0.48		0.55		0.75		0.68	

[a] *r* = Pearson product moment correlation coefficient (a measure of precision), SD = standard deviation, *v* = variance ratio from equation 6 (used as a measure of scale shift from the concordance line), *u* = difference of means from equation 6 (used as a measure a location shift from the concordance line), C_b = Bias coefficient (a measure of accuracy), *CCC* = Concordance correlation coefficient (1 = perfect agreement; 0 = no agreement)

Table 2.6. Average air temperature and relative humidity, and total rainfall during the 2021, 2022, and 2023 growing seasons collected from CFAES weather stations located in five Ohio Counties.

	Wayne			Franklin			Wood			Clark			Huron		
Variable[a]	2021	2022	2023	2021	2022	2023	2021	2022	2023	2021	2022	2023	2021	2022	2023
T	17	17	16	19	18	18	18	18	17	18	18	17	18	17	11
RH	79	77	75	73	70	70	78	75	76	79	76	76	78	74	63
Rain	597	681	429	521	706	478	648	610	508	559	546	389	747	427	478

[a]T = daily average air temperature (°C), RH = daily average relative humidity (%), and Rain = total rainfall (mm) for the period from April 19 to November 19.

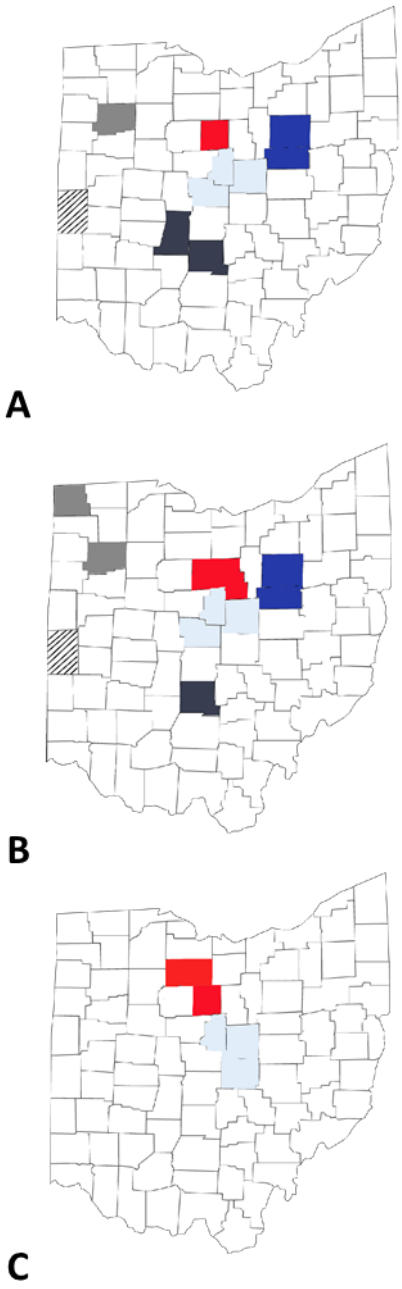

Fig. 2.1. Map of Ohio showing counties from which corn fields were sampled in 2021 (**A**), 2022 (**B**) and 2023 (**C**). Colors/pattern represent production regions: Gray = Region 1, Red = Region 2, Blue = Region 3, Pale-blue = Region 4, Dark gray = Region 5, and White with lines = Region 6.

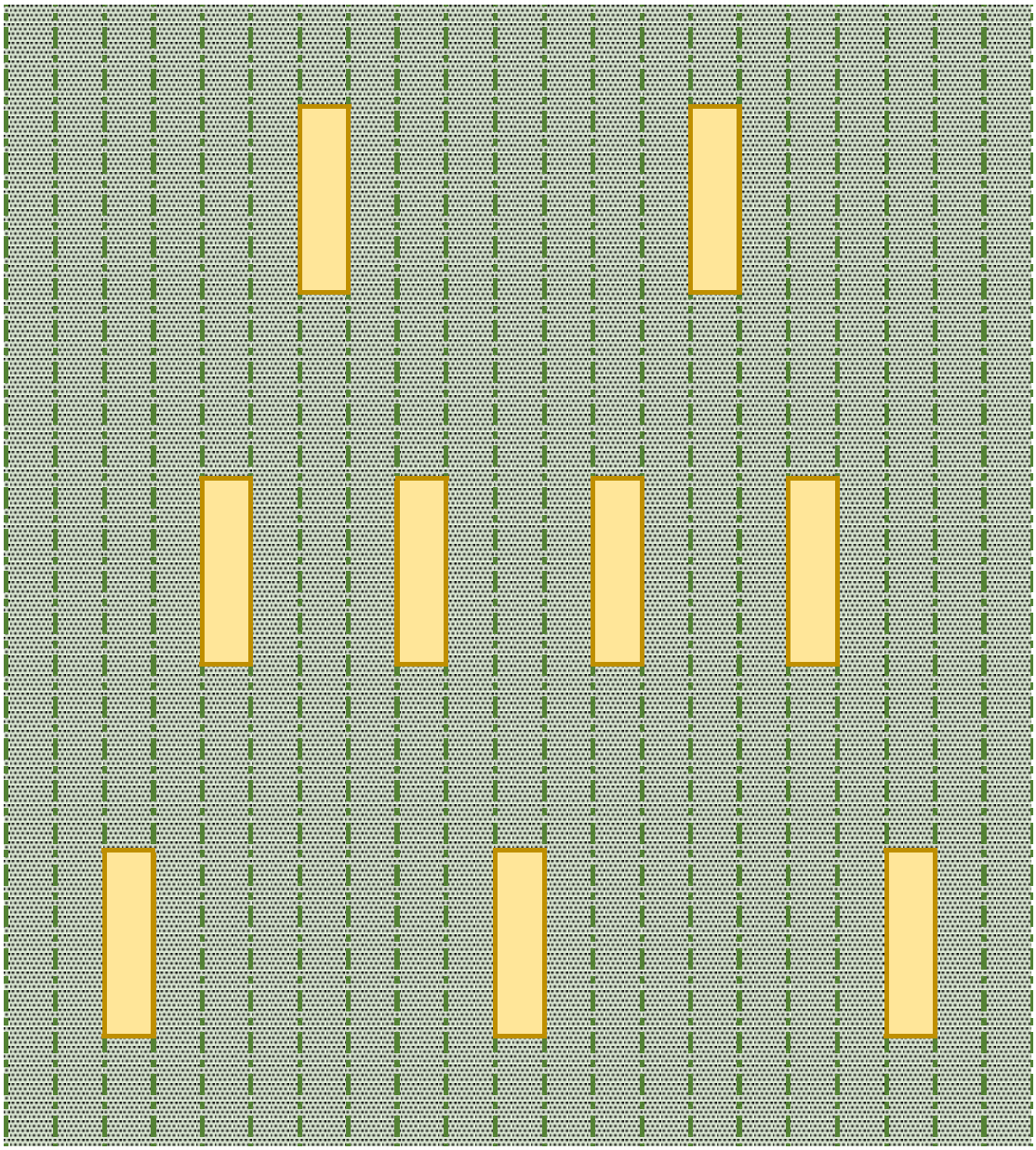

Fig. 2.2. Hand sampling design showing the M-shape pattern of transects (yellow rectangles) consisting of pairs of maize rows (green dotted lines) from which 10 randomly selected ears were collected.

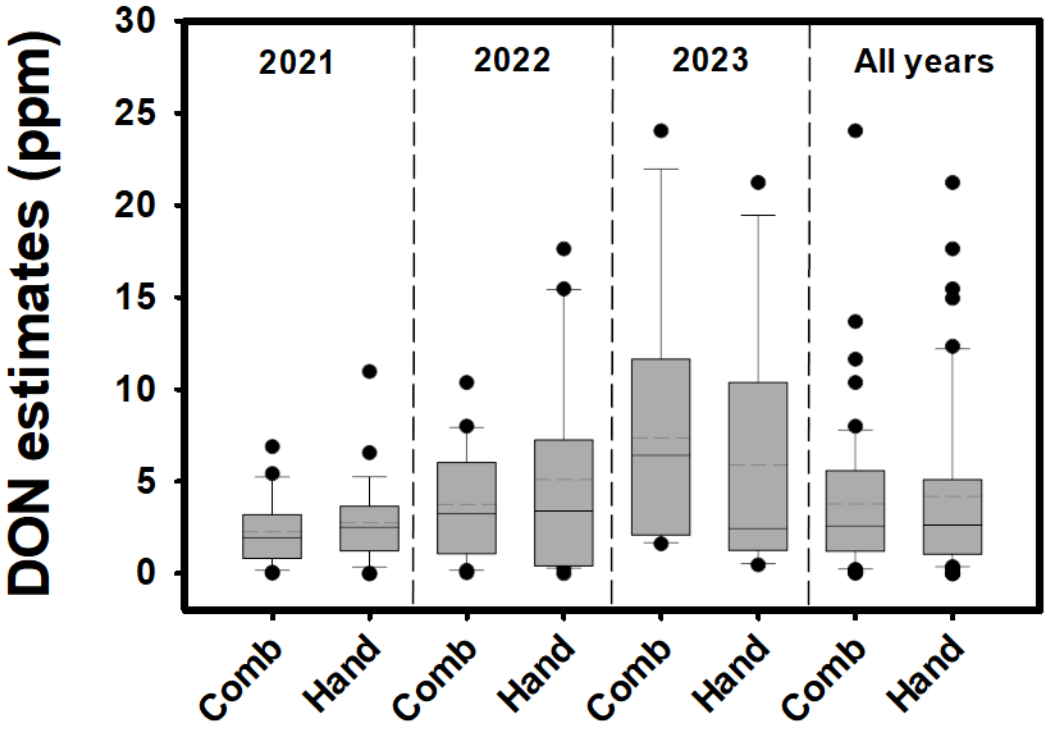

Fig. 2.3. Boxplots showing the distribution of estimated field-level mean deoxynivalenol (DON) contamination (ppm) of maize grain for samples collected from commercial fields using hand- and combine-sampling methods (Comb and Hand, respectively) during the 2021, 2002, and 2023 growing seasons and pooled across seasons. Broken and solid lines within each box represent means and medians, respectively, while the top and bottom lines of the box represent the 75th and 25th percentiles of the data, respectively. Vertical bars extending beyond the boxes represent extreme data points. The vertical dashed lines serve to separate years.

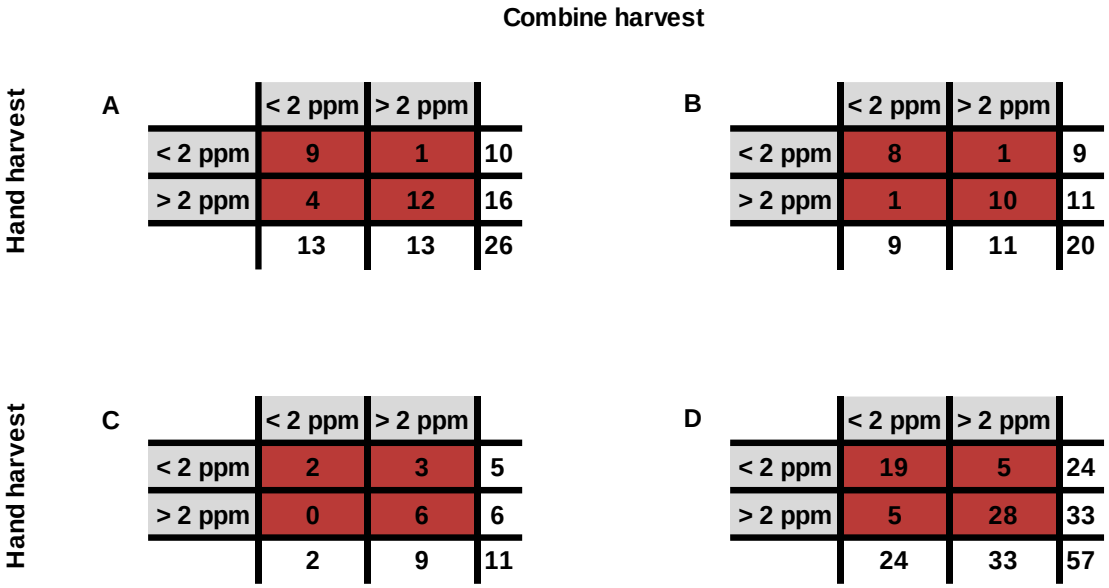

Fig. 2.4. Contingency tables showing the number of fields in which mean DON was estimated to be ≥ 2 ppm for both the hand- and combine-sampling methods, < 2 ppm for the two methods, ≥ 2 ppm for one method and < 2 ppm for the other, and < 2 ppm for one method and ≥ 2 ppm for the other for samples collected from commercial fields during the 2021 (**A**), 2002 (**B**), and 2023 (**C**) growing seasons and pooled across seasons (**D**).

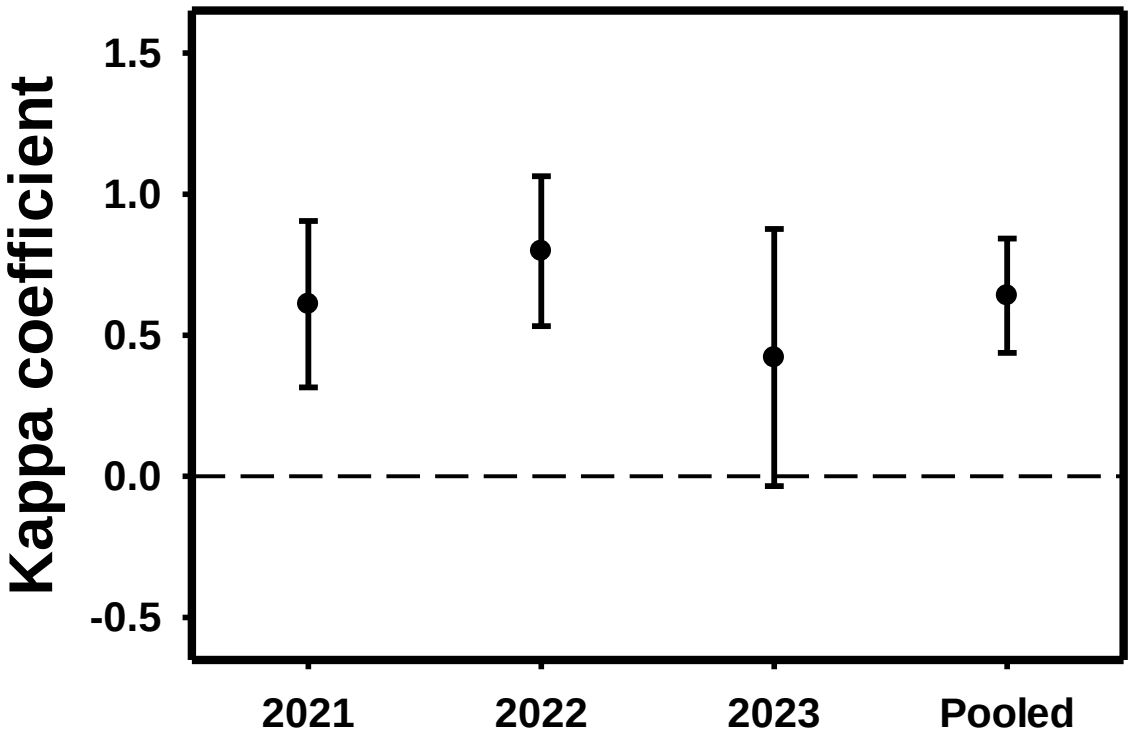

Fig. 2.5 Interval plot showing Cohen Kappa coefficients (dots) for each growing season and pooled across seasons with their corresponding 95% confidence intervals. Coefficients with confidence intervals that intercept the 0 broken reference lines are not significantly different from zero.

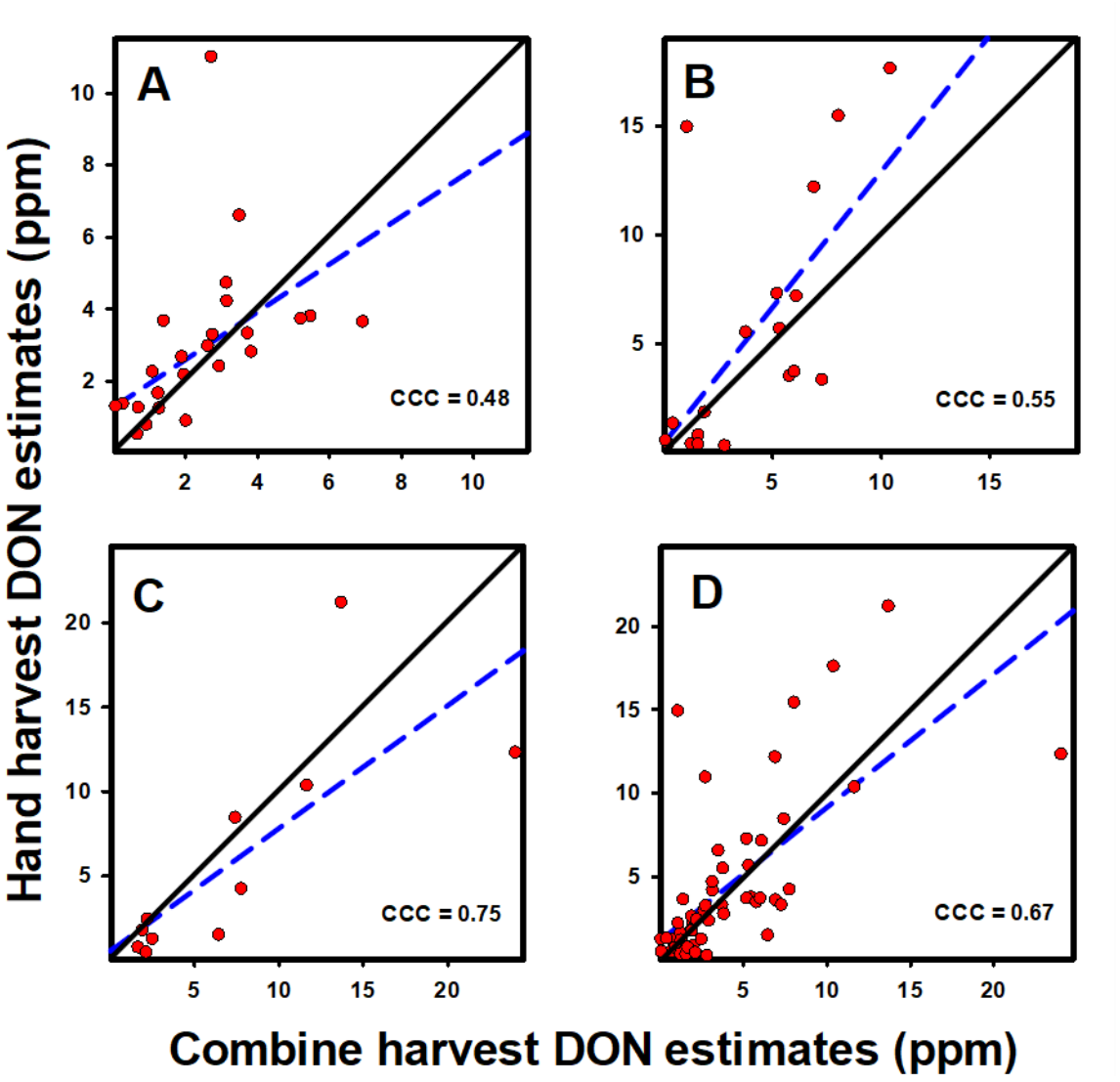

Fig. 2.6 Estimated mean DON contamination (ppm) of corn grain sampled from commercial fields using hand- and combine-sampling methods in each of three growing seasons (**A** = 2021; **B** = 2022; **C** = 2023; **D** = Pooled data). Solid black 45° lines indicate perfect agreement between sampling methods (CCC = 1). Broken blue lines indicate the best-fit lines of the data. CCC = Concordance correlation coefficient (1 = perfect agreement and 0 = no agreement).

Chapter 3: Heterogeneity of DON Contamination of Maize Grain at Multiple Spatial Scales

ABSTRACT

Deoxynivalenol (DON) contamination maize grain infected with the toxigenic, necrotrophic fungus *Fusarium graminearum*, the primary causal agent of Gibberella ear rot (GER), is a major economic concern for maize production in Ohio. DON reduces the market value of the crop and poses a threat to human and animal health. Understanding the heterogeneity of DON contamination at multiple spatial scales is important for developing sampling protocols and evaluating DON management strategies. Eighty-four to 367 and 254 to 989 samples were collected by hand (hand-sampling) or with a combine (combine-sampling), respectively, from 11 to 29 commercial maize fields for DON quantification at the end of the 2021, 2022, and 2023 growing seasons. Heterogeneity of DON contamination at multiple spatial scales was characterized for DON incidence by fitting a generalized linear mixed models to the incidence data using the complementary log-log (CLL) link function. To characterize the heterogeneity of field-levels mean DON contamination (ppm), unconditional hierarchical linear models were fitted to the DON data. Estimated variances and mean square errors from the model fit were then used to estimate variance partition coefficients for each level of the spatial scale and intracluster correlation coefficients. With DON as a continuous response, variability between fields within regions was the highest source of heterogeneity with combine-sampling in all cases, whereas sample/transect accounted for the highest proportion of total variability with hand-

sampling in 2021 and 2023, but not in 2022. Low intracluster correlation coefficients (ICC) indicated that this high transect-level variability with hand-sampling was most likely due to ear-to-ear variability. For DON as a binary response, field was the greatest source of variability on the CLL link scale. High ICCs indicated a high degree of similarity of DON contamination status (above or below 2 ppm DON) of ears within a cluster on the CLL link scale. These results suggest that combine-sampling tended to yield less variable field-level mean DON estimates than hand-sampling, and that the high transect heterogeneity with hand-sampling was mostly due to ear-to-ear variability.

INTRODUCTION

Gibberella ear rot (GER) and associated mycotoxin contamination of maize grain continues to be a cause for concern in the state of Ohio (Dalla Lana et al. 2021). This ear disease, caused predominantly by the toxigenic, necrotrophic ascomycete fungus *Fusarium graminearum* in the United States (US), reduces grain quality and yield components (Dalla Lana et al. 2022; Vigier et al. 2001). Infection is followed by contamination of the grain with mycotoxins such as deoxynivalenol (DON), DON derivatives, and zearalenone, among others (Desjardins 2006; Jimenez et al. 1996), depending on the chemotype of the pathogen population, production practices, and environmental conditions (Alexander et al. 2011; Hooker and Schaafsma 2005; Llorens et al. 2004). DON contamination reduces the market value of the crop and makes grain unsafe for human and animal consumption because it may cause vomiting, feed refusal, low weight gain, and reproductive disorders in livestock (Pestka et al. 1987; Schaafsma et al. 2009; Vesonder et al. 1976) if contaminated feed is consumed. For this reason, the US food and drug administration (2010) set allowable limits for DON contamination in wheat depending on its end use. For

maize, however, DON thresholds for grain commercialization are usually established by grain buyers, often based on the supply and demand and market prices of grain. Farmers may face grain rejection or price reductions when DON contamination exceeds market-established thresholds.

Although the control of GER is important from a yield loss perspective, the reduction of mycotoxin contamination is often the ultimate goal of GER management programs. However, direct or indirect approaches for evaluating the efficacy of management programs against the toxin remain a challenge because of high variability in DON and disparities between the level of contamination and visual symptoms of GER in commercial fields. Successful reduction in GER with resistance or fungicides does not always lead to correspondingly successful reduction in DON below critical thresholds. In addition, DON contamination may still increase after the implementation of the most successful GER management programs. Relationships between disease severity and DON contamination have been studied for GER in maize and Fusarium head blight (FHB) in wheat, a related disease caused by the same pathogen. For FHB, a linear relationship between FHB index (similar to GER severity) and DON contamination is often reported (Beyer et al. 2007, 2010; Paul et al. 2006). However, the strength of this relationship varies (Paul et al. 2005, 2006) as influenced by factors such as late-season weather conditions (Moraes et al. 2023) and cultivar resistance (Sneller et al. 2012). In some cases, low FHB index were reported to be associated with relatively high DON levels and vice versa (Cowger and Arellano 2010; Gilbert et al. 2002; Mesterhazy et al. 1999).

In contrast, GER severity and DON contamination were reported to have a positive exponential-type relationships (Bolduan et al. 2009; Reid and Sinha 1998; Reid et al. 2000)

that was also be influenced by hybrid resistance (Dalla Lana et al. 2022). However, as was the case with the *F. graminearum*-wheat pathosystem, asymptomatic maize grain with higher-than-expected levels of DON has also been observed in *F. graminearum*-maize pathosystem (Dalla Lana et al. 2021). This naturally increases the complexity of disease scouting, as researchers and farmers might not always be able to rely on visual symptoms alone as a measure of DON contamination when making grain handling, management, and marketing decisions. Although visual symptoms of GER may be relatively easier and cheaper to quantify, and can be quantified pre-harvest, well before DON contamination is usually quantified, as Madden and Paul (2020) demonstrated for the association between FHB and DON in *F. graminearum*-wheat pathosystem, visual symptoms may be weak surrogate for DON. Consequently, effort to manage DON must focus on the toxin itself rather that visual symptoms as a surrogate. This would require sampling to assess the efficacy of DON management and mitigation programs, and relatedly, an understanding to the spatial heterogeneity of DON contamination in commercial fields to develop sampling protocols.

To our knowledge, there is no published data on the spatial variation of DON in production fields. Previous studies indicated that GER and FHB were randomly distributed within fields, suggesting the DON may also be randomly distributed (Del Ponte et al. 2003; Oerke et al. 2010; Schmale III et al. 2005a, b). However, most of those studies did not account for fields with the presence of crop residue, where *Fusarium* spore deposition patterns and infection appeared to be more aggregated (Del Ponte et al. 2003; Schmale III et al. 2005a). In our study to assess the agreement between sampling methods for DON quantification in maize grain (Chapter 2), our findings suggested that high variability in

DON contamination within fields affected the agreement between hand- and combine-sampling. This variability could be explained, at least in part, by differences in silking (R1 growth stage) among plants, the presence of insects that wound ears and create entry points for the pathogen, variations in microclimate, and the amount of Fusarium-infested residue in a field and associated spore production.

A thorough understanding of variability is essential for developing effective sampling protocols for mycotoxin quantification, which is crucial for accurately evaluating management strategies such as fungicide efficacy in on-farm trials, largescale resistance screening, and the validation of DON forecasting systems. Therefore, the specific objectives of this study were to (i) characterize the heterogeneity of DON contamination at different spatial scales and (ii) determine the spatial distribution pattern of the toxin. To accomplish these objectives, fields across the state of Ohio were grouped into production regions based on typical weather patterns and topographical features, and hand- and combine-sampled for DON in 2021, 2022, and 2023. Unconditional hierarchical linear models and generalized linear mixed models were fitted to the data and variance partition and intracluster correlation coefficients were estimated to characterize heterogeneity of DON contamination of grain at multiple spatial scales and to determine its distribution pattern.

MATERIALS AND METHODS

Site selection, sampling, and deoxynivalenol quantification. Commercial maize fields across the state of Ohio were hand- and/or combine-sampled for DON at the end of the 2021, 2022, and 2023 growing seasons. Twenty-nine, twenty-one, and eleven fields were sampled by combine, whereas twenty-seven, twenty-eight and eleven were hand-

sampling in 2021, 2022, and 2023, respectively. No specific criteria were used for selecting individual fields; this mostly depended on the availability of commercial farms and the willingness of producers to collaborate. However, the regions of the state in which the fields were located were selected on the basis on the history of occurrence of GER and DON contamination of grain (based on feedback from stakeholders and extension educators), and local weather patterns and topographical features.

Samples were collected from fields in Crawford, Darke, Delaware, Holmes, Knox, Licking, Madison, Morrow, Pickaway, Putnam, Richland, Seneca, Wayne, and Williams counties, representing six production regions (Fig 3.1). In some cases, fields were managed based on the Ohio Agronomic Guide (Lindsey et al. 2017), but the specifics were left to the discretion of the producers and crop advisors. The agricultural practices used and other metadata for each field can be found in Table 2.1 in Chapter 2. Percentage of maize surface crop residue cover was estimated in all fields in 2021 and 2022 using a line transect method (Morrison et al. 1993) to determine the incidence (presence or absence) of residue every 3.2 meters along a 30.48-meter-long tape.

Ear samples were collected by hand (hereafter referred to as Hand-sampling) after physiological maturity, but before mechanical harvest, whereas grain samples were collected onboard a combine during harvest (hereafter referred to as Combine-sampling). With Hand-sampling, a two-stage cluster sampling approach was used to collect 10 ears from each of nine approximately 12-m-long transects (clusters; pair of row sections) along an “M”-shape pattern across a field. Five ears were arbitrarily harvested from each of the two rows of a transect. For Combine-sampling, a grain sample of approximately 110 to 450 g was collected from the grain stream of the combine every two hectares, approximately,

or 25,4000 kg of grain. The sampling designs were recommended but not always rigorously followed by all growers.

All samples were collected in paper bags, appropriately labelled with field coordinates and other metadata, shipped or transported to the laboratory, and stored on greenhouse benches with the bags open to facilitate drying to approximately 14% moisture. Prior to storage, husks were removed from Hand-harvested ears, and GER severity and the incidence of insect damage were rated as described in Chapter 2. After drying, ears were threshed, and the grain were pooled by transect, forming separate transect/cluster samples in 2021 and 2022. In 2023, grain from individual ears from each hand-harvested transect were kept separate as individual ear samples. Sub-samples were drawn from each combine-harvested sample, and each hand-harvested cluster and ear samples; homogenized and individually ground; and samples of ground grain were sent for DON analysis. Additional post-harvest grain processing details can be found in Chapter 2.

Data analysis. *Heterogeneity of DON contamination as a continuous response*. The heterogeneity of DON contamination of maize grain in commercial fields was estimated as a continuous response using DON estimates in parts per million (ppm). Separate unconditional hierarchical linear models (equation 1) were fitted to the data for each sampling method x growing season combination to estimate variability of DON at multiple spatial scales. The spatial scale considered were Regions (R), Fields within regions (F), and samples (transect in the cases of hand-sampling) within fields within regions (S). R, F, and S were considered random effects in the model and were assumed to be independent. Total variance was partitioned into variance components representing variability between-regions (σ^2_{region}), between fields within regions (σ^2_{field}), and between

samples within field within regions (σ^2_{sample}). This was done by fitted to the following random-effects model:

$$y_{ijt} = \mu + R_i + F(R)_{ij} + S(FR)_{ijt} \quad (1)$$

where y_{ijt} is the DON value of the *t*th sample/transect within the *j*th field of the *i*th region, μ is the overall expected value (mean), R_i is the effect of the *i*th region, $F(R)_{ij}$ is the effect of the *j*th field within the *i*th region, and $S(FR)_{ijt}$ is the effect of the *t*th sample (transect in the case of hand-sampling) within the *j*th field of the *i*th region. Models (equation 1) were fitted using the MIXED procedure in SAS (SAS Institute, Cary, NC) with the type III sums of squares method to estimate variance components.

Variance partition coefficients (VPCs). The variance components estimated from the fit of equation 1 to the data were used to estimate variance partition coefficients (VPCs) for each sampling method x year combination. VPCs were then used to estimate of the proportion of the total variability attributable to regions (equation 3a), fields within region (equation 3b), and samples within fields within regions (equation 3c) using the following equations:

$$VPC_{region} = \frac{\sigma^2_{region}}{\sigma^2_{region}+\sigma^2_{field}+\sigma^2_{sample}} \quad (2a)$$

$$VPC_{field} = \frac{\sigma^2_{field}}{\sigma^2_{region}+\sigma^2_{field}+\sigma^2_{sample}} \quad (2b)$$

$$VPC_{sample} = \frac{\sigma^2_{sample}}{\sigma^2_{region}+\sigma^2_{field}+\sigma^2_{sample}} \quad (2c)$$

where the terms are as defined above.

Variability of DON contamination within fields. DON variability among transects and ears within transects was estimated using data from hand-harvested grain samples

collected from the 11 fields in 2023 by again fitting an unconditional hierarchical linear model to the data as:

$$y_{jt} = \mu + T_j + E(T)_{jt} \quad (3)$$

where y_{jt} is the DON estimate of the t*th* ear within the *j*th transect, μ is the overall expected value (mean), T_j is the effect of the *j*th transect, and $E(T)_{jt}$ is the effect of the *t*th ear within the *j*th transect. Ear and transect were considered independent random effects in the model. The model (equation 2) was again fitted using the Mixed procedure in SAS (SAS Institute, Cary, NC) with the type III sums of squares method to estimate variance components.

Intracluster correlation coefficient (ICC). Results from the fit of equation 3 to the data were used to estimate ICCs as measures of agreement in DON contamination between ears within transects. ICC was estimated for each of the 11 fields sampled during the 2023 growing season as:

$$ICC = \frac{\sigma^2_{transect}}{\sigma^2_{transect}+\sigma^2_{ear}} = \frac{\widehat{MSBS}-\widehat{MSWS}}{\widehat{MSBS}+(k-1)\widehat{MSWS}} \quad (4)$$

where $\widehat{MSBS}$ is the estimated mean square between transects, $\widehat{MSWS}$ the estimated mean square within transects, and *k* is the number of ears harvested and assayed for DON within a transect. Positive ICC values would indicate that DON contamination of ears from the same transect would be more similar than contamination of ears from different transects, whereas negative ICC values would indicate that DON contamination is highly variable among ears in the same transect. ICC values close to 1 would indicate that ears from the same transacts have very similar levels of DON contamination. On the other hand, ICC values close to 0 would be indicative of ears within the same transect having very different levels of contamination.

Heterogeneity of DON as a binary response at three spatial scales. The incidence of DON contamination was estimated as the proportion of contaminated ears as ($I = Y/n$) in each transect, where Y is the numbers of ears with DON contamination above the detection limit of 0.05 ppm and n is the total number of ears sampled from each transect (10 in most cases). Only hand-sampling data from the 2023 growing season for which there as individual ear sample DON estimates were used in the analysis. Heterogeneity was characterized by fitting the following generalized linear mixed model (GLMM) to the complementary loc-log (CLL) link function of I:

$$g(I_{ijt}) = \eta_{ijt} = \mu + R_i + F(R)_{ij} + T(FR)_{ijt} \quad (5)$$

where $g(I_{ijt})$ is the CLL link function, η_{ijt} is the linear predictor, μ is the expected value (mean) on the link scale, R_i and $F(R)_{ij}$ are as defined above, and $T(FR)_{ijt}$ is the effect of the tth transect within the jth field within the ith region. R, F, and T were considered normal distribution independent random effects in the model with means of 0 and constant variances of σ^2_{region}, σ^2_{field}, and $\sigma^2_{transect}$. Equation 5 was fitted to I using the GLIMMIX procedure in SAS with the Laplace option and the CLL link function.

Variance estimates obtained from the fit of equation 5 to I were used to estimate the intracluster correlation coefficient (ϕ) as a measure of the similarity of DON contamination among transects within field and regions on the CLL link scale as:

$$\phi = \frac{\sigma^2_{region} + \sigma^2_{field}}{\sigma^2_{region} + \sigma^2_{field} + \sigma^2_{transect}} \quad (6)$$

where the terms are as defined above. Equation 6 provides a measure of the proportion of the total variance that is due to variability between for regions and fields. A ϕ value close to 1 indicates that transects within fields and regions tend to have similar chance of being contaminated with DON above the LOD on the link scale (i.e., transect variance is low

compared to region and field variance). Likelihood-ratio test and profile confidence intervals were performed to test the significance of the random effects using the covtest/cl(type=profile) statement in GLIMMIX as well as to test the null hypothesis that $\sigma^2_{region} = \sigma^2_{field}$ and $\sigma^2_{field} = \sigma^2_{Transect}$.

In order to obtain variance estimates on the original scale of the data, the inverse CLL link function (equation 7) was determined using the delta method to estimate the probability of DON contamination at the average value of the random effects (i.e., estimated DON incidence on the original scale) as:

$$\hat{p} = 1 - \exp\left(-\exp(\hat{\mu})\right) \tag{7}$$

The corresponding variance is given by:

$$var(\hat{p}) = \sigma^2_{total} * [(1-\hat{p})^2 * (-\ln(1-\hat{p}))^2] \tag{8}$$

where σ^2_{total} is the total variance on the CLL link scale estimated by adding the individual variance components.

In order to obtain intracluster correlation coefficient on the scale of the original data (ρ), we followed the approach described in Kriss et al. (2012) of assuming nonlinearity of the link function and considering Transect to follow a Bernoulli distribution. Values from equations 7 and 8 were used in the following formula determined by Murray (1998) and Kriss et al. (2012) as:

$$\rho = \frac{var(\hat{p})}{var(\hat{p}) + p(1-\hat{p})} \tag{9}$$

where $p(1-p)$ is defined as the variance of a Bernoulli distribution, $\hat{p}$ is estimated disease incidence on the original scale (equation 7) and $var(\hat{p})$ its variance (equation 8).

RESULTS

Exploratory data analysis. DON contamination of grain varied among growing seasons and sampling methods, and for a given sampling method, among regions, fields within regions, and samples/transects within field and region (Fig 3.2, 3.3, and 3.4). For both sampling methods, estimates of mean DON were higher in 2023 than in 2021 or 2022. In the latter two seasons (2021 and 2022) means, averaged across regions, fields, and samples, were higher with hand-sampling (2.74 and 4.59 ppm) than with combine-sampling (2.20 and 3.67 ppm), whereas in 2023, combine-sampling yielded grain with a higher mean level of contamination (7.51 ppm) than hand-sampling (5.94 ppm) (Table 3.1). Across the three years, the maximum level of contamination was observed with hand-sampling, ranging from 26.50 to 146.10 ppm, compared to 15.80 to 35.80 with combine-sampling (Table 3.1).

Variability in DON contamination, based on estimated variances and standard deviations of the means, followed a similar pattern to that observed for the means, with lower values with combine-sampling than with hand-sampling in any given year, and higher values in 2023 than in 2022 or 2022 with either sampling method (Table 3.1). Variances ranged from 0.04 to 7.60, 0.19 to 21.48, and 25.58 to 106.29 for combine samples and from 0.82 to 15.96, 0.89 to 65.26, and 32.21 to 287.38 for hand samples for 2021, 2022, and 2023, respectively (Fig. 3.2). Fields with the highest levels of mean DON contamination were in Regions 3, 4, and 5 in 2021, Regions 2, 3, and 4 in 2022, and Region 2 in 2023 (Fig. 3.2). In 2021 and 2022, the range of field-level mean DON (difference between the highest and lowest field-level means) was highest in Region 4, but higher in Region 2 than in Region 4 in 2023 (Fig. 3.4).

In 2023, the only year in which DON contamination was quantified in grain from individual ears within transects within fields (Fig. 3.5), ears from fields located in Region 2 were generally more contaminated that ears sampled from fields in Region 4. Individual ear sample means ranged from 0 to 146.10 ppm in Region 2 and from 0 to 39.50 in Region 4 (Fig. 3.5). DON variability among ears were generally higher among ears from fields in Region 2, particularly those that were heavily contaminated, than from fields in Region 4. Fifty percent of the data in the four most contaminated field in region 2 were between 0.70 and 15.95 ppm in Crawford_1 (interquartile range [IQR] = 15.25 ppm), between 2.10 and 37.88 ppm in Crawford_4 (IQR = 35.78 ppm), between 0.03 and 14.48 ppm in Crawford_5 (IQR = 14.45 ppm), and between 0.64 and 10.55 ppm in Seneca_1 (IQR = 9.91 ppm). IQRs for fields in Region 4 ranged from 0 to 4.05 ppm.

Heterogeneity of DON as a continuous response. Variance estimates for regions, fields within regions, and samples/transects within fields within regions from the fit of equation 1 are shown in Table 3.2. Region was the level in spatial scale with the lowest DON heterogeneity with both sampling methods in all three years, representing only 7, 4, and 12% of the total variability with hand-sampling and 9, 0.3, and 13% with combine-sampling in 2021, 2022, and 2023, respectively. Sample (transect in the case of hand-sampling) within field and region was the second highest source of variability with combine-sampling in all years, representing 34 to 41% of the total variance. In contrast, transect was the greatest source of variability in all but one year (2022), accounting for 62% of the toral variance in 2021, 44% in 2022, and 74% in 2023. Field represented the highest proportion of the total variance with combine-sampling in all three seasons,

accounting for 50, 62, and 51% of the total variance in 2021, 2022, and 2023, respectively (Table 3.2).

To gain a better understanding of the high variability observed between transects in 2023, results from the fit of equation 3 to the DON data were used to estimate ICC and determine ear-to-ear variability in DON contamination within transects in the 11 fields. For all fields in 2023, the ICC values were very low (< 0.25), with negative values in some fields (Crawford_1, Crawford_2, and Morrow_1; Table 3). Positive ICC values would indicate that in Crawford_3, Crawford_4 Crawford_5, Knox_1, Knox_2, Knox_3, Licking_1, and Seneca_1, DON contamination of ears from the same transect were more similar than contamination of ears from different transects, whereas negative ICC values for Crawford_1, Crawford_2, and Morrow_1 would indicate that DON contamination is highly variable among ears in the same transect. Overall, low ICC values (considerably lower than 1) indicate that ear-to-ear variability was considerably higher than transect-to-transect variability.

Heterogeneity of DON as a binary response. Close to 50% of the 989 ears samples across the 11 field in 2023 had DON contamination above the detection limit. Estimated DON incidence (*I*) varied among Regions, Field within Regions, and Transect within Fields within Regions, ranging from 0 to 1 across fields and transects in Region 2 and from 0 to 0.9 in Region 4. In Region 2, 50% of the transects had *I* values between 0.40 and 0.90, whereas in the Region 4, the corresponding values were 0.10 and 0.50. Estimated *I* on the CLL link scale (μ) from the fit of equation 5 was -0.57 with a standard error of 0.43 (Table 3.4). This means that, on the original data scale, based on the inverse link of CLL (equation

7), the overall probability of an ear being contaminated with DON ($\widehat{\boldsymbol{p}}$) above the detection limit was 0.43 (Table 3.4).

Estimated variances were similar for Region and Transect within Field within Region, 0.26 and 0.21, respectively, but considerably higher for Fields within Regions (0.53). When partitioning the variance components obtained from the fit of equation 5 in a way similar to what was done in equation 2, variability among fields was the highest source of DON incidence heterogeneity on the CLL scale, accounting for 52% of total variance, followed variability among regions accounting for 26% of the total variance, and transects with 21% of the total. However, based on the likelihood-ratio test, only the variances for Field within Region and Transect within Field and Region were significantly different from 0. The variance for Region, although high, had wide confidence intervals (0 to 6.4), which as likely due to the low number of regions (n = 2).

Intracluster correlation coefficient on the CLL scale (ϕ), equation 6**,** was high ($\phi = 0.78$), indicating that transects within fields within regions tended to have similar values of DON incidence on the CLL scale. While on the original scale, the estimated intracluster correlation coefficient of DON incidence (ρ) was low (ρ = 0.29), indicating that ears within transects were likely to have similar DON contamination levels compared to ears from other transects, fields, or regions.

DISCUSSION

Spatial heterogeneity of plant diseases is an important component of the epidemiology of pathosystems that researchers use to develop effective management programs. Several studies have focused the heterogeneity of FHB in wheat at multiple

spatial scales based on disease incidence or severity (Kriss et al. 2012; Moraes et al. 2021; Wilhelm and Jones 2005). Findings from these studies allowed for the development of sampling protocols for FHB and provided a clearer understand the distribution pattern of the pathogen/disease within and between fields and regions. However, to our knowledge, no such studies have been done on GER, and specifically, on DON contamination of grain, which is increasing in occurrence and levels of contamination of maize grain in Ohio and some neighboring states (Dalla Lana et al. 2020). Here, we sampled commercial corn fields using two sampling protocols and characterized the heterogeneity of DON contamination of maize grain at multiple spatial scales in terms of level of contamination and incidence.

Estimated mean DON contamination (ppm) varied among years, regions, fields and sampling method. There are several possible reasons for the observed differences in baselines DON contamination between years, regions, and fields, including different environmental conditions, hybrid resistance, and cultural practices. Dalla Lana et al. (2021) demonstrated that DON contamination increased with increases in the number of hours with high relative humidity (>90%) and temperature above 20°C. Although in-field weather data were not collected as part of this study, field-to-field differences in microclimatic conditions might have contributed to differences in DON at different spatial scales. In addition, differences among fields in agricultural practices that are known to affect *F. graminearum* survival and spore production may have also contributed to the observed heterogeneity in DON contamination.

For instance, most of the fields sampled in 2023, some of which had very high levels of DON contamination, did not receive a fungicide treatment. Eli et al. (2021) reposted that an application of pydiflumetofen at the R1 growth stage led to a 50%

reduction in DON content in Ontario, Canada. However, these findings were not consistent with those reported by Anderson et al. (2017) who did not see a reduction in DON contamination following the application of DMI and QoI fungicides to some fields in Indiana, USA. Hybrid resistance was also shown to reduce DON contamination of grain, and although information on the resistance of the hybrids used in our studies were not available, relatively low DON contamination in some fields may have been due to the resistance of the hybrids used. The range of field-levels mean DON contamination of grain from the commercial fields sampled in our study was comparable to those reported by Dalla Lana et al. (2021), allowing us to evaluate the heterogeneity of naturally occurring levels of DON in commercial fields.

Heterogeneity of DON contamination of grain (in ppm) at the three spatial scales, estimated based on variance components, was lowest at the highest level in the spatial hierarchy (regions in our case). In all years, variability among regions accounted for 4 to 12% of total variability with hand-sampling and 0.3 to 13% with combine-sampling. Contrary to what was observed with hand-sampling, except for 2022, with combine-sampling, variability between fields within regions was the highest source of variability. This reflects, at least in part, the effects of the field-specific factors given above on DON contamination. The difference between hand- and combine-sampling in terms of transect being the highest source of variable with hand-sampling was likely the results of lower in-field variability with combing-sampling compared to hand-sampling, due to the formers resulting in more homogenized and representatives samples being collected than the latter. In several fields, more combine samples were collected across a wider area than hand simples. Although mean DON contamination was fairly comparable between combine- and

hand-sampling, the latter tended to have more extreme values than the former, which likely led to higher heterogeneity within fields with hand-sampling.

With hand sampling, transects within fields within regions (the lowest level in the hierarchy) accounted for the highest proportion of the total variability (except in 2022). In order to better understand this effect, intracluster correlation coefficients (ICC) values were estimated using the hand-sampling data from 2023. ICC was very low, with most fields having values closer to 0 than to 1, and some even had negative ICC values. Low ICC suggested that ears within transects had different levels of DON (ppm) while transects had very similar estimates. Although negative ICC are not common in theory, they are possible when the numerator of equation 4 is negative. Thus, when the within transect (ear variability) mean squares is higher than the between transect mean square it is possible to obtain negative ICC values. This implies that ear-to-ear variability was high and most of the heterogeneity occurred at the ear level (Lohr 2010).

These results suggest that with combine sampling one is more likely to have less variability between DON estimates within field, but these estimates may be highly variable when compared with other fields, and that from hand-sampling there is more within field variability likely due to ear-to-ear differences in DON levels. Although VPCs estimates indicated that variability between transects tended to be higher with hand sampling (when estimating DON as a continuous response), ICC showed that transect-to-transect variability was mostly due to ear-to-ear variability and that transects alone was less variable when compared to ear variability. These results were consistent with those from Moraes et al. (2021), who conducted a similar study to characterize the heterogeneity of FHB index (severity in FHB research) in inoculated research plots. In that study, the spatial scale was

(physically) much smaller, only including differences between plots, clusters within plots, and spikes within clusters within plots. They showed that FHB index was more variable between wheat spikes (the equivalent of corn ears in our study) than between plots. However, since the two studies were quite different, one should exercise caution when comparing results between the two.

When characterizing the heterogeneity of DON as a binary response (DON incidence). Intracluster correlation on the CLL scale (ϕ) was high (ϕ = 0.78), indicating that transects within the same field and region tend to have similar estimates of expected DON incidence on the CLL scale. A high ϕ value also indicated that the variability between fields within regions and between regions were higher than variability between transects (the lowest level on the spatial scale). When estimating DON as a binary response, difference in contamination levels (ppm) of samples/transect did not account for variability, therefore, heterogeneity between transects tends to be lower compared to estimating heterogeneity of DON as a continuous variable. On the original scale, estimated intracluster correlation (ρ) was low, but different from zero ($\rho = 0.29$), indicating that DON contamination of ears within transect was not randomly distributed (following binomial distribution theory where $\rho = 0$).

Kriss et al. (2012) characterized the heterogeneity of FHB incidence in wheat fields at three spatial scales, variability between counties (equivalent to region in our research), fields within counties, and sites within fields and counties (equivalent to transects within fields and regions in our analysis). As was the case in our study, they demonstrated that FHB incidence, on the CLL link scale, was most variable at the higher level of the spatial scales, while variability was lowest between sites within fields and counties (the lowest in

the spatial scale hierarchy). Their intracluster correlation results were similar to ours, with ϕ values considerably high, ranging from 0.88 to 0.99, and ρ values low. High field-to-field variation was also found by Wilhelm and Jones (2005). However, their research focused on fitting binomial or beta-binomial distribution to FHB incidence data at four spatial scales, they did not attempt to characterize spatial heterogeneity as was done in our research or by Moraes et al. (2021) and Kriss et al. (2012). The authors attributed high between-field variability in FHB index to differences in agricultural practices (tillage, crop rotation, and planting date).

In conclusion, combine-sampling tended to yield less variable field-level mean DON estimates than hand-sampling. DON estimates from hand sampling tended to be more variable within fields, with the heterogeneity being mostly due to ear-to-ear variability, as the variability between transects was relatively low according to ICC and ϕ values. This would imply that ears can be pooled by transect to obtain a composite transect sample, but the sample size for ears should be increased to help reduce within field variability with hand-sampling. High variability in DON contamination between fields was common, regardless of sampling methods, and this heterogeneity could be explained by differences in agricultural practices, microclimates among field, and complex interactions involving these factors. Future research should focus on increasing sample sizes at the field, transect/sample, and ear levels, and formally evaluate the effects of production practices, local weather conditions, and relatedly, baseline GER severity and DON contamination on DON heterogeneity in production fields.

REFERENCES

Alexander, N. J., McCormick, S. P., Waalwijk, C., van der Lee, T., and Proctor, R. H. 2011. The genetic basis for 3-ADON and 15-ADON trichothecene chemotypes in *Fusarium*. Fungal Genet. Biol. 48:485–495.

Anderson, N. R., Romero Luna, M. P., Ravellette, J. D., and Wise, K. A. 2017. Impact of foliar fungicides on Gibberella ear rot and deoxynivalenol levels in Indiana corn. Plant Health Progress 18:186–191.

Beyer, M., Klix, M. B., and Verreet, J.-A. 2007. Estimating mycotoxin contents of *Fusarium*-damaged winter wheat kernels. Int. J. Food Microbiol. 119:153–158.

Bolduan, C., Miedaner, T., Schipprack, W., Dhillon, B. S., and Melchinger, A. E. 2009. Genetic variation for resistance to ear rots and mycotoxins contamination in early european maize inbred lines. Crop Sci. 49:2019–2028.

Cowger, C., and Arrellano, C. 2010. Plump kernels with high deoxynivalenol linked to late *Gibberella zeae* infection and marginal disease conditions in winter wheat. Phytopathology 100: 719-728.

Dalla Lana, F., Madden, L. V., and Paul, P. A. 2021a. Logistic models derived via lasso methods for quantifying the risk of natural contamination of maize grain with deoxynivalenol. Phytopathology 111:2250–2267.

Dalla Lana, F., Madden, L. V., and Paul, P. A. 2021b. Natural occurrence of maize Gibberella ear rot and contamination of grain with mycotoxins in association with weather variables. Plant Dis. 105:114–126.

Del Ponte, E. M., Shah, D. A., and Bergstrom, G. C. 2003. Spatial patterns of Fusarium head blight in new york wheat fields suggest role of airborne inoculum. Plant Health Progress 4:6.

Desjardins, A. E. 2006. Fusarium mycotoxins: chemistry, genetics, and biology. J. Agric. Sci. 145:539–539.

Eli, K., Schaafsma, A. W., Limay-Rios, V., and Hooker, D. C. 2021. Effect of pydiflumetofen on Gibberella ear rot and *Fusarium* mycotoxin accumulation in maize grain. World Mycotoxin J. 14:495–512.

Gilbert, J., Abramson, D., McCallum, B., and Clear, R. 2002. Comparison of Canadian *Fusarium graminearum* isolates for aggressiveness, vegetative compatibility, and production of ergosterol and mycotoxins. Mycopathologia 153:209–215.

Hooker, D. C., and Schaafsma, A. W. 2005. Agronomic and environmental impacts on concentrations of deoxynivalenol and fumonisin B1 in corn across Ontario. Can. J. Plant Pathol. 27:347–356.

Jiménez, M., Máñez, M., and Hernández, E. 1996. Influence of water activity and temperature on the production of zearalenone in corn by three *Fusarium* species. Int. J. Food Microbiol. 29:417–421.

Kang, Z., and Buchenauer, H. 1999. Immunocytochemical localization of *Fusarium* toxins in infected wheat spikes by *Fusarium culmorum*. Physiol. Mol. Plant Pathol. 55:275–288.

Kriss, A. B., Paul, P. A., and Madden, L. V. 2012. Characterizing heterogeneity of disease incidence in a spatial hierarchy: a case study from a decade of observations of Fusarium head blight of wheat. Phytopathology 102:867–877.

Lana, F. D., Madden, L. V., Carvalho, C. P., and Paul, P. A. 2022. Impact of Gibberella ear rot on grain quality and yield components in maize as influenced by hybrid reaction. Plant Dis. 106:3061–3075.

Lana, F. D., Paul, P. A., Minyo, R., Thomison, P., and Madden, L. V. 2020. Stability of hybrid maize reaction to Gibberella ear rot and deoxynivalenol contamination of grain. Phytopathology 110:1908–1922.

Lindsey, L. E., Lentz, E., Michel, A., Tilmon, K., Culman, S., and Paul, P. 2017. Small grain production. Pages 69-81 in: Ohio Agronomy Guide, 15th Ed. D. Barker, S. Culman, A. Dorrance, J. Fulton, R. Haden, E. Lentz, A. Lindsey, L. Lindsey, M. Loux, E. McCoy, A. Michel, J. Noel, P. Paul, M. Sulc, P. Thomison, K. Tilmon, and J. Witter, eds. The Ohio State University, Columbus, OH.

Llorens, A., Mateo, R., Hinojo, M. J., Valle-Algarra, F. M., and Jiménez, M. 2004. Influence of environmental factors on the biosynthesis of type B trichothecenes by isolates of *Fusarium* spp. from Spanish crops. Int. J. Food Microbiol. 94:43–54.

Lohr, S. L. 2010. Sampling: Design and Analysis. 2nd ed. Brooks/Cole, Boston, MA.

Madden, L. V., and Paul, P. A. 2020. Is disease intensity a good surrogate for yield loss or toxin contamination? A case study with Fusarium head blight of wheat. Phytopathology 110:1632–1646.

Mesterházy, Á., Bartók, T., Mirocha, C. G., and Komoróczy, R. 1999. Nature of wheat resistance to Fusarium head blight and the role of deoxynivalenol for breeding. Plant Breed. 118:97–110.

Moraes, W. B., Madden, L. V., Baik, B.-K., Gillespie, J., and Paul, P. A. 2023. Environmental conditions after Fusarium head blight visual symptom development affect contamination of wheat grain with deoxynivalenol and deoxynivalenol-3-glucoside. Phytopathology 113:206–224.

Moraes, W. B., Madden, L. V., and Paul, P. A. 2022. Characterizing heterogeneity and determining sample sizes for accurately estimating wheat Fusarium head blight index in research plots. Phytopathology 112:315–334.

Morrison, J. E., Huang, C. H., Lightle, D. T., and Daughtry, C. S. 1993. Residue measurement techniques. J. Soil Water Conserv. 48:478-483.

Oerke, E.-C., Meier, A., Dehne, H.-W., Sulyok, M., Krska, R., and Steiner, U. 2010. Spatial variability of Fusarium head blight pathogens and associated mycotoxins in wheat crops. Plant Pathol. 59:671–682.

Paul, P. A., Lipps, P. E., and Madden, L. V. 2006. Meta-analysis of regression coefficients for the relationship between Fusarium head blight and deoxynivalenol content of wheat. Phytopathology 96:951–961.

Paul, P. A., Lipps, P. E., and Madden, L. V. 2005. Relationship between visual estimates of Fusarium head blight intensity and deoxynivalenol accumulation in harvested wheat grain: A meta-analysis. Phytopathology 95: 1225-1236.

Pestka, J. J., Lin, W.-S., and Miller, E. R. 1987. Emetic activity of the trichothecene 15-acetyldeoxynivalenol in swine. Food Chem. Toxicol. 25:855–858.

Reid, L. M., and Sinha, R. C. 1998. Maize maturity and the development of Gibberella ear rot symptoms and deoxynivalenol after inoculation. Eur. J. Plant Pathol. 104:147–154.

Reid, L. M., Zhu, X., Savard, M. E., Sinha, R. C., and Vigier, B. 2000. Pre-harvest accumulation of deoxynivalenol in sweet corn ears inoculated with *Fusarium graminearum*. Food Addit. Contam. 17:689–701.

Schaafsma, A. W., Limay-Rios, V., Paul, D. E., and Miller, J. D. 2009. Mycotoxins in fuel ethanol co-products derived from maize: a mass balance for deoxynivalenol. J. Sci. Food Agric. 89:1574–1580.

Schmale, D. G., Shah, D. A., and Bergstrom, G. C. 2005. Spatial patterns of viable spore deposition of Gibberella zeae in wheat fields. Phytopathology 95:472–479.

Schmale III, D. G., Bergstrom, G. C., and Shah, D. A. 2005. Spatial patterns of viable spore deposition of the corn ear rot pathogen, *Gibberella zeae*, in first-year corn fields. Can. J. Plant Pathol. 27:225–233.

Sneller, C., Guttieri, M., Paul, P., Costa, J., and Jackwood, R. 2012. Variation for resistance to kernel infection and toxin accumulation in winter wheat infected with *Fusarium graminearum*. Phytopathology 102:306–314.

U.S. Food and Drug Administration. 2010. Guidance for industry and FDA: advisory levels for deoxynivalenol (DON) in finished wheat products for human consumption and grains and grain by-products used for animal feed. Available: https://www.fda.gov/regulatory-information/search-fda-guidance-documents/guidanceindustry-and-fda-advisory-levels-deoxynivalenol-don-finished-wheat-products-human.

Vesonder, R. F., Ciegler, A., Jensen, A. H., Rohwedder, W. K., and Weisleder, D. 1976. Co-identity of the refusal and emetic principle from *Fusarium*-infected corn. Appl. Environ. Microbiol. 31:280–285.

Vigier, B., Reid, L. M., Dwyer, L. M., Stewart, D. W., Sinha, R. C., Arnason, J. T., and Butler, G. 2001. Maize resistance to Gibberella ear rot: symptoms, deoxynivalenol, and yield1. Can. J. Plant Pathol. 23:99–105.

Wilhelm, K. P., and Jones, R. K. 2005. Meso- and microscale patterns of Fusarium head blight in spring wheat fields in Minnesota. Plant Dis. 89:474–479.

Table 3.1. Summary statistics for deoxynivalenol (DON; ppm) contamination of maize grain sampled by combine and hand from fields across the state of Ohio at the 2021, 2022, and 2023 growing seasons.

	Combine			Hand		
Statistic[a]	2021	2022	2023	2021	2022	2023
N	367	251	84	239	254	989
Mean	2.20	3.67	7.51	2.74	4.59	5.94
SD	2.31	3.80	8.66	3.42	6.38	13.62
Minimum	0.03	0.03	0.40	0.03	0.03	0.03
25th percentile	0.72	1.00	2.10	0.59	0.47	0.03
Median	1.60	2.40	4.35	1.70	2.00	0.03
75th percentile	3.00	5.30	8.95	3.40	6.20	4.10
Maximum	15.80	21.70	35.80	26.50	40.80	146.10
Range	15.78	21.68	35.40	26.48	40.78	146.08

[a] N = Number of samples collected with either sampling method in each growing season, SD = Standard deviation, and Range is the difference between the maximum and minimum.

Table 3.2. Estimated variances[a] for deoxynivalenol (DON) contamination of maize grain at three spatial scales (regions, fields within regions, and samples or transects within fields within regions) and their standard errors (SE) based on the fit of equation 1, and variance partition coefficients[b] (VPCs; equation 2) for each level in the spatial hierarchy in 2021, 2022, and 2023.

		2021			2022			2023		
Method[c]	Source[d]	Variance[a]	SE	VPC	Variance	SE	VPC	Variance	SE	VPC
Hand	Region	0.80	1.16	0.07	1.78	4.83	0.04	23.18	40.71	0.12
	Field	3.79	1.46	0.31	21.75	7.12	0.52	28.65	14.26	0.14
	Transect	7.47	0.73	0.62	18.17	1.71	0.44	147.81	6.68	0.74
Combine	Region	0.51	0.81	0.09	0.06	3.29	0.003	11.00	27.25	0.13
	Field	2.88	1.16	0.50	10.46	5.39	0.62	42.43	24.53	0.51
	Sample	2.37	0.18	0.41	6.24	0.58	0.37	28.48	4.71	0.34

[a] Total variances were partitioned with the type III sum of squares method, [b] VPCs when multiplied by 100 provide an estimates of the percentage of variability accounted for by each spatial scale, [c] sampling method used, hand- and combine-sampling, and [d] indicate the levels in the spatial hierarchy for which the total variability was partitioned.

Table 3.3. Estimated variances for deoxynivalenol (DON) contamination in maize grain at two spatial scales (Transect and Ear within transects) and their standard errors (SE) based on the fit of equation 3, and respective intracluster correlation coefficient (ICC; equation 4) for data from hand-sampled grain scale in 2023.

Field[a]	Source[b]	Variance[c]	SE	ICC[d]
Crawford_1	Transect	-0.48	0.47	-0.040
	Ear	12.47	1.98	
Crawford_2	Transect	-6.58	7.76	-0.033
	Ear	206.79	32.49	
Crawford_3	Transect	7.21	5.61	0.155
	Ear	39.41	6.19	
Crawford_4	Transect	1.52	27.46	0.003
	Ear	510.03	80.14	
Crawford_5	Transect	117.57	82.52	0.201
	Ear	468.09	73.55	
Knox_1	Transect	0.06	0.33	0.010
	Ears	5.84	0.92	
Knox_2	Transects	0.03	0.62	0.003
	Ears	11.61	1.82	
Knox_3	Transects	4.12	2.83	0.213
	Ears	15.21	2.39	
Licking_1	Transects	3.43	5.24	0.048
	Ears	68.30	10.73	
Morrow_1	Transects	-0.28	2.28	-0.006
	Ears	45.94	7.22	
Seneca_1	Transects	27.24	18.81	0.210
	Ears	102.46	16.10	

[a] List of fields that were sampled with combine- and hand-sampling methods, coded based on the county of origin with a number indicating the specific field sampled within that county, [b] sources of variation representing the two levels in the spatial scale, [c]variances estimated using moment-based model, negative variances are possible, and [d]ICC - negative values are possible when the mean squares of the within-subject is higher than the mean squares between-subjects.

Table 3.4. Statistics characterizing the heterogeneity of the incidence of deoxynivalenol (DON) contamination of grain from maize ears hand-sampling from commercial fields in Ohio in 2023 based on the fit of equation 5, including estimated mean DON incidence on the complementary log-log link scale (μ) and its standard errors (SE), probability of DON contamination ($\hat{p}$)**,** variance partition coefficients (VPC) for the three levels in spatial scale (Region, Fields within Region, and Transects within Fields within Region), the lower (LCL) and upper (UCL) limits the 95% confidence intervals around VPC, likelihood-ratio test, and estimated of intracluster correlation coefficients.

μ (SE)	$\hat{p}$	ρ[a]	ϕ[b]	Source[c]	Variance (SE)	VPC	LCL	UCL	Ratio test[d]
-0.57 (0.43)	0.43	0.29	0.78	Region	0.263 (0.37)	0.26	0	6.4	1.57
				Field	0.530 (0.27)	0.52	0.2	1.7	41.47*
				Transect	0.214 (0.08)	0.21	0.09	0.41	18.58*

[a] Intracluster correlation coefficient on the original incidence scale (equation 9) indicating the degree of similarity of the contamination status (contaminated or not) of maize ears within transects within fields and regions, [b] intracluster correlation coefficient (equation 6) indicating the degree of similarity of the complementary log-log link of expected probability of contamination status (contaminated or not) of transects within fields and within regions, [c]levels in the spatial hierarchy, [d] likelihood-ratio test to test the significance of the random effects, and [*]indicates that a variance estimate was significantly different from zero.

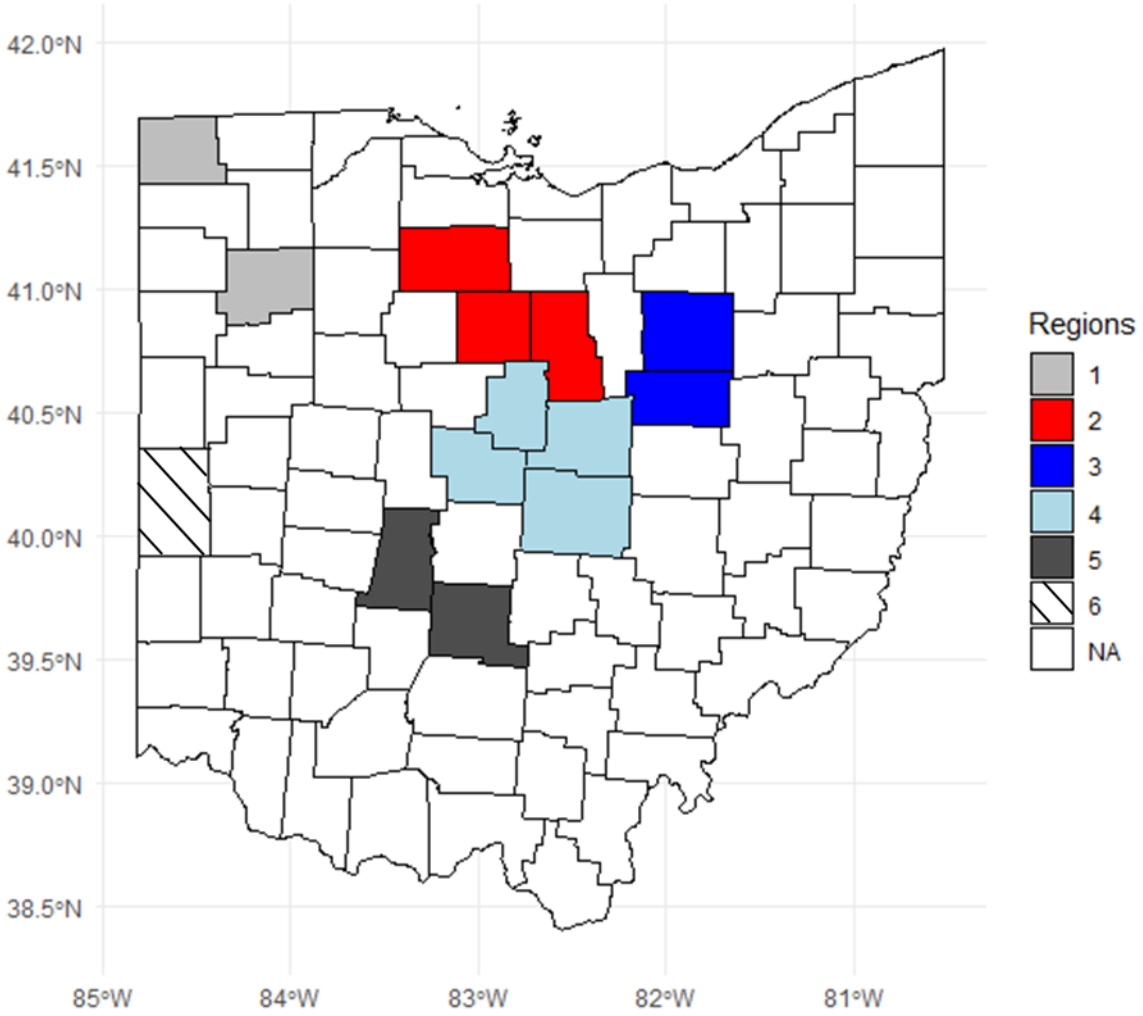

Fig. 3.1. Map of Ohio showing counties from which corn fields were sampled in 2021, 2022 and 2023. Colors/pattern represent production regions: Gray = Region 1, Red = Region 2, Blue = Region 3, Pale-blue = Region 4, Dark gray = Region 5, and White with lines = Region 6.

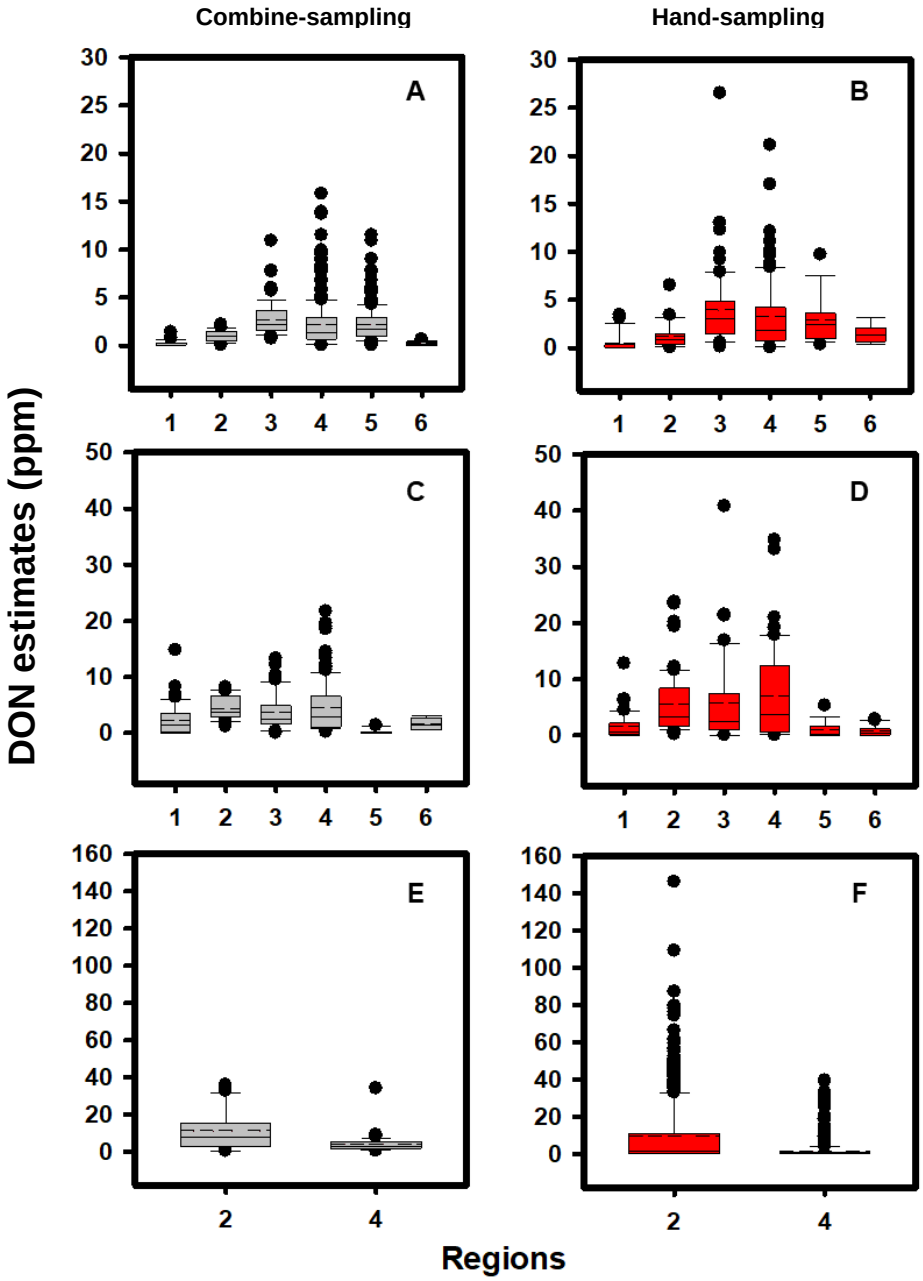

Fig. 3.2. Boxplots showing the distribution of deoxynivalenol (DON) contamination (ppm) of maize grain for samples collected from commercial fields using hand- and combine-sampling methods grouped by regions in 2021 (A and B), 2022 (C and D), and 2023 (E and F). Broken and solid lines within each box represent means and medians, respectively, while the top and bottom lines of the box represent the 75th and 25th percentiles of the data, respectively. Vertical bars extending beyond the boxes represent extreme data points. For combine-sampling, dots represent DON estimates for individual samples, whereas for hand-sampling, dots represent transect means in 2021 and 2022, and estimates for individual ears in 2023.

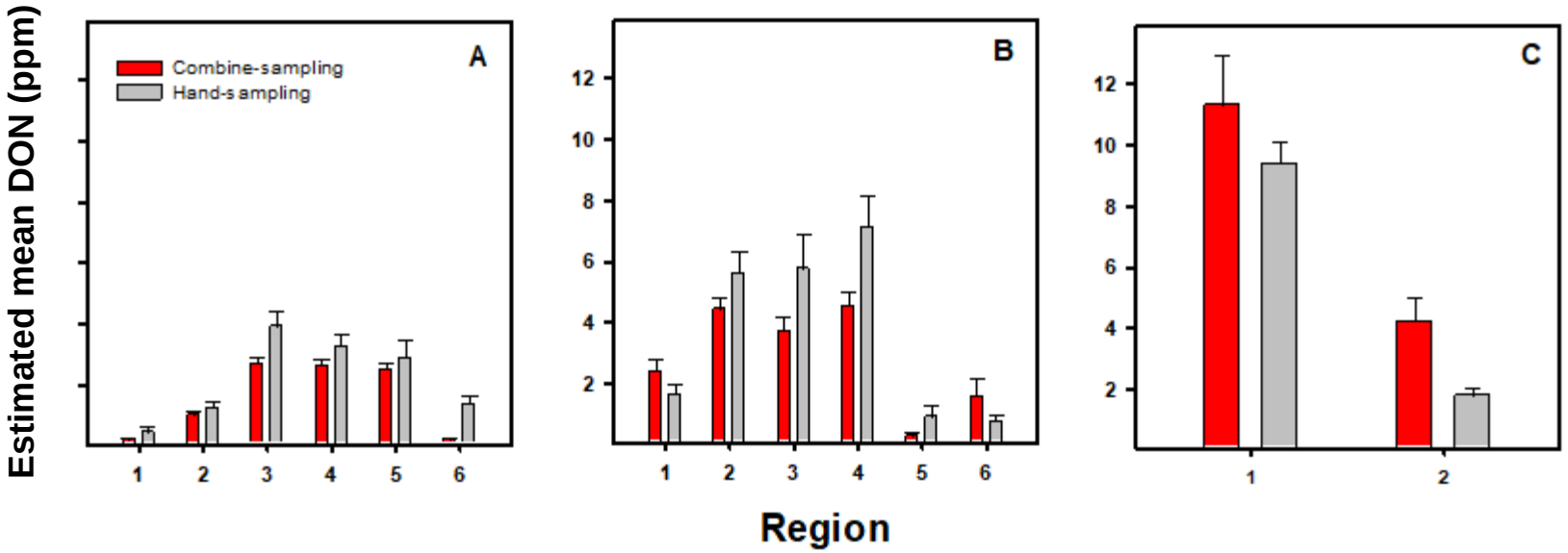

Fig. 3.3. Estimated mean deoxynivalenol (DON) contamination (ppm) of maize grain hand- and combine-sampled from fields in different production regions across the state of Ohio 2021 (A), 2022 (B), and 2023 (C). Error bars are standard errors of the mean.

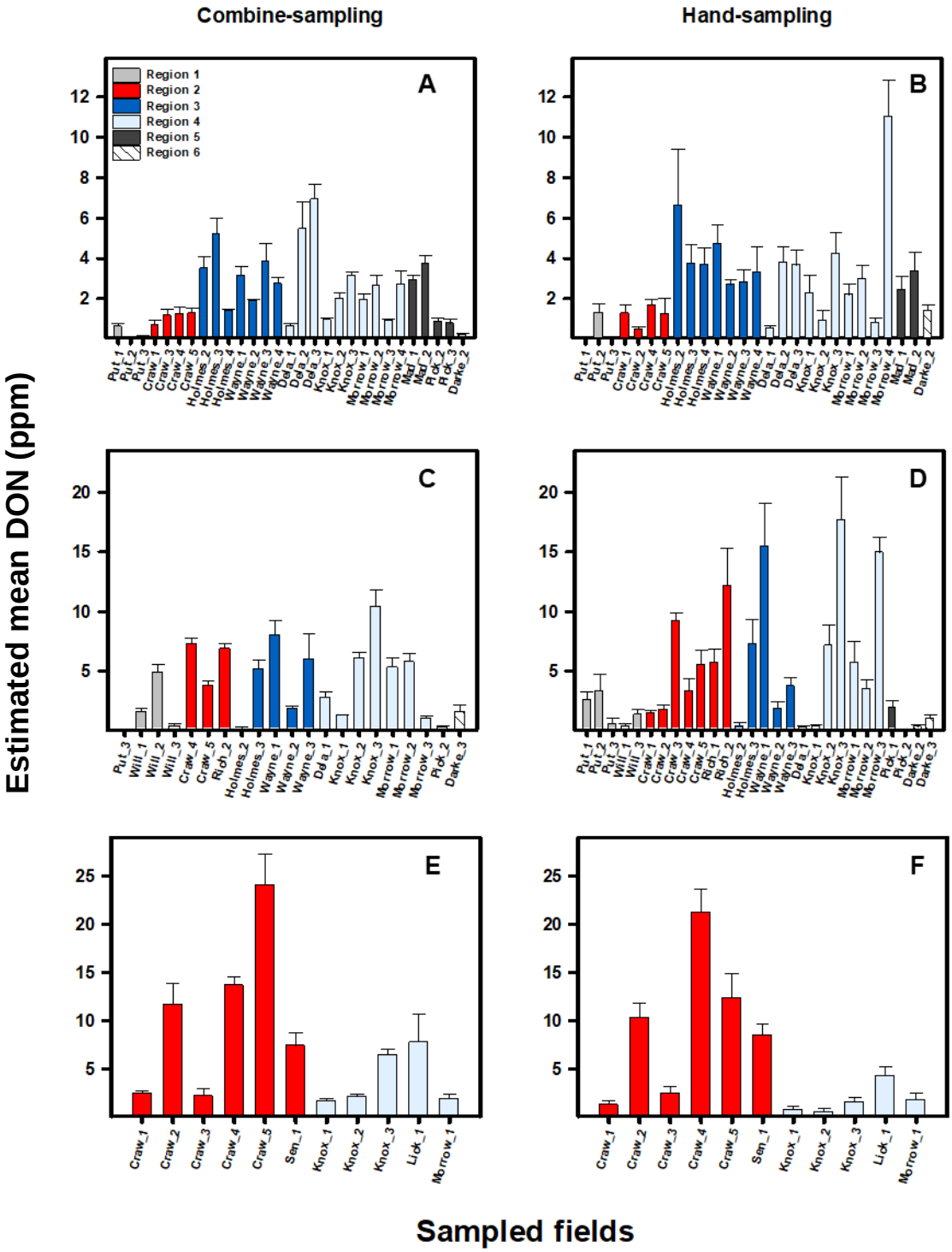

Fig. 3.4. Estimated field-level mean deoxynivalenol (DON) contamination of maize grain (ppm) hand- and combine-sampled from fields in different production regions across the state of Ohio in 2021 (A and B), 2002 (C and D), and 2023 (E and F). Fields are labelled with abbreviations for county names and numbers for specific fields within that county. Error bars are standard errors of the mean.

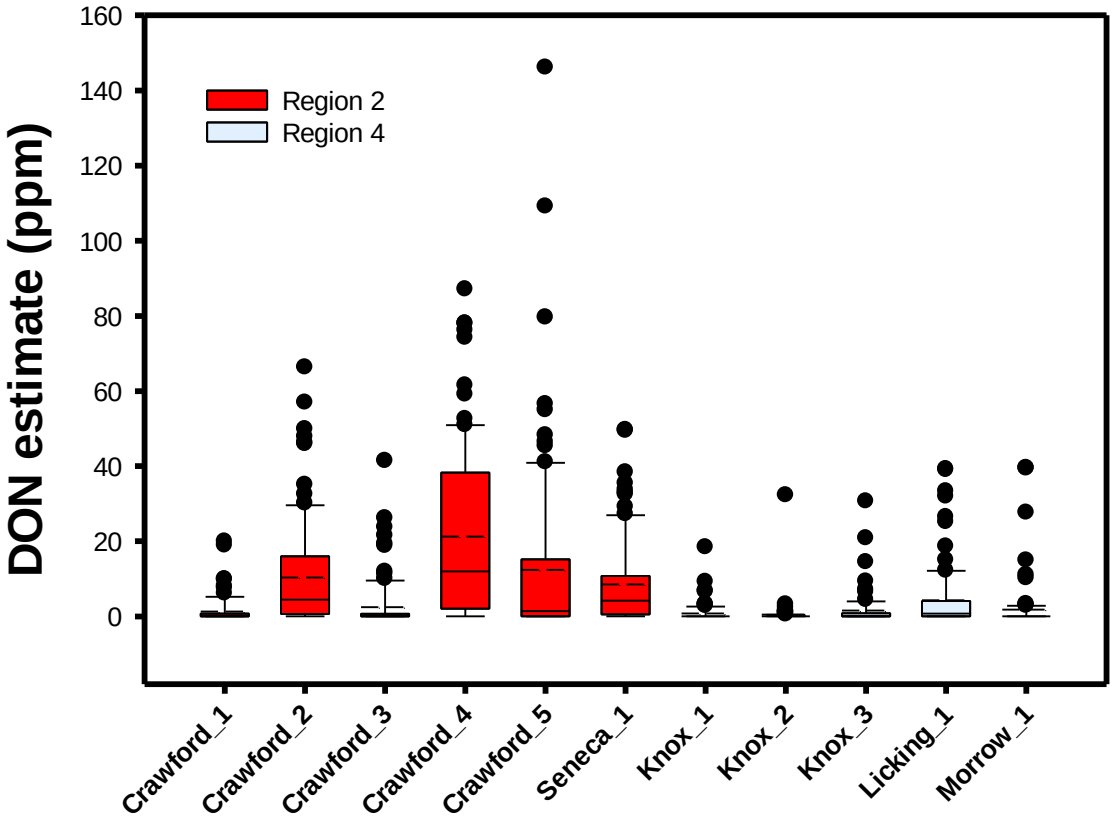

Fig. 3.5. Boxplots showing the distribution of deoxynivalenol (DON) contamination (ppm) of maize grain across ears hand-sampled from commercial fields in 2023. Broken and solid lines within each box represent means and medians, respectively, while the top and bottom lines of the box represent the 75th and 25th percentiles of the data, respectively. Vertical bars extending beyond the boxes represent extreme data points. Fields are labelled with abbreviations for county names and numbers for specific fields within that county.

BIBLIOGRAPHY

Akinsanmi, O. A., Backhouse, D., Simpfendorfer, S., and Chakraborty, S. 2006. Genetic diversity of Australian *Fusarium graminearum* and *F. pseudograminearum*. Plant Pathol. 55:494–504.

Alexander, N. J., McCormick, S. P., Waalwijk, C., van der Lee, T., and Proctor, R. H. 2011. The genetic basis for 3-ADON and 15-ADON trichothecene chemotypes in *Fusarium*. Fungal Genet. Biol. 48:485–495.

Ali, M. L., Taylor, J. H., Jie, L., Sun, G., William, M., Kasha, K. J., Reid, L. M., and Pauls, K. P. 2005. Molecular mapping of QTLs for resistance to Gibberella ear rot, in corn, caused by *Fusarium graminearum*. Genome 48:521–533.

Anderson, N. R., Romero Luna, M. P., Ravellette, J. D., and Wise, K. A. 2017. Impact of foliar fungicides on Gibberella ear rot and deoxynivalenol levels in Indiana Corn. Plant Health Progress 18:186–191.

Andriolli, C. F., Casa, R. T., Kuhnem, P. R., Bogo, A., Zancan, R. L., and Reis, E. M. 2016. Timing of fungicide application for the control of Gibberella ear rot of maize. Trop. Plant Pathol. 41:264–269.

Atanasova-Penichon, V., Pons, S., Pinson-Gadais, L., Picot, A., Marchegay, G., Bonnin-Verdal, M.-N., Ducos, C., Barreau, C., Roucolle, J., Sehabiague, P., Carolo, P., and Richard-Forget, F. 2012. Chlorogenic acid and maize ear rot resistance: a dynamic study investigating *Fusarium graminearum* development, deoxynivalenol production, and phenolic acid accumulation. Mol. Plant-Microbe in. 25:1605–1616.

Awika, J. M. 2011. Major cereal grains production and use around the world. In advances in cereal science: implications to food processing and health promotion. ACS Symposium Series. American Chemical Society pp. 1–13.

Baird, R. E., Mullinix, B. G., Peery, A. B., and Lang, M. L. 1997. Diversity and longevity of the soybean debris mycobiota in a no-tillage system. Plant Dis. 81:530–534.

Beliën, T., Van Campenhout, S., Robben, J., and Volckaert, G. 2006. Microbial endoxylanases: effective weapons to breach the plant cell-wall barrier or, rather, triggers of plant defense systems?. Mol. Plant-Microbe in. 19:1072–1081.

Beyer, M., Klix, M. B., and Verreet, J.-A. 2007. Estimating mycotoxin contents of *Fusarium*-damaged winter wheat kernels. Int. J. Food Microbiol. 119:153–158.

Beyer, M., Röding, S., Ludewig, A., and Verreet, J. A. 2004. Germination and survival of *Fusarium graminearum* macroconidia as affected by environmental factors. J. Phytopathol. 152:92–97.

Bolduan, C., Miedaner, T., Schipprack, W., Dhillon, B. S., and Melchinger, A. E. 2009. Genetic variation for resistance to ear rots and mycotoxins contamination in early European maize inbred lines. Crop Sci. 49:2019–2028.

Bottalico, A., and Perrone, G. 2002. Toxigenic *Fusarium* species and mycotoxins associated with head blight in small-grain cereals in Europe. In Mycotoxins in Plant Disease: Under the aegis of COST Action 835 'Agriculturally Important Toxigenic Fungi 1998-2003', EU project (QLK 1-CT-1998-01380), and ISPP 'Fusarium Committee,' eds. A. Logrieco, J. A. Bailey, L. Corazza, and B. M. Cooke. Springer.

Boutigny, A. L., Ward, T. J., Ballois, N., Iancu, G., and Ioos, R. 2014. Diversity of the *Fusarium graminearum* species complex on French cereals. Eur. J. Plant Pathol. 138:133–148.

Boutigny, A. L., Ward, T. J., Van Coller, G. J., Flett, B., Lamprecht, S. C., O'Donnell, K., and Viljoen, A. 2011. Analysis of the *Fusarium graminearum* species complex from wheat, barley and maize in South Africa provides evidence of species-specific differences in host preference. Fungal Genet. Biol. 48:914–920.

Broders, K. D., Lipps, P. E., Paul, P. A., and Dorrance, A. E. 2007. Evaluation of *Fusarium graminearum* associated with corn and soybean seed and seedling disease in Ohio. Plant Dis. 91:1155–1160.

Burlakoti, R. R., Neate, S. M., Adhikari, T. B., Gyawali, S., Salas, B., Steffenson, B. J., and Schwarz, P. B. 2011. Trichothecene profiling and population genetic analysis of Gibberella zeae from barley in North Dakota and Minnesota. Phytopathology 101:687–695.

Butrón, A., Reid, L. M., Santiago, R., Cao, A., and Malvar, R. A. 2015. Inheritance of maize resistance to Gibberella and Fusarium ear rots and kernel contamination with deoxynivalenol and fumonisins. Plant Pathol. 64:1053–1060.

Caldwell, R. W., Tuite, J., Stob, M., and Baldwin, R. 1970. Zearalenone production by *Fusarium* species. Appl. Microbiol. 20:31–34.

Chungu, C., Mather, D. E., Reid, L. M., and Hamilton, R. I. 1996. Inheritance of kernel resistance to *Fusarium graminearum* in maize. J. of Hered. 87:382–385.

Cohen, J. 1960. A coefficient of agreement for nominal scales. Educ. Psychol. Meas. 20:37–46.

Cossette, F., and Miller, J. D. 1995. Phytotoxic effect of deoxynivalenol and Gibberella ear rot resistance of com. Nat. Toxins 3:383–388.

Cowger, C., and Arrellano, C. 2010. Plump kernels with high deoxynivalenol linked to late *Gibberella zeae* infection and marginal disease conditions in winter wheat. Phytopathology 100: 719-728.

Da Fonseca, R. R., Smith, B. D., Wales, N., Cappellini, E., Skoglund, P., Fumagalli, M., Samaniego, J. A., Carøe, C., Ávila-Arcos, M. C., Hufnagel, D. E., Korneliussen, T. S., Vieira, F. G., Jakobsson, M., Arriaza, B., Willerslev, E., Nielsen, R., Hufford, M. B., Albrechtsen, A., Ross-Ibarra, J., and Gilbert, M. T. P. 2015. The origin and evolution of maize in the Southwestern United States. Nat. Plants 1:1–5.

Dalla Lana, F., Madden, L. V., and Paul, P. A. 2021a. Logistic models derived via lasso methods for quantifying the risk of natural contamination of maize grain with deoxynivalenol. Phytopathology 111:2250–2267.

Dalla Lana, F., Madden, L. V., and Paul, P. A. 2021b. Natural occurrence of maize Gibberella ear rot and contamination of grain with mycotoxins in association with weather variables. Plant Dis. 105:114–126.

David Miller, J., Culley, J., Fraser, K., Hubbard, S., Meloche, F., Ouellet, T., Lloyd Seaman, W., Seifert, K. A., Turkington, K., and Voldeng, H. 1998. Effect of tillage practice on Fusarium head blight of wheat. Can. J. Plant Pathol. 20:95–103.

Del Ponte, E. M., Shah, D. A., and Bergstrom, G. C. 2003. Spatial patterns of Fusarium head blight in New York wheat fields suggest role of airborne inoculum. Plant Health Progress 4:6.

Desjardins, A. E. 2006. Fusarium mycotoxins: chemistry, genetics and biology. J. Agric. Sci. 145:539–539.

Desjardins, A. E., and Proctor, R. H. 2011. Genetic diversity and trichothecene chemotypes of the *Fusarium graminearum* clade isolated from maize in Nepal and identification of a putative new lineage. Fungal Biol. 115:38–48.

Dill-Macky, R., and Jones, R. K. 2000. The effect of previous crop residues and tillage on Fusarium head blight of wheat. Plant Dis. 84:71–76.

Dufault, N. S., De Wolf, E. D., Lipps, P. E., and Madden, L. V. 2006. Role of temperature and moisture in the production and maturation of *Gibberella zeae* perithecia. Plant Dis. 90:637–644.

Edite Bezerra da Rocha, M., Freire, F. da C. O., Erlan Feitosa Maia, F., Izabel Florindo Guedes, M., and Rondina, D. 2014. Mycotoxins and their effects on human and animal health. Food Control 36:159–165.

Eli, K., Schaafsma, A. W., Limay-Rios, V., and Hooker, D. C. 2021. Effect of pydiflumetofen on Gibberella ear rot and *Fusarium* mycotoxin accumulation in maize grain. World Mycotoxin J. 14:495–512.

Enerson, P. M., and Hunter, R. B. 1980. Response of maize hybrids to artificially inoculated ear mold incited by *Gibberella zeae*. Can. J. Plant Sci. 60:1463–1465.

Federal Grain Inspection Service-United States Department of Agriculture. 2016. Inspecting grain: practical procedures for grain handlers. Available: https://www.ams.usda.gov/sites/default/files/media/PracticalProceduresBook2017.pdf

Federal Grain Inspection Service-United States Department of Agriculture. 2023. Mycotoxin handbook. Available at: https://www.ams.usda.gov/sites/default/files/media/MycotoxinHB.pdf

Feinberg, B., and McLaughlin, C. S. 1989. Biochemical mechanism of action of trichothecene mycotoxins. 1st ed. In Trichothecene Mycotoxicosis Pathophysiologic Effects (1989), CRC Press, Boca Raton, Fl.

Foroud, N. A., and Eudes, F. 2009. Trichothecenes in cereal grains. Int. J. Mol. Sci. 10:147–173.

Francl, L., Shaner, G., Bergstrom, G., Gilbert, J., Pedersen, W., Dill-Macky, R., Sweets, L., Corwin, B., Jin, Y., Gallenberg, D., and Wiersma, J. 1999. Daily inoculum levels of *Gibberella zeae* on wheat spikes. Plant Dis. 83:662–666.

Gilbert, J., Abramson, D., McCallum, B., and Clear, R. 2002. Comparison of Canadian *Fusarium graminearum* isolates for aggressiveness, vegetative compatibility, and production of ergosterol and mycotoxins. Mycopathologia 153:209–215.

Harris, L. J., Desjardins, A. E., Plattner, R. D., Nicholson, P., Butler, G., Young, J. C., Weston, G., Proctor, R. H., and Hohn, T. M. 1999. Possible role of trichothecene mycotoxins in virulence of *Fusarium graminearum* on maize. Plant Dis. 83:954–960.

Hesseltine, C. W., and Bothast, R. J. 1977. Mold development in ears of corn from tasseling to harvest. Mycologia 69:328–340.

Hooker, D. C., and Schaafsma, A. W. 2005. Agronomic and environmental impacts on concentrations of deoxynivalenol and fumonisin B1 in corn across Ontario. Can. J. Plant Pathol. 27:347–356.

Iram, A., Cekmecelioglu, D., and Demirci, A. 2020. Distillers' dried grains with solubles (DDGS) and its potential as fermentation feedstock. Appl. Microbiol. Biotechnol. 104:6115–6128.

Islam, M. N., Tabassum, M., Banik, M., Daayf, F., Fernando, W. G. D., Harris, L. J., Sura, S., and Wang, X. 2021. Naturally occurring *Fusarium* species and mycotoxins in oat grains from Manitoba, Canada. Toxins 13:670.

Jiménez, M., Máñez, M., and Hernández, E. 1996. Influence of water activity and temperature on the production of zearalenone in corn by three *Fusarium* species. Int. J. Food Microbiol. 29:417–421.

Kang, Z., and Buchenauer, H. 1999. Immunocytochemical localization of *Fusarium* toxins in infected wheat spikes by *Fusarium culmorum*. Physiol. Mol. Plant Pathol. 55:275–288.

Kawakami, A., Kato, N., Sasaya, T., Tomioka, K., Inoue, H., Miyasaka, A., and Hirayae, K. 2015. Gibberella ear rot of corn caused by *Fusarium asiaticum* in Japan. J. Gen. Plant Pathol. 81:324–327.

Kebebe, A. Z., Reid, L. M., Zhu, X., Wu, J., Woldemariam, T., Voloaca, C., and Xiang, K. 2015. Relationship between kernel drydown rate and resistance to Gibberella ear rot in maize. Euphytica 201:79–88.

Keller, M. D., Bergstrom, G. C., and Shields, E. J. 2014. The aerobiology of *Fusarium graminearum*. Aerobiologia 30:123–136.

Khatibi, P. A., McMaster, N. J., Musser, R., and Iii, D. G. S. 2014. Survey of mycotoxins in corn distillers' dried grains with solubles from seventy-eight ethanol plants in twelve states in the U.S. in 2011. Toxins 6:1155–1168.

Khonga, E. B., and Sutton, J. C. 1988. Inoculum production and survival of *Gibberella zeae* in maize and wheat residues. Can. J. Plant Pathol. 10:232–239.

Kriss, A. B., Paul, P. A., and Madden, L. V. 2012. Characterizing heterogeneity of disease incidence in a spatial hierarchy: a case study from a decade of observations of Fusarium head blight of wheat. Phytopathology 102:867–877.

Kuhnem, P. R., Ward, T. J., Silva, C. N., Spolti, P., Ciliato, M. L., Tessmann, D. J., and Del Ponte, E. M. 2016. Composition and toxigenic potential of the *Fusarium graminearum* species complex from maize ears, stalks and stubble in Brazil. Plant Pathol. 65:1185–1191.

Lana, F. D., Madden, L. V., Carvalho, C. P., and Paul, P. A. 2022. Impact of Gibberella ear rot on grain quality and yield components in maize as influenced by hybrid reaction. Plant Dis. 106:3061–3075.

Lana, F. D., Paul, P. A., Minyo, R., Thomison, P., and Madden, L. V. 2020. Stability of hybrid maize reaction to Gibberella ear rot and deoxynivalenol contamination of grain. Phytopathology 110:1908–1922.

Lee, S.-H., Lee, J.-K., Nam, Y.-J., Lee, S.-H., Ryu, J.-G., and Lee, T. 2010. Population structure of *Fusarium graminearum* from maize and rice in 2009 in Korea. Plant Pathol. J. 26:321–327.

Leplat, J., Friberg, H., Abid, M., and Steinberg, C. 2013. Survival of *Fusarium graminearum*, the causal agent of Fusarium head blight. Agron. Sustain. Dev. 33:97–111.

Lin, L. I.-K. 1989. A concordance correlation coefficient to evaluate reproducibility. Biometrics 45:255–268.

Lindsey, L. E., Lentz, E., Michel, A., Tilmon, K., Culman, S., and Paul, P. 2017. Small grain production. Pages 69-81 in: Ohio Agronomy Guide, 15th Ed. D. Barker, S. Culman, A. Dorrance, J. Fulton, R. Haden, E. Lentz, A. Lindsey, L. Lindsey, M. Loux, E. McCoy, A. Michel, J. Noel, P. Paul, M. Sulc, P. Thomison, K. Tilmon, and J. Witter, eds. The Ohio State University, Columbus, OH.

Liu, K. 2011. Chemical composition of distillers grains, a review. J. Agric. Food Chem. 59:1508–1526.

Llorens, A., Mateo, R., Hinojo, M. J., Valle-Algarra, F. M., and Jiménez, M. 2004. Influence of environmental factors on the biosynthesis of type B trichothecenes by isolates of *Fusarium* spp. from Spanish crops. Int. J. Food Microbiol. 94:43–54.

Lohr, S. L. 2010. Sampling: Design and Analysis. 2nd ed. Brooks/Cole, Boston, MA.

Machado, F. J., Kuhnem, P. R., Casa, R. T., McMaster, N., Schmale, D. G., Vaillancourt, L. J., and Del Ponte, E. M. 2021. The dominance of *Fusarium meridionale* over *F. graminearum* causing Gibberella ear rot in Brazil may be due to increased aggressiveness and competitiveness. Phytopathology 111:1774–1781.

Madden, L. V., and Paul, P. A. 2020. Is disease intensity a good surrogate for yield loss or toxin contamination? A case study with Fusarium head blight of wheat. Phytopathology 110:1632–1646.

Madden, L. V., Hughes, G., and Van Den Bosch, F. 2007. The Study of Plant Disease Epidemics. American Phytopathological Society, St. Paul, MN.

Magarini, A., Passera, A., Ghidoli, M., Casati, P., and Pilu, R. 2023. Genetics and environmental factors associated with resistance to *Fusarium graminearum*, the causal agent of Gibberella ear rot in maize. Agronomy 13:1836.

Maldonado-Ramirez, S. L., Schmale, D. G., Shields, E. J., and Bergstrom, G. C. 2005. The relative abundance of viable spores of *Gibberella zeae* in the planetary boundary layer suggests the role of long-distance transport in regional epidemics of Fusarium head blight. Agric. For. Meteorol. 132:20–27.

Matsuoka, Y., Vigouroux, Y., Goodman, M. M., Sanchez G., J., Buckler, E., and Doebley, J. 2002. A single domestication for maize shown by multilocus microsatellite genotyping. Proc. Natl. Acad. Sci. 99:6080–6084.

McHugh, M. L. 2012. Interrater reliability: the kappa statistic. Biochem. Med. 22:276–282.

McMullen, M., Bergstrom, G., De Wolf, E., Dill-Macky, R., Hershman, D., Shaner, G., and Van Sanford, D. 2012. A unified effort to fight an enemy of wheat and barley: Fusarium head blight. Plant Dis. 96:1712–1728.

Mesterházy, Á., Bartók, T., Mirocha, C. G., and Komoróczy, R. 1999. Nature of wheat resistance to Fusarium head blight and the role of deoxynivalenol for breeding. Plant Breed. 118:97–110.

Miller, J. D., Young, J. C., and Trenholm, H. L. 1983. *Fusarium* toxins in field corn. I. Time course of fungal growth and production of deoxynivalenol and other mycotoxins. Can. J. Bot. 61:3080–3087.

Miller, S. S., Reid, L. M., and Harris, L. J. 2007. Colonization of maize silks by *Fusarium graminearum*, the causative organism of gibberella ear rot. Can. J. Bot. 85:369–376.

Mohammadi, M., Anoop, V., Gleddie, S., and Harris, L. J. 2011. Proteomic profiling of two maize inbreds during early Gibberella ear rot infection. Proteomics 11:3675–3684.

Moraes, W. B., Madden, L. V., and Paul, P. A. 2022. Characterizing heterogeneity and determining sample sizes for accurately estimating wheat Fusarium head blight index in research plots. Phytopathology 112:315–334.

Moraes, W. B., Madden, L. V., Baik, B.-K., Gillespie, J., and Paul, P. A. 2023. Environmental conditions after Fusarium head blight visual symptom development affect contamination of wheat grain with deoxynivalenol and deoxynivalenol-3-glucoside. Phytopathology 113:206–224.

Morrison, J. E., Huang, C. H., Lightle, D. T., and Daughtry, C. S. 1993. Residue measurement techniques. J. Soil Water Conserv. 48:478-483.

Mueller, D. S., Wise, K. A., Sisson, A. J., Allen, T. W., Bergstrom, G. C., Bissonnette, K. M., Bradley, C. A., Byamukama, E., Chilvers, M. I., Collins, A. A., Esker, P. D., Faske, T. R., Friskop, A. J., Hagan, A. K., Heiniger, R. W., Hollier, C. A., Isakeit, T., Jackson-Ziems, T. A., Jardine, D. J., Kelly, H. M., Kleczewski, N. M., Koehler, A. M., Koenning, S. R.,

Malvick, D. K., Mehl, H. L., Meyer, R. F., Paul, P. A., Peltier, A. J., Price, P. P., Robertson, A. E., Roth, G. W., Sikora, E. J., Smith, D. L., Tande, C. A., Telenko, D. E. P., Tenuta, A. U., Thiessen, L. D., and Wiebold, W. J. 2020. Corn yield loss estimates due to diseases in the United States and Ontario, Canada, from 2016 to 2019. Plant Health Progress 21:238–247.

Munkvold, G. P. 2003. Epidemiology of *Fusarium* diseases and their mycotoxins in maize ears. Eur. J. Plant Pathol. 109:705–713.

Nielsen, L. K., Jensen, J. D., Rodríguez, A., Jørgensen, L. N., and Justesen, A. F. 2012. *TRI12* based quantitative real-time PCR assays reveal the distribution of trichothecene genotypes of *F. graminearum* and *F. culmorum* isolates in Danish small grain cereals. Int. J.Food Microbiol. 157:384–392.

Nyvall, R. F. 1970. Chlamydospores of *Fusarium roseum 'graminearum'* as survival structures. Phytopathology 60:1175-1177.

O. Zamir, L., J. Gauthier, M., A. Devor, K., Nadeau, Y., and Sauriol, F. 1989. Trichodiene is a precursor to trichothecenes. J. Chem. Soc., Chem. Commun. 0:598–600.

O'Donnell, K., Kistler, H. C., Tacke, B. K., and Casper, H. H. 2000. Gene genealogies reveal global phylogeographic structure and reproductive isolation among lineages of *Fusarium graminearum*, the fungus causing wheat scab. Proc. Natl. Acad. Sci. 97:7905–7910.

O'Donnell, K., Ward, T. J., Aberra, D., Kistler, H. C., Aoki, T., Orwig, N., Kimura, M., Bjørnstad, Å., and Klemsdal, S. S. 2008. Multilocus genotyping and molecular phylogenetics resolve a novel head blight pathogen within the *Fusarium graminearum* species complex from Ethiopia. Fungal Genet. Biol. 45:1514–1522.

O'Donnell, K., Ward, T. J., Geiser, D. M., Corby Kistler, H., and Aoki, T. 2004. Genealogical concordance between the mating type locus and seven other nuclear genes supports formal recognition of nine phylogenetically distinct species within the *Fusarium graminearum* clade. Fungal Genet. Biol. 41:600–623.

Oerke, E.-C., Meier, A., Dehne, H.-W., Sulyok, M., Krska, R., and Steiner, U. 2010. Spatial variability of Fusarium head blight pathogens and associated mycotoxins in wheat crops. Plant Pathol. 59:671–682.

Ohio Law and Administrative Rules. 2010. Section 926.31 - Ohio revised code | Ohio laws. Available: https://codes.ohio.gov/ohio-revised-code/section-926.31

Parker, N. S., Anderson, N. R., Richmond, D. S., Long, E. Y., Wise, K. A., and Krupke, C. H. 2017. Larval western bean cutworm feeding damage encourages the development of Gibberella ear rot on field corn. Pest Manag. Sci. 73:546–553.

Paul, P. A. 2020. Gibberella ear rots showing up in corn: how to tell it apart from other ear rots. Agronomic Crops Network. Ohio State Univ. Extension. Available: https://agcrops.osu.edu/newsletter/corn-newsletter/2020-34/gibberella-ear-rots-showing-corn-how-tell-it-apart-other-ear-rots .

Paul, P. A., El-Allaf, S. M., Lipps, P. E., and Madden, L. V. 2004. Rain splash dispersal of *Gibberella zeae* within wheat canopies in Ohio. Phytopathology 94:1342–1349.

Paul, P. A., Lipps, P. E., and Madden, L. V. 2005. Relationship between visual estimates of Fusarium head blight intensity and deoxynivalenol accumulation in harvested wheat grain: A meta-analysis. Phytopathology 95: 1225-1236.

Paul, P. A., Lipps, P. E., and Madden, L. V. 2006. Meta-analysis of regression coefficients for the relationship between Fusarium head blight and deoxynivalenol content of wheat. Phytopathology 96:951–961.

Pereyra, S. A., and Dill-Macky, R. 2008. Colonization of the residues of diverse plant species by *Gibberella zeae* and their contribution to Fusarium head blight inoculum. Plant Dis. 92:800–807.

Pestka, J. J. 2010. Deoxynivalenol: mechanisms of action, human exposure, and toxicological relevance. Arch. Toxicol. 84:663–679.

Pestka, J. J., Lin, W.S., and Miller, E. R. 1987. Emetic activity of the trichothecene 15-acetyldeoxynivalenol in swine. Food Chem. Toxicol. 25:855–858.

Petronaitis, T., Simpfendorfer, S., and Hüberli, D. 2021. Importance of Fusarium spp. In Wheat to Food Security: A Global Perspective. in: Plant Diseases and Food Security in the 21st Century, eds. Peter Scott, Richard Strange, Lise Korsten, and Maria Lodovica Gullino. Cham: Springer International Publishing.

Pfordt, A., Ramos Romero, L., Schiwek, S., Karlovsky, P., and von Tiedemann, A. 2020. Impact of environmental conditions and agronomic practices on the prevalence of *Fusarium* species associated with ear- and stalk rot in maize. Pathogens 9:236.

Przemieniecki, S., Tomasz, K., and Korzekwa, K. 2015. Chemotypes and geographic distribution of the *Fusarium graminearum* species complex. Environmental Biotechnology 10:45–54.

Puri, K. D., and Zhong, S. 2010. The 3ADON population of *Fusarium graminearum* found in North Dakota is more aggressive and produces a higher level of DON than the prevalent 15ADON population in spring wheat. Phytopathology 100:1007–1014.

Qiu, J., and Shi, J. 2014. Genetic relationships, carbendazim sensitivity and mycotoxin production of the *Fusarium graminearum* populations from maize, wheat and rice in eastern China. Toxins 6:2291–2309.

Reid, L. M., and Hamilton, R. I. 1997. Breeding maize for ear rot resistance in Canada. Cereal Res. Commun. 25:639–642.

Reid, L. M., and Sinha, R. C. 1998. Maize maturity and the development of Gibberella ear rot symptoms and deoxynivalenol after inoculation. Eur. J. Plant Pathol. 104:147–154.

Reid, L. M., Mather, D. E., and Hamilton, R. I. 1996. Distribution of deoxynivalenol in *Fusarium graminearum*-infected maize ears. Phytopathology 86: 110-114.

Reid, L. M., Mather, D. E., Bolton, A. T., and Hamilton, R. I. 1994. Evidence for a gene for silk resistance to *Fusarium graminearum* schw. ear rot of maize. J. Hered. 85:118–121.

Reid, L. M., Mather, D. E., Hamilton, R. I., and Bolton, A. T. 1992. Diallel analysis of resistance in maize to *Fusarium graminearum* infection via the silk. Can. J. Plant Sci. 72:915–923.

Reid, L. M., Zhu, X., and Ma, B. L. 2001. Crop rotation and nitrogen effects on maize susceptibility to Gibberella (*Fusarium graminearum*) ear rot. Plant Soil 237:1–14.

Reid, L. M., Zhu, X., Savard, M. E., Sinha, R. C., and Vigier, B. 2000. Pre-harvest accumulation of deoxynivalenol in sweet corn ears inoculated with *Fusarium graminearum*. Food Addit. Contam. 17:689–701.

Ross, S. M. 2017. Introductory Statistics. Fourth edition ed. Academic Press, Burlington, MA.

Russell, W. A. 1993. Achievements of Maize Breeders in North America. in: International Crop Science I. John Wiley & Sons, Ltd. Madison, WI.

Salas, B., Steffenson, B. J., Casper, H. H., Tacke, B., Prom, L. K., Fetch, T. G., and Schwarz, P. B. 1999. *Fusarium* species pathogenic to barley and their associated mycotoxins. Plant Dis. 83:667–674.

Sampietro, D. A., Díaz, C. G., Gonzalez, V., Vattuone, M. A., Ploper, L. D., Catalan, C. A. N., and Ward, T. J. 2011. Species diversity and toxigenic potential of *Fusarium graminearum complex* isolates from maize fields in northwest Argentina. Int. J. Food Microbiol. 145:359–364.

Schaafsma, A. W., Hooker, D. C., Baute, T. S., and Illincic-Tamburic, L. 2002. Effect of bt-corn hybrids on deoxynivalenol content in grain at harvest. Plant Dis. 86:1123–1126.

Schaafsma, A. W., Limay-Rios, V., Paul, D. E., and Miller, J. D. 2009. Mycotoxins in fuel ethanol co-products derived from maize: a mass balance for deoxynivalenol. J. Sci. Food Agric. 89:1574–1580.

Schaafsma, A. W., Tamburic-Ilincic, L., and Hooker, D. C. 2005. Effect of previous crop, tillage, field size, adjacent crop, and sampling direction on airborne propagules of *Gibberella zeae/Fusarium graminearum*, Fusarium head blight severity, and deoxynivalenol accumulation in winter wheat. Can. J. Plant Pathol. 27:217–224.

Schmale III, D. G., Arntsen, Q. A., and Bergstrom, G. C. 2005. The forcible discharge distance of ascospores of *Gibberella zeae*. Can. J. Plant Pathol. 27:376–382.

Schmale, D. G., Bergstrom, G. C., and Shah, D. A. 2005a. Spatial patterns of viable spore deposition of the corn ear rot pathogen, *Gibberella zeae*, in first-year corn fields. Can.J. Plant Pathol. 27:225–233.

Schmale, D. G., Shah, D. A., and Bergstrom, G. C. 2005b. Spatial patterns of viable spore deposition of *Gibberella zeae* in wheat fields. Phytopathology 95:472–479.

Sneller, C., Guttieri, M., Paul, P., Costa, J., and Jackwood, R. 2012. Variation for Resistance to Kernel Infection and Toxin Accumulation in Winter Wheat Infected with Fusarium graminearum. Phytopathology 102:306–314.

Starkey, D. E., Ward, T. J., Aoki, T., Gale, L. R., Kistler, H. C., Geiser, D. M., Suga, H., Tóth, B., Varga, J., and O'Donnell, K. 2007. Global molecular surveillance reveals novel Fusarium head blight species and trichothecene toxin diversity. Fungal Genet. Biol. 44:1191–1204.

Suga, H., Karugia, G. W., Ward, T., Gale, L. R., Tomimura, K., Nakajima, T., Miyasaka, A., Koizumi, S., Kageyama, K., and Hyakumachi, M. 2008. Molecular Characterization of the Fusarium graminearum Species Complex in Japan. Phytopathology 98:159–166.

Sutton, J. C. 1982. Epidemiology of wheat head blight and maize ear rot caused by Fusarium graminearum. Can. J. Plant Pathol. 4:195–209.

Sutton, J. C., and Baliko, W. 1981. Methods for quantifying partial resistance to Gibberellazeae in maize ears. Can. J. Plant Pathol. 3:26–32.

Sutton, J. C., Baliko, W., and Liu, H. J. 1980. Fungal colonization and zearalenone accumulation in maize ears injured by birds. Can. J. Plant Sci. 60:453–461.

Tarr, S. A. J. 1972. The dispersal of plant pathogens. In Principles of Plant Pathology, ed. S. A. J. Tarr. London: Macmillan Education UK. Palgrave, London.

Trail, F., and Common, R. 2000. Perithecial development by Gibberella zeae: a light microscopy study. Mycologia 92:130–138.

Trail, F., Gaffoor, I., and Vogel, S. 2005. Ejection mechanics and trajectory of the ascospores of Gibberella zeae (anamorph Fuarium graminearum). Fungal Genet. Biol. 42:528–533.

Trail, F., Xu, H., Loranger, R., and Gadoury, D. 2002. Physiological and environmental aspects of ascospore discharge in Gibberella zeae (anamorph Fusarium graminearum). Mycologia 94:181–189.

Tschanz, A. T., Horst, R. K., and Nelson, P. E. 1976. The Effect of Environment on Sexual Reproduction of Gibberella Zeae. Mycologia 68:327–340.

U.S. Food and Drug Administration. 2010. Guidance for Industry and FDA: Advisory Levels for Deoxynivalenol (DON) in Finished Wheat Products for Human Consumption and Grains and Grain By-Products used for Animal Feed. Available: https://www.fda.gov/regulatory-information/search-fda-guidance-documents/guidanceindustry-and-fda-advisory-levels-deoxynivalenol-don-finished-wheat-products-human.

USDA-NASS. 2023. Corn & Other Feedgrains. Available at: https://www.ers.usda.gov/topics/crops/corn-and-other-feedgrains/.

USDA-NASS. 2024a. Corn acreage planted. Available at: https://www.nass.usda.gov/Charts_and_Maps/graphics/cornac.pdf

USDA-NASS. 2024b. Corn production. Available at: https://www.nass.usda.gov/Charts_and_Maps/graphics/cornprod.pdf

USDA-NASS. 2024c. Corn Yield. Available at: https://www.nass.usda.gov/Charts_and_Maps/graphics/cornyld.pdf

Vesonder, R. F., Ciegler, A., Jensen, A. H., Rohwedder, W. K., and Weisleder, D. 1976. Co-identity of the refusal and emetic principle from Fusarium-infected corn. Appl. Environ. Microbiol. 31:280–285.

Vigier, B., Reid, L. M., Dwyer, L. M., Stewart, D. W., Sinha, R. C., Arnason, J. T., and Butler, G. 2001. Maize resistance to gibberella ear rot: symptoms, deoxynivalenol, and yield1. Can. J. Plant Pathol. 23:99–105.

Visconti, A., Chelkowski, J., Solfrizzo, M., and Bottalico, A. 1990. Mycotoxins in corn ears naturally infected with Fusarium graminearum and F. crookwellense. Can. J. Plant Pathol. 12:187–189.

Walker, S. L., Leath, S., Hagler, W. M., and Murphy, J. P. 2001. Variation Among Isolates of Fusarium graminearum Associated with Fusarium Head Blight in North Carolina. Plant Dis. 85:404–410.

Ward, T. J., Clear, R. M., Rooney, A. P., O'Donnell, K., Gaba, D., Patrick, S., Starkey, D. E., Gilbert, J., Geiser, D. M., and Nowicki, T. W. 2008. An adaptive evolutionary shift in Fusarium head blight pathogen populations is driving the rapid spread of more toxigenic Fusarium graminearum in North America. Fungal Genet. Biol. 45:473–484.

Wilhelm, K. P., and Jones, R. K. 2005. Meso- and Microscale Patterns of Fusarium Head Blight in Spring Wheat Fields in Minnesota. Plant Dis. 89:474–479.

Willyerd, K. T., Thomison, P., and Paul, P. A. 2016. Gibberella Ear Rot and Mycotoxins in Corn: Sampling, Testing, and Storage. Ohio State Univ. Extension. Available: https://ohioline.osu.edu/factsheet/plpath-cer-04

Wu, F., Groopman, J. D., and Pestka, J. J. 2014. Public Health Impacts of Foodborne Mycotoxins. Annu. Rev. Food Sci. Technol. 5:351–372.

Wu, Q.-H., Wang, X., Yang, W., Nüssler, A. K., Xiong, L.-Y., Kuča, K., Dohnal, V., Zhang, X.-J., and Yuan, Z.-H. 2014. Oxidative stress-mediated cytotoxicity and metabolism of T-2 toxin and deoxynivalenol in animals and humans: an update. Arch Toxicol. 88:1309–1326.

Xu, X., and Nicholson, P. 2009. Community Ecology of Fungal Pathogens Causing Wheat Head Blight. Annu. Rev. Phytopathol. 47:83–103.

Xu, X.-M., Parry, D. W., Nicholson, P., Thomsett, M. A., Simpson, D., Edwards, S. G., Cooke, B. M., Doohan, F. M., Monaghan, S., Moretti, A., Tocco, G., Mule, G., Hornok, L., Béki, E., Tatnell, J., and Ritieni, A. 2008. Within-field variability of Fusarium head blight pathogens and their associated mycotoxins. Eur. J. Plant Pathol. 120:21–34.

Xue, A. G., Chen, Y., Seifert, K., Guo, W., Blackwell, B. A., Harris, L. J., and Overy, D. P. 2019. Prevalence of Fusarium species causing head blight of spring wheat, barley and oat in Ontario during 2001–2017. Can. J. Plant Pathol. 41:392–402.

Xue, A. G., Cober, E., Voldeng, H. D., Voldeng, H. D., Babcock, C., and Clear, R. M. 2007. Evaluation of the pathogenicity of Fusarium graminearum and Fusarium pseudograminearum on soybean seedlings under controlled conditions. Can. J. Plant Pathol. 29:35–40.

Yli-Mattila, T., Gagkaeva, T., Ward, T. J., Aoki, T., Kistler, H. C., and O'Donnell, K. 2009. A novel Asian clade within the Fusarium graminearum species complex includes a newly discovered cereal head blight pathogen from the Russian Far East. Mycologia 101:841–852.

Zeller, K. A., Bowden, R. L., and Leslie, J. F. 2004. Population differentiation and recombination in wheat scab populations of Gibberella zeae from the United States. Mol. Ecol. 13:563–571.